Thermal convection in icy moons' oceans: influence of tidal heating

Daphné Lemasquerier[1,2], Carver Bierson[3], Krista Soderlund[3]

[1]UTIG, JSG, University of Texas at Austin, Austin, TX, USA
[2]School of Mathematics and Statistics, University of St Andrews, UK
[3]Arizona State University, Tempe, AZ, USA

IPAM – Rotating Turbulence: Interplay and Separability of Bulk and Boundary Dynamic (RTI2025)
Los Angeles -- January 27-31, 2024

Krista Soderlund
(UTIG)

Carver Bierson
(ASU)

Icy moons

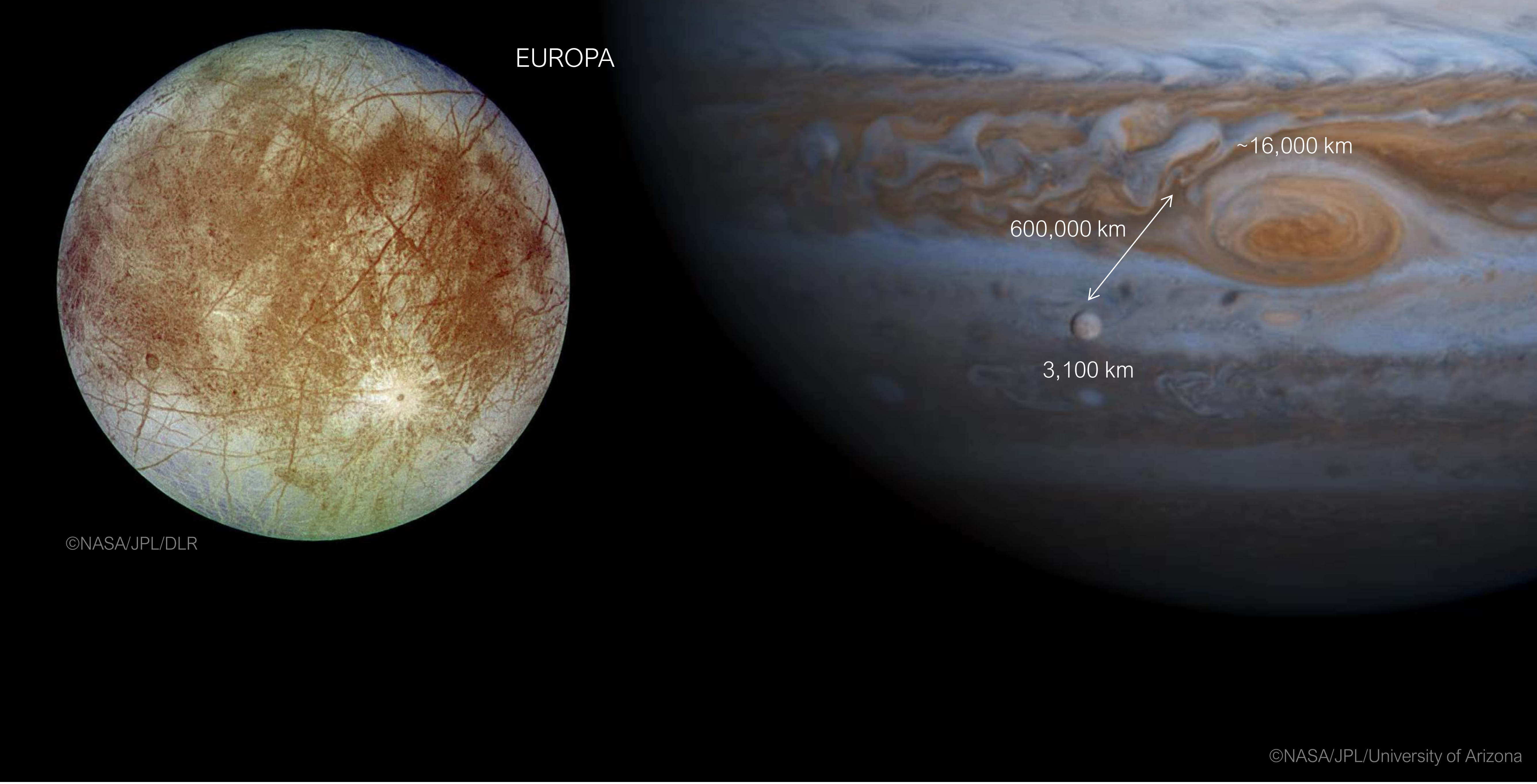
EUROPA
~16,000 km
600,000 km
3,100 km
©NASA/JPL/DLR
©NASA/JPL/University of Arizona

Icy moons

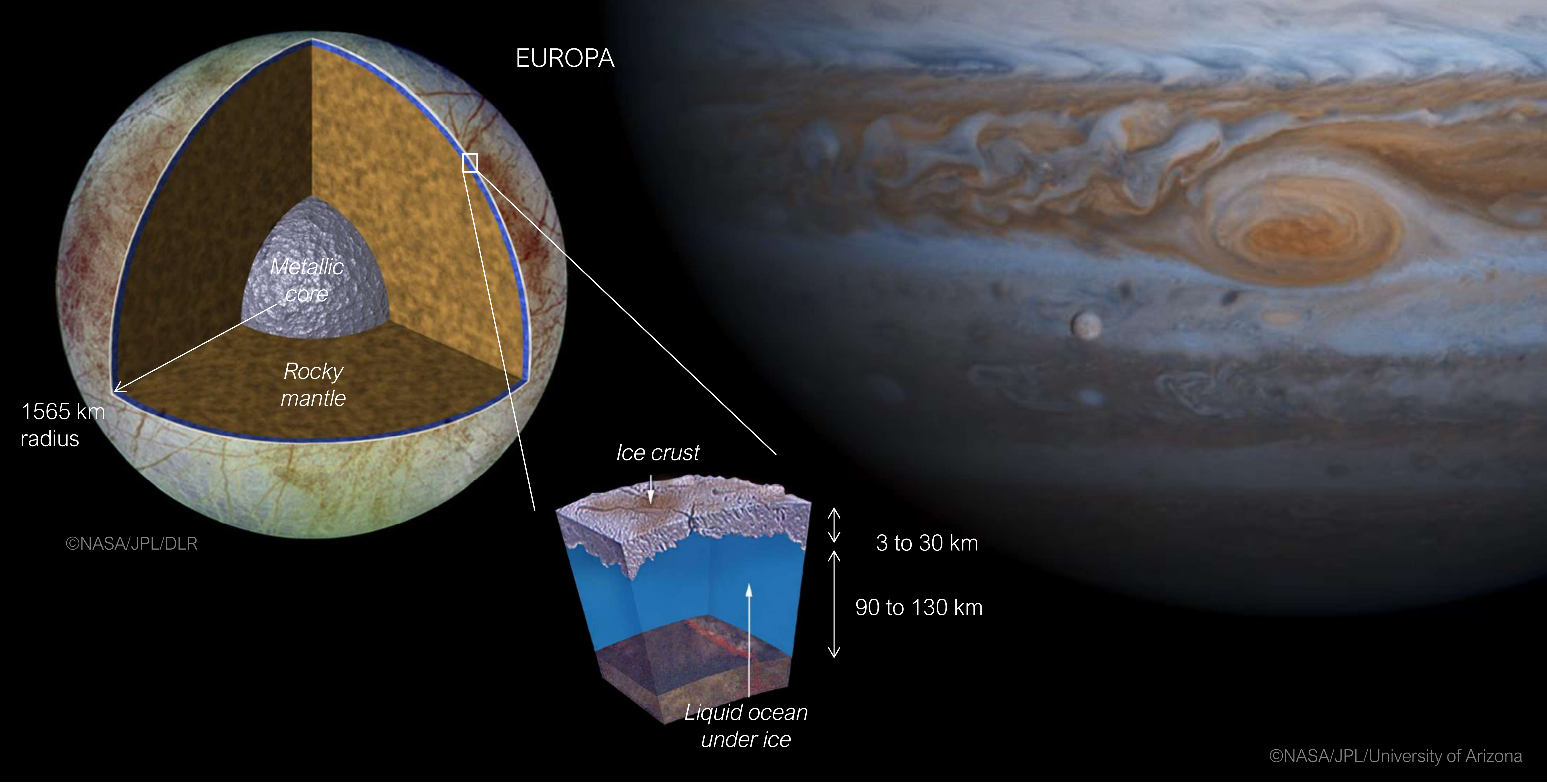
EUROPA
Metallic core
Rocky mantle
1565 km radius
©NASA/JPL/DLR
Ice crust
3 to 30 km
90 to 130 km
Liquid ocean under ice
©NASA/JPL/University of Arizona

Icy moons

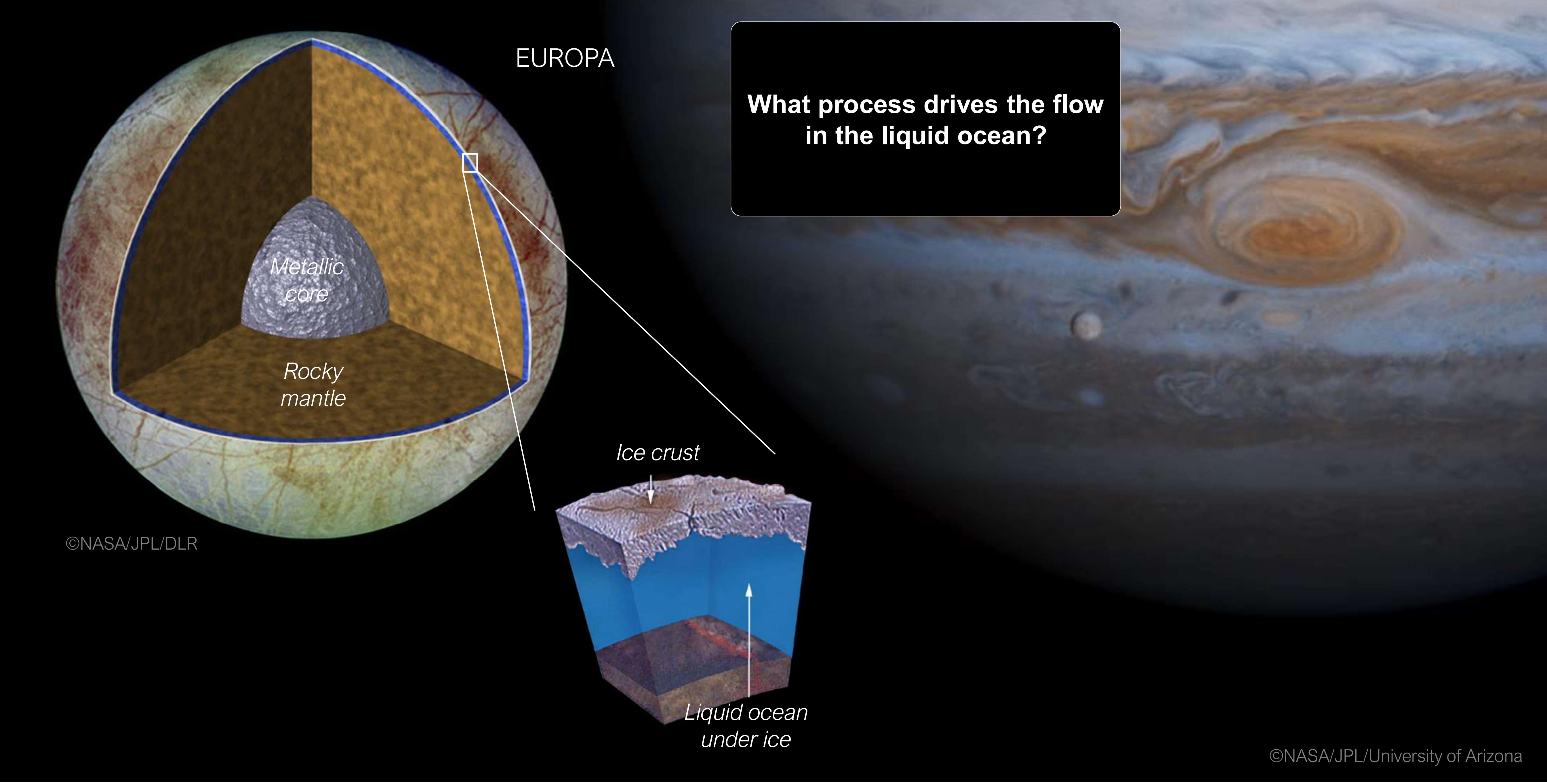
EUROPA
Metallic core
Rocky mantle
Ice crust
Liquid ocean under ice
What process drives the flow in the liquid ocean?

Icy moons

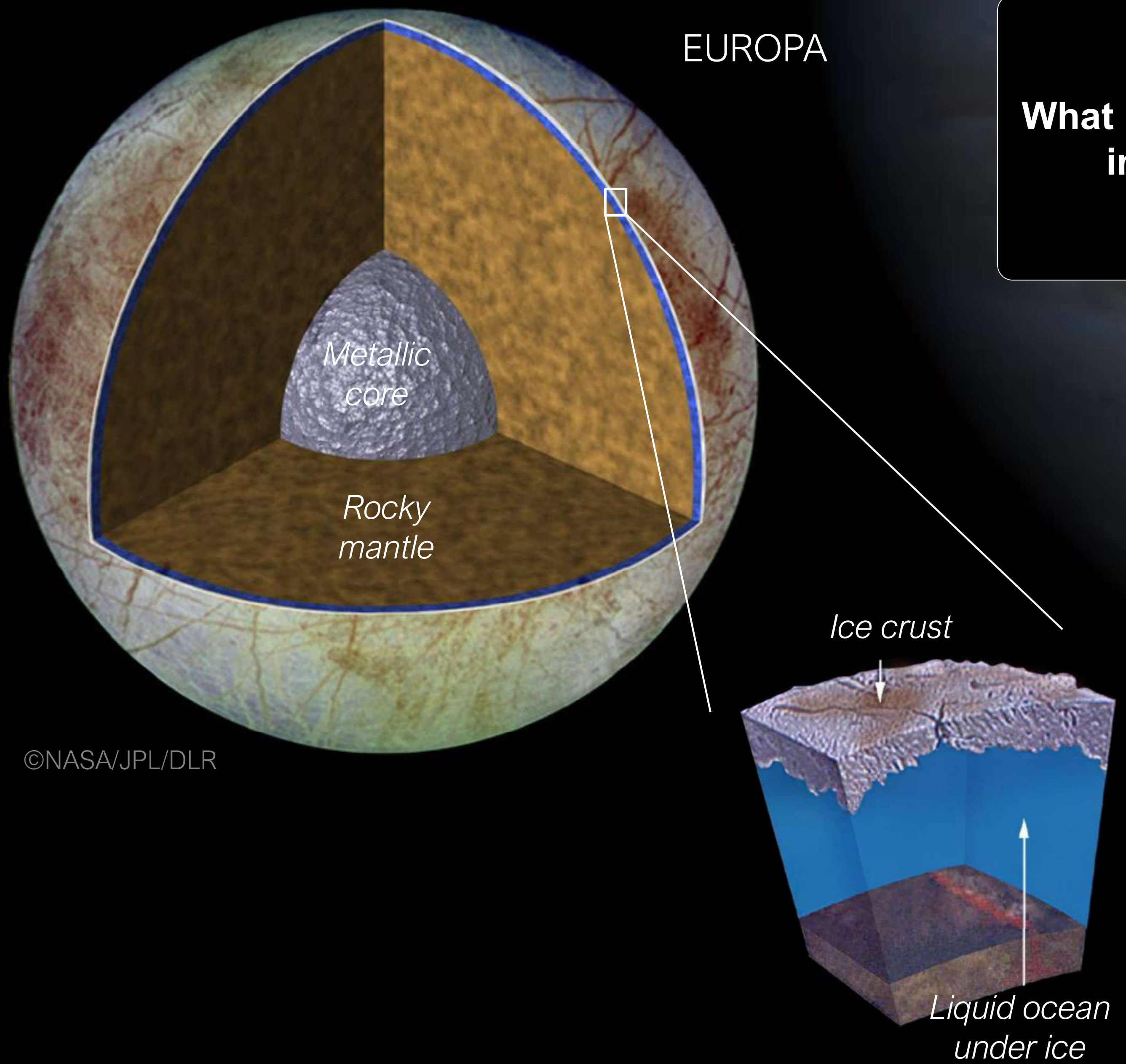

What process drives the flow in the liquid ocean?

- → Temperature gradients?
- → Salinity gradients?
- → Mechanical forcing (tides, libration)?

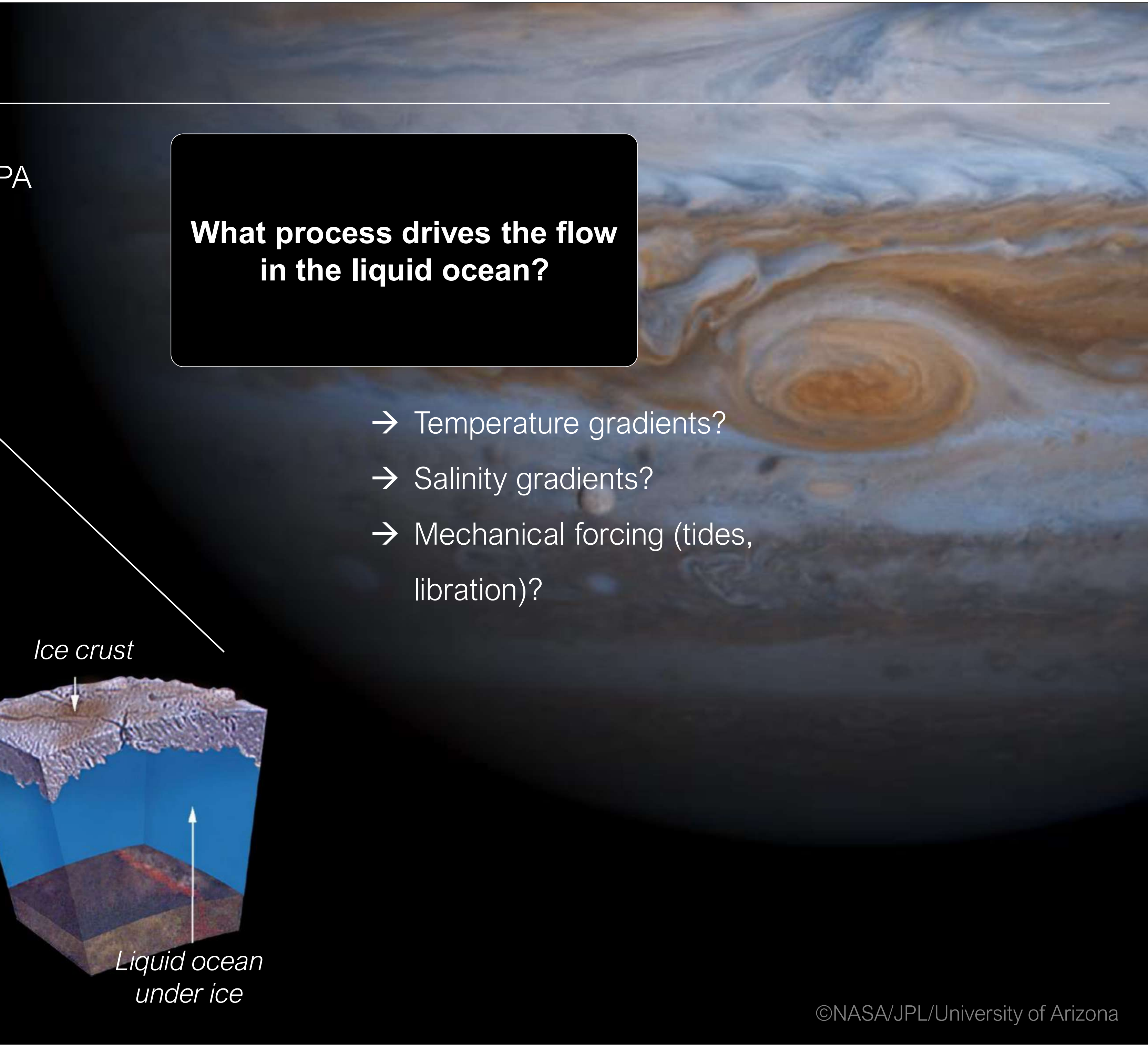

Icy moons

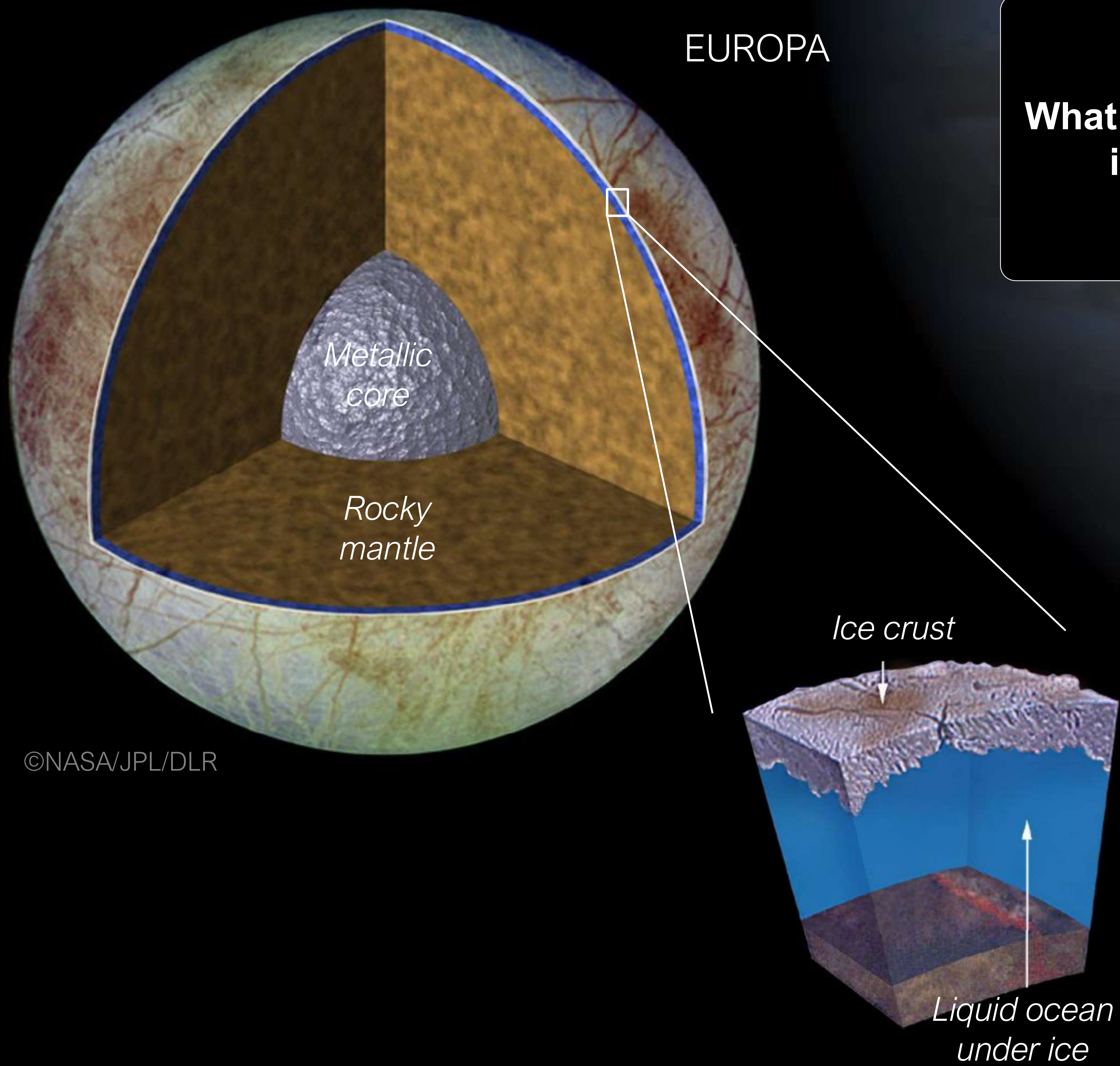

What process drives the flow in the liquid ocean?

→ **Temperature gradients?**

→ Salinity gradients?

→ Mechanical forcing (tides, libration)?

Icy moons

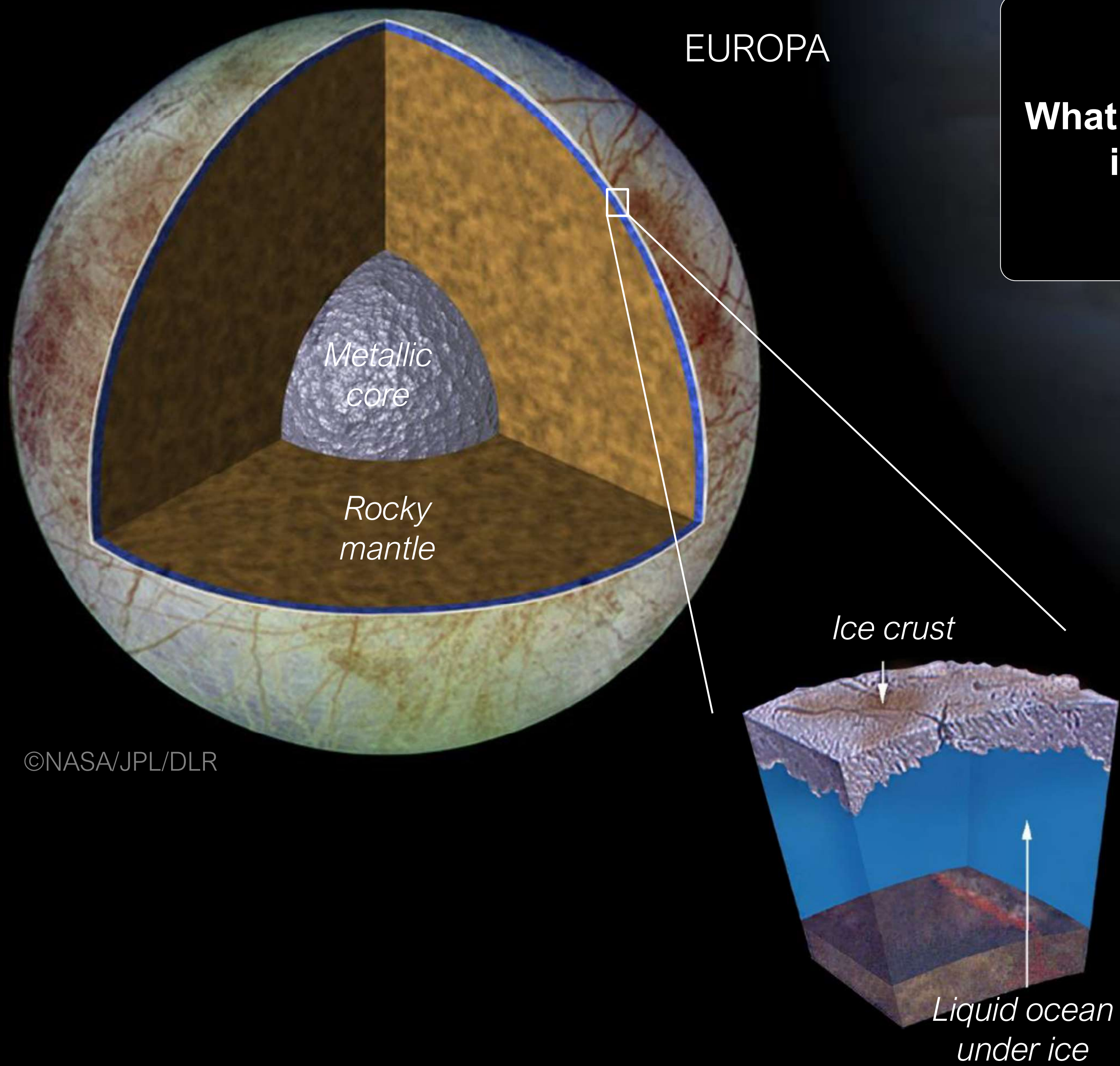

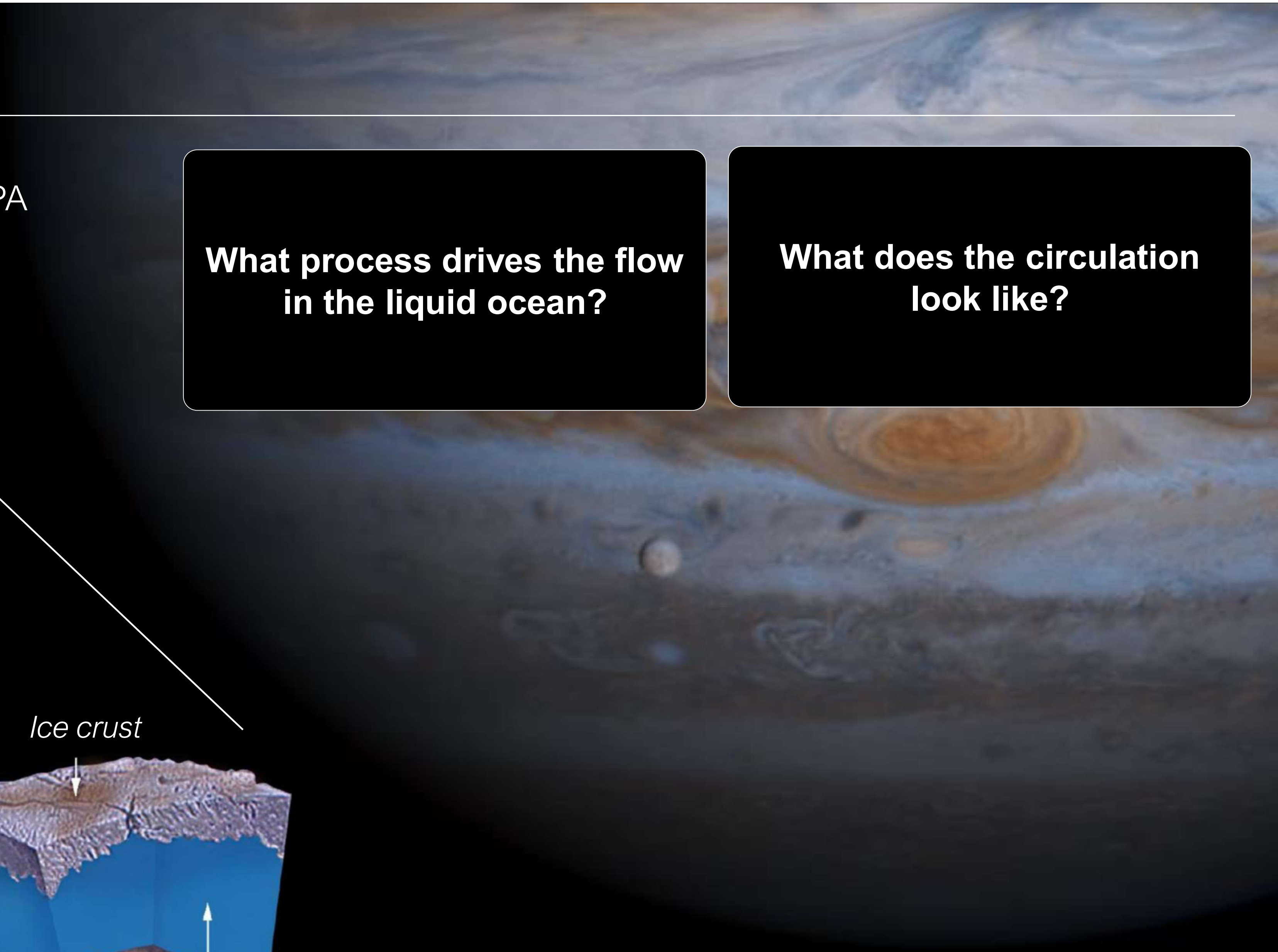

What process drives the flow in the liquid ocean?

What does the circulation look like?

Icy moons

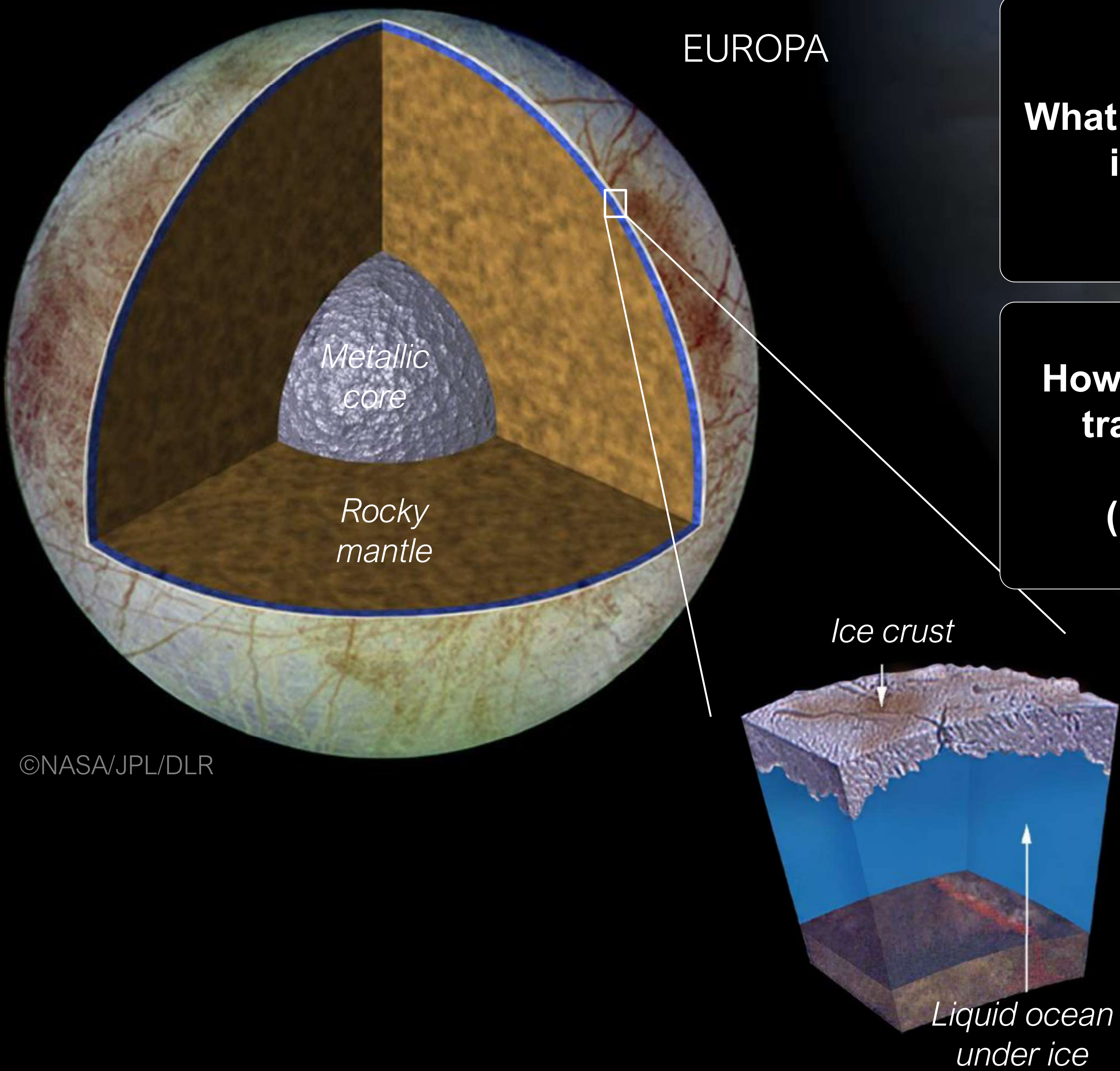

What process drives the flow in the liquid ocean?

What does the circulation look like?

How are heat and materials transported across the ocean?
(mantle → ice crust)

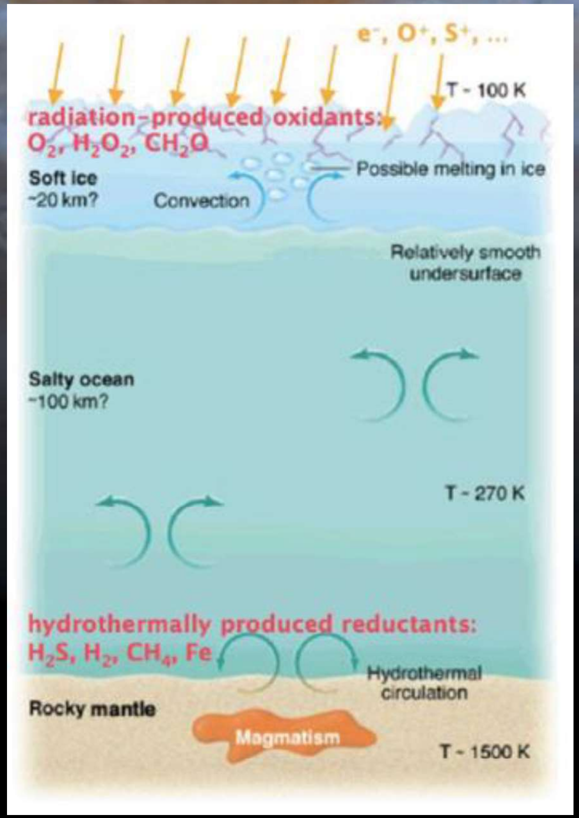

Pappalardo (2010), after Stevenson (2000)

Icy moons

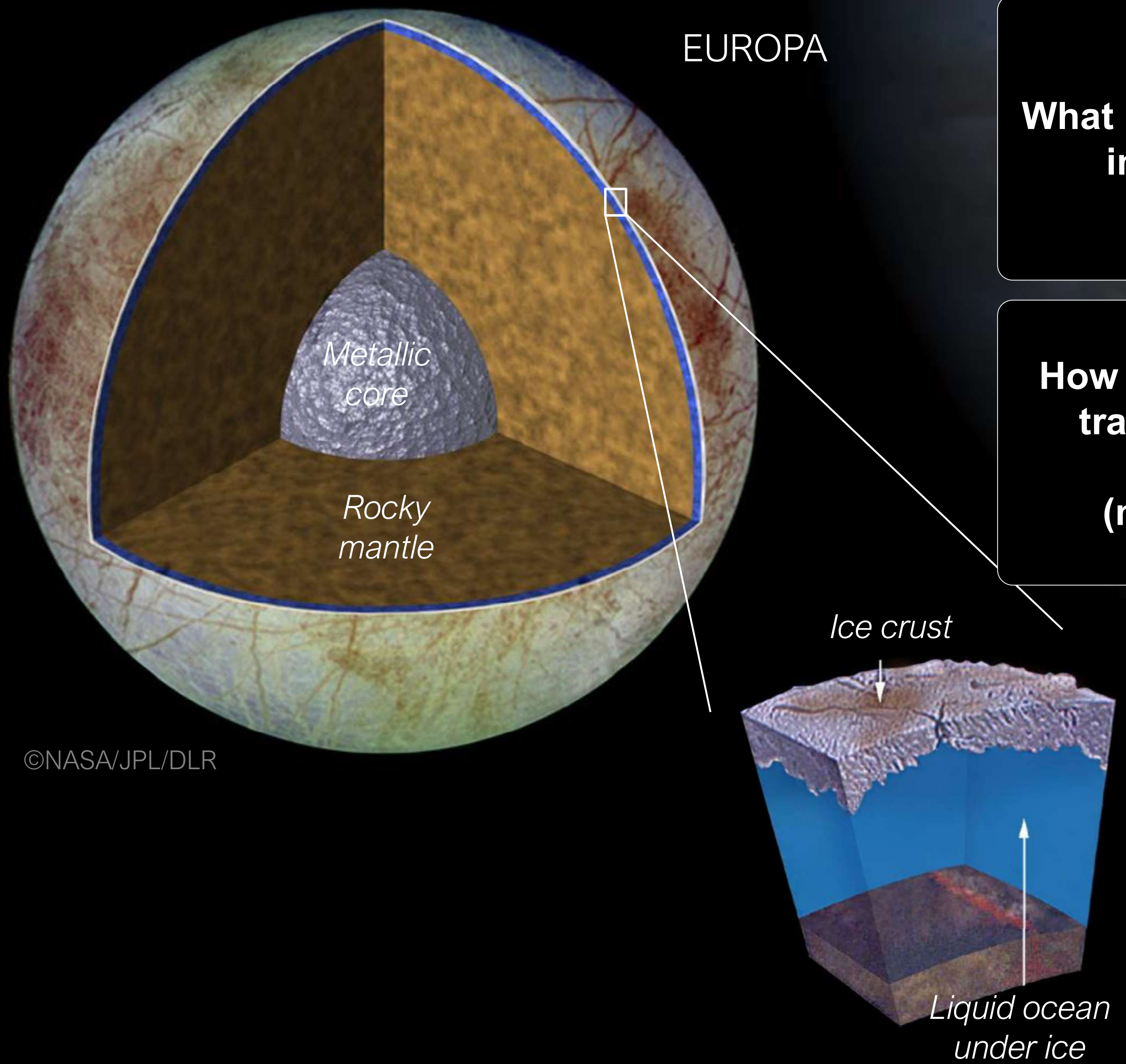

What process drives the flow in the liquid ocean?

What does the circulation look like?

How are heat and materials transported across the ocean? (mantle → ice crust)

What is the nature of the dynamical and thermal coupling between the ocean and the ice crust?

Icy moons

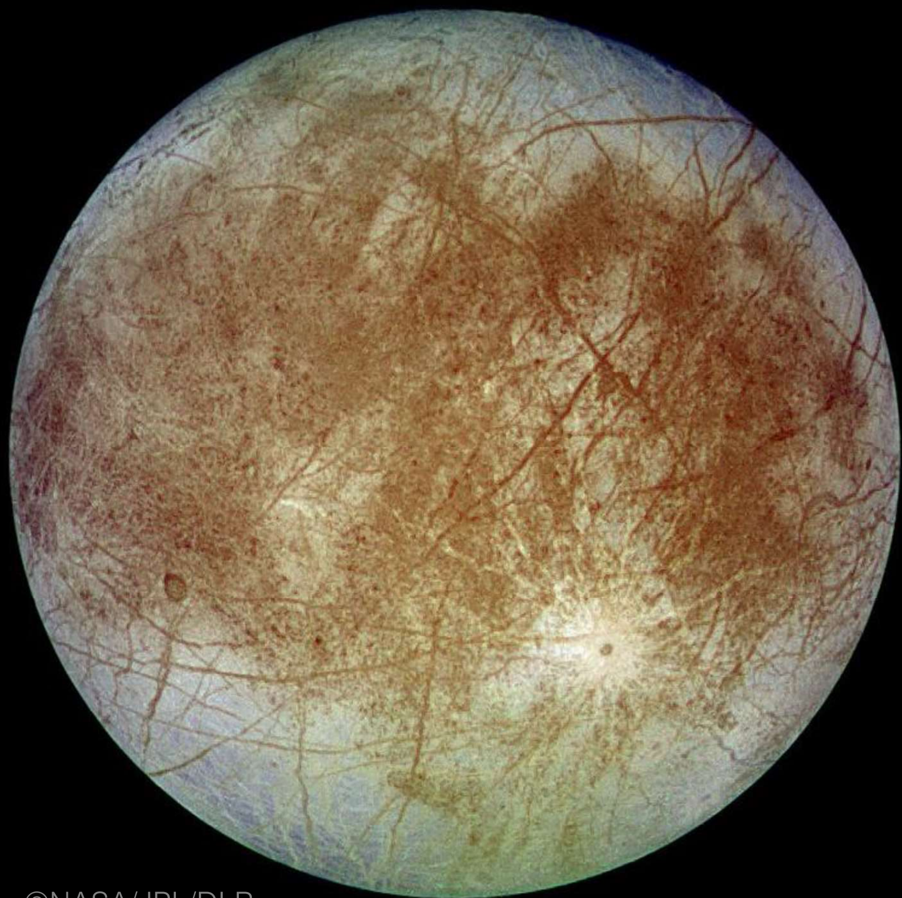

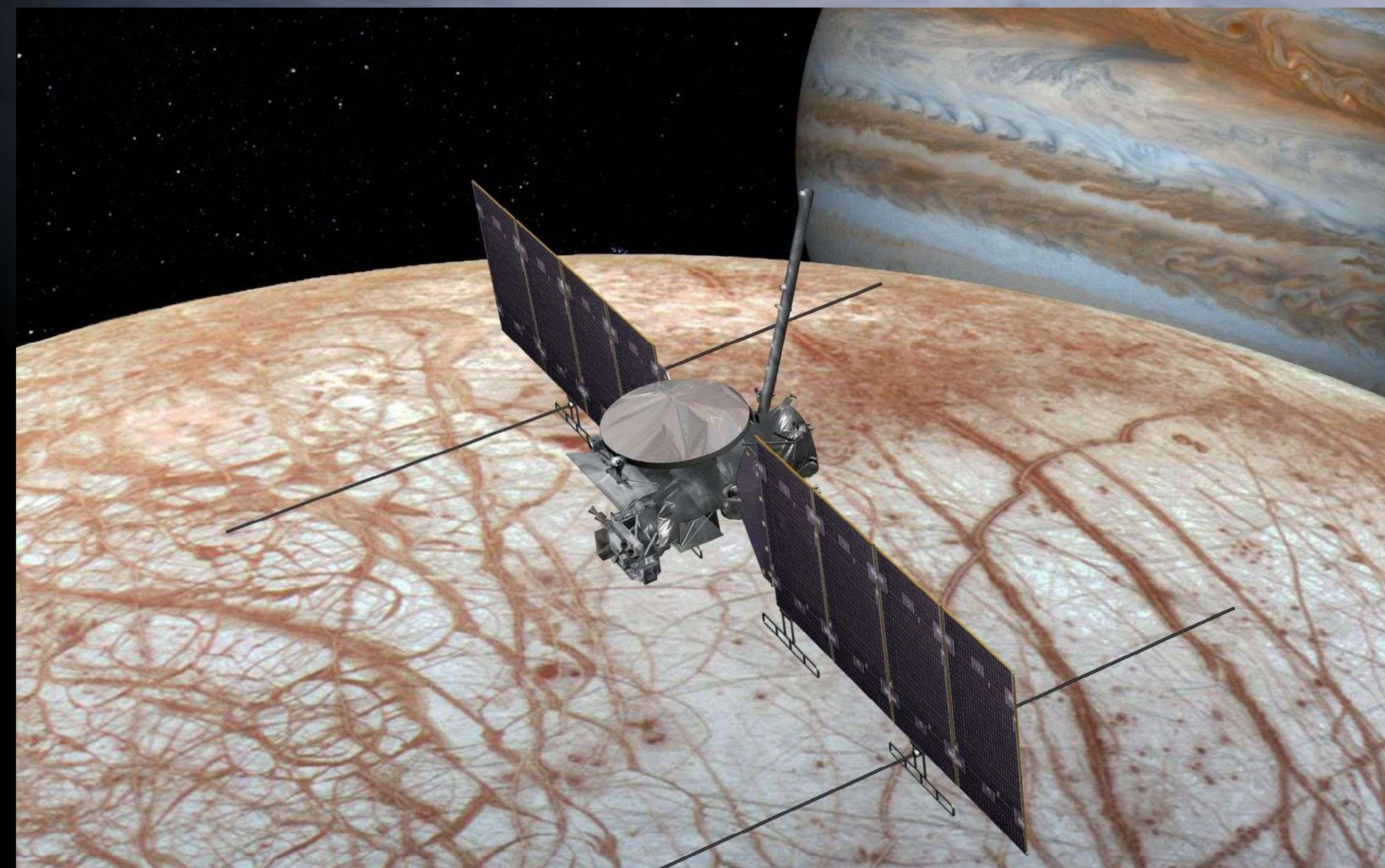

Europa Clipper (NASA)
launch: 2024
arrival: 2030

Tidal heating

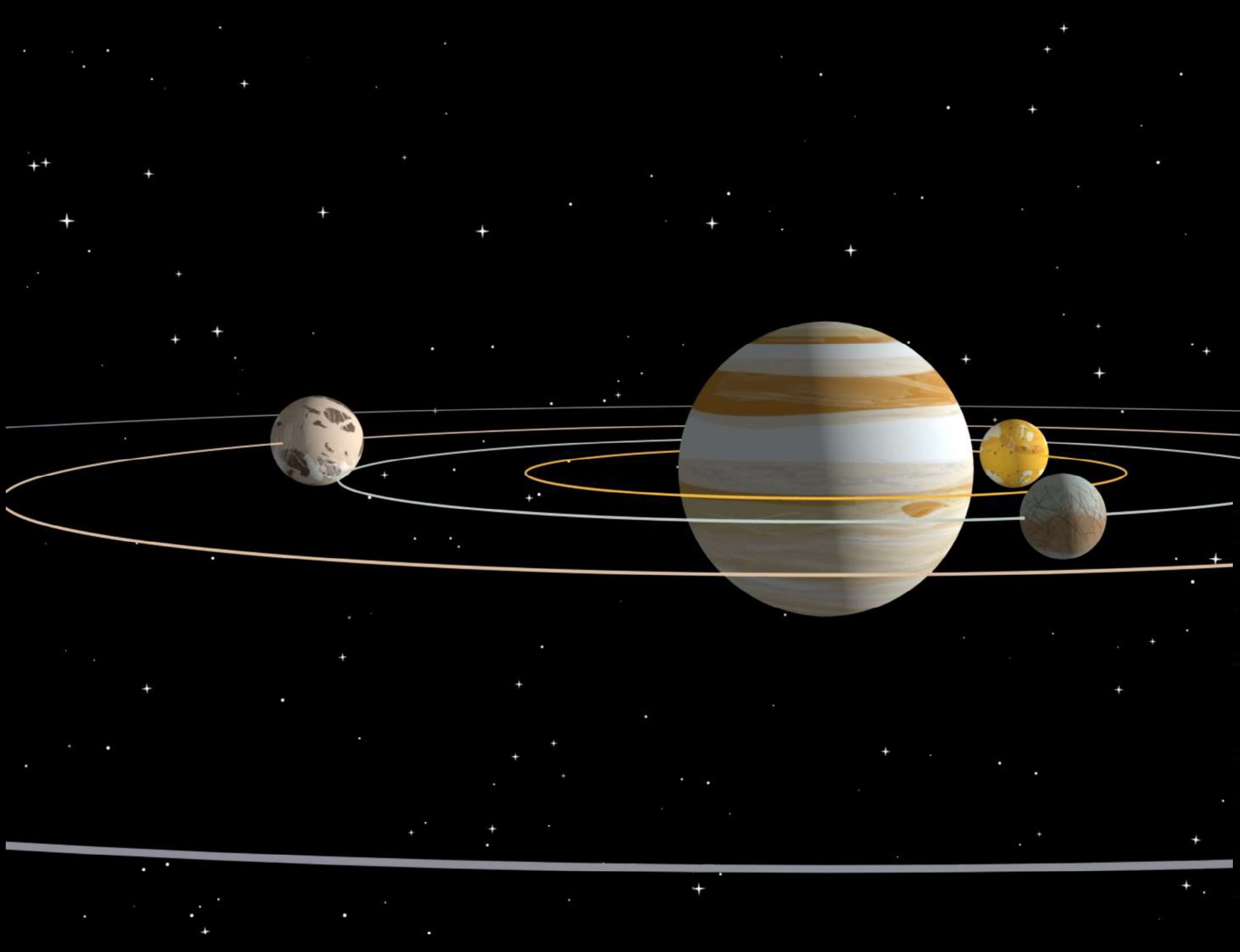

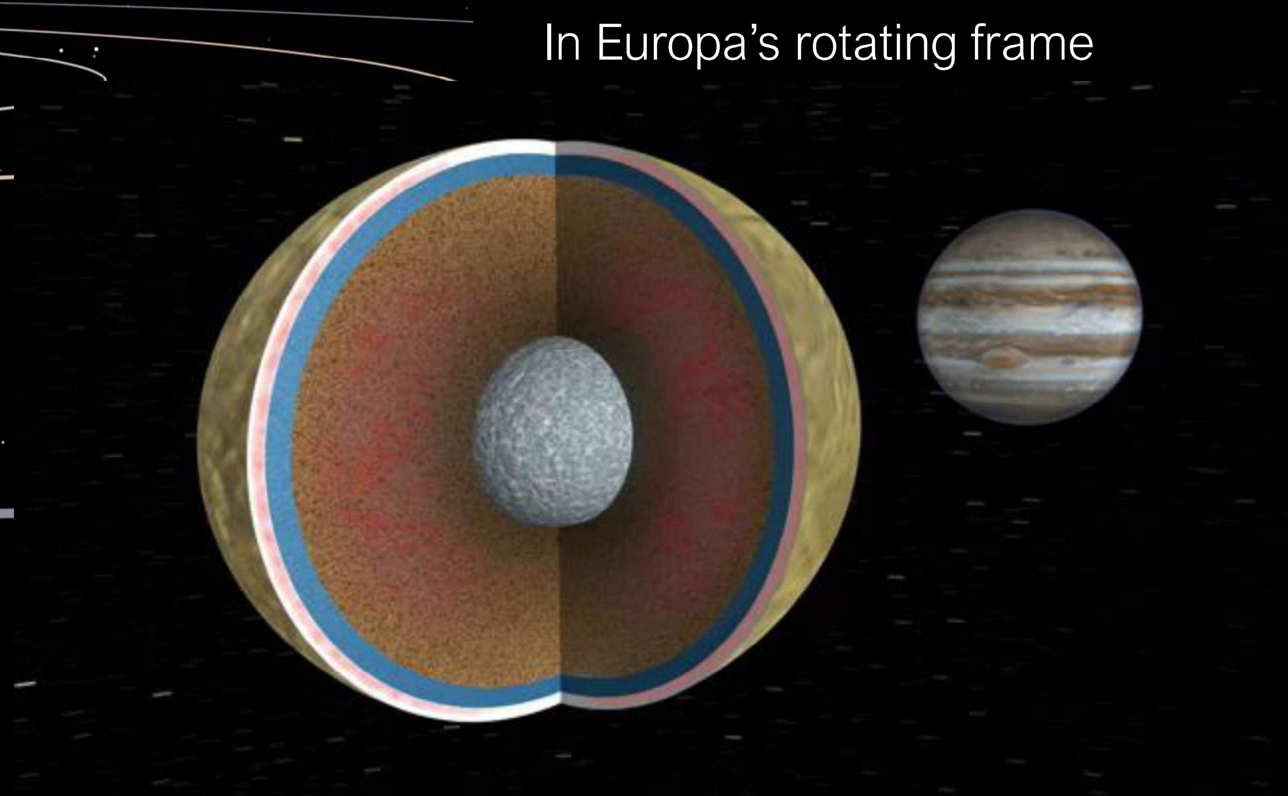

Tidal heating

Tidal dissipation model for Europa
(Carver Bierson, ASU, see also Beuthe 2013; Sotin+ 2009; Tobie+ 2005)

- Eccentricity tides
- Tidal heating of viscoelastic materials [Roberts and Nimmo, 2008]
- Andrade rheology [Bierson and Nimmo, 2016]
- Multi-layered body

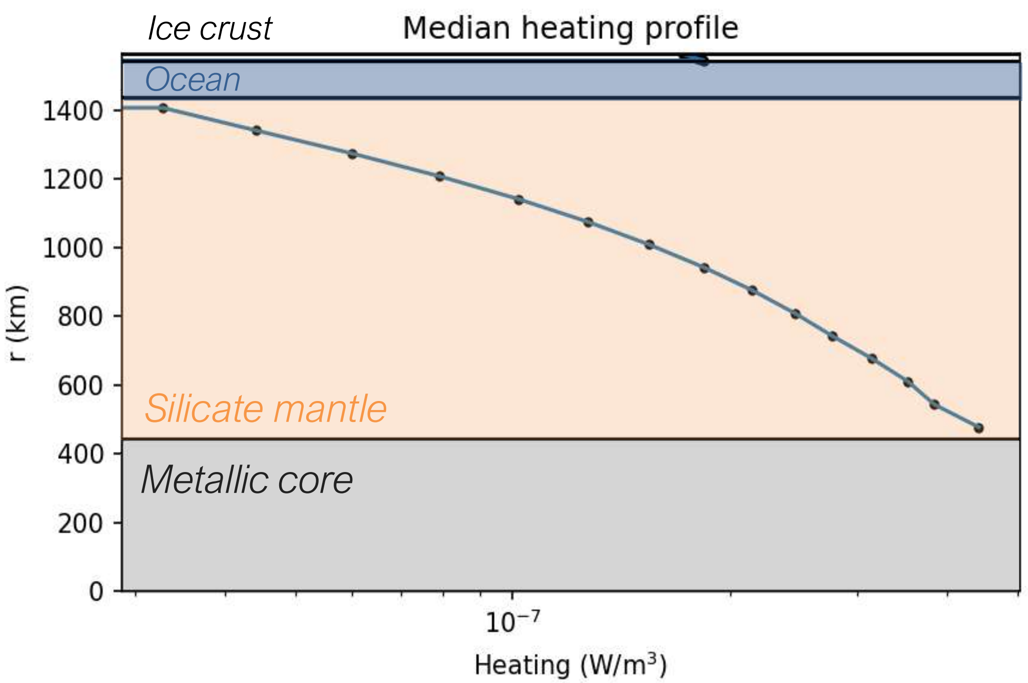

Tidal heating

Tidal dissipation model for Europa
(Carver Bierson, ASU, see also Beuthe 2013; Sotin+ 2009; Tobie+ 2005)

- Eccentricity tides
- Tidal heating of viscoelastic materials [Roberts and Nimmo, 2008]
- Andrade rheology [Bierson and Nimmo, 2016]
- Multi-layered body

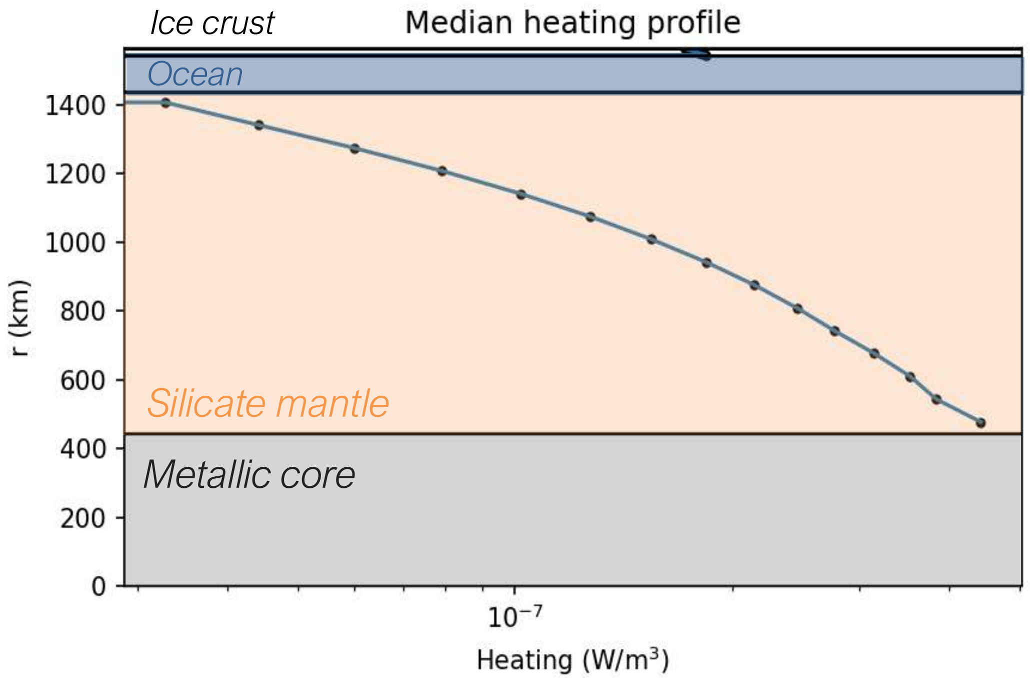

Heat flux at the top of the mantle (mW/m^2)

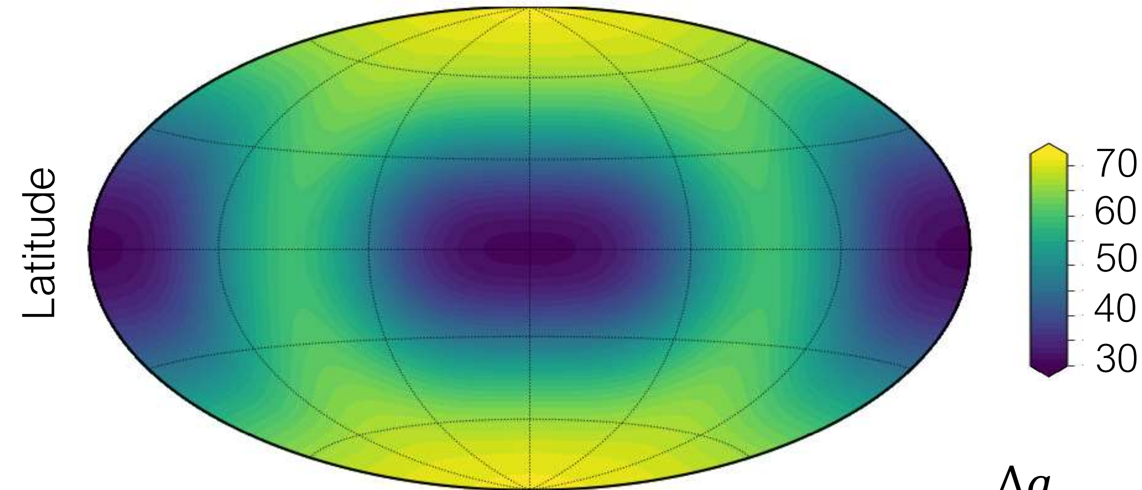

$$q^* = \frac{\Delta q}{q_0} \sim O(1)$$

Dominant spherical harmonics:

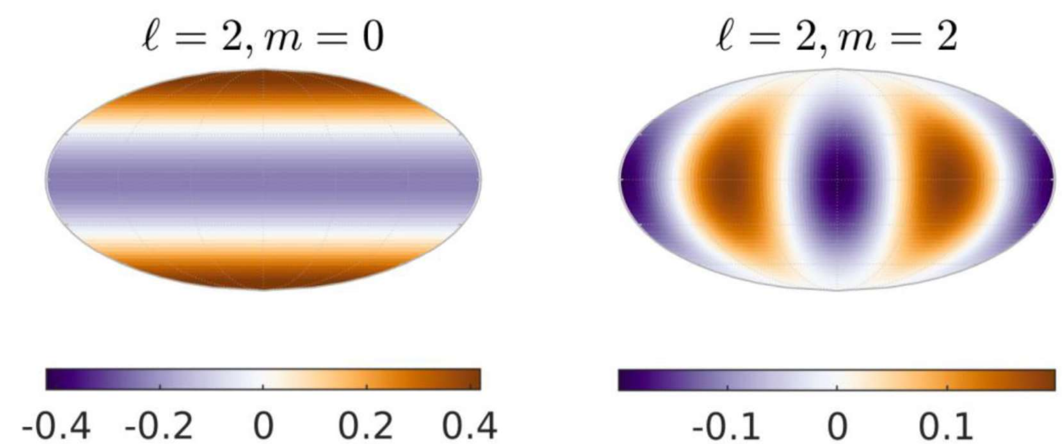

Tidal heating – melting?

Běhounkova+ (2021): magmatism in Europa's mantle
- 3D modelling of heat production by tidal+radiogenic heating
- Model transfer of heat and melting

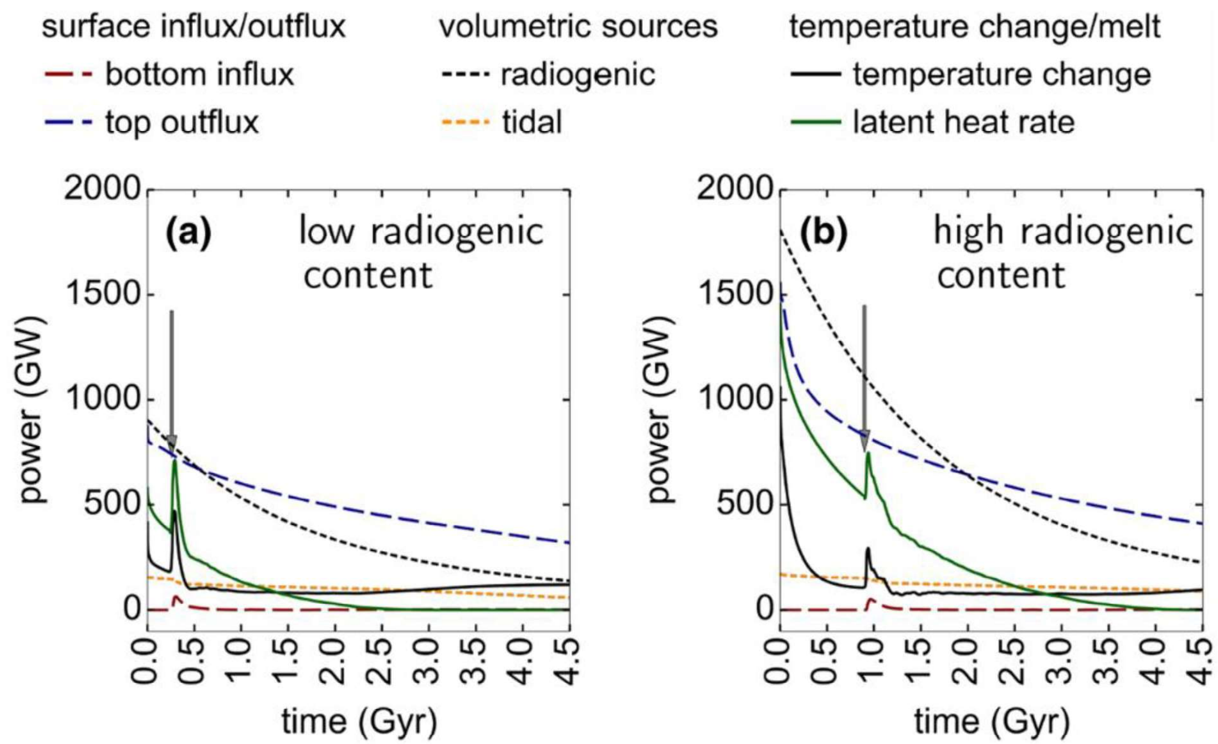

Tidal heating – melting?

Běhounkova+ (2021): magmatism in Europa's mantle

- 3D modelling of heat production by tidal+radiogenic heating
- Model transfer of heat and melting

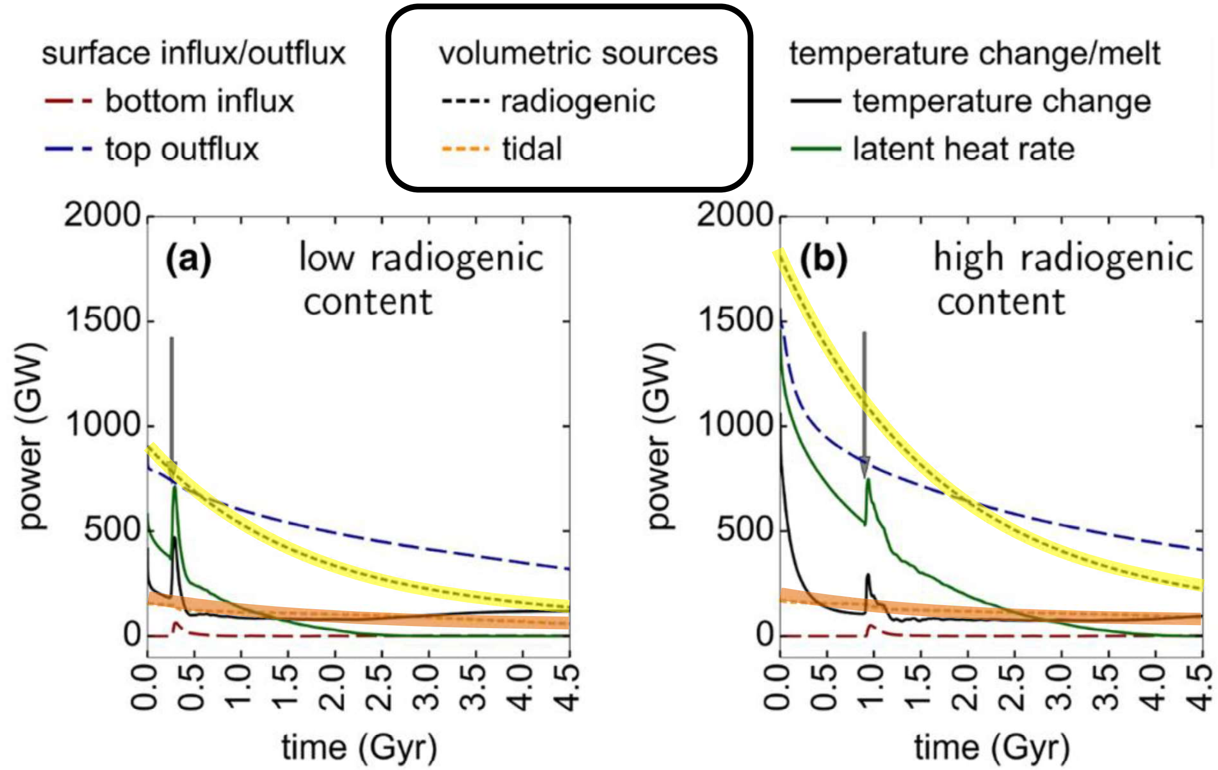

Tidal heating – melting?

Běhounkova+ (2021): magmatism in Europa's mantle

- 3D modelling of heat production by tidal+radiogenic heating
- Model transfer of heat and melting

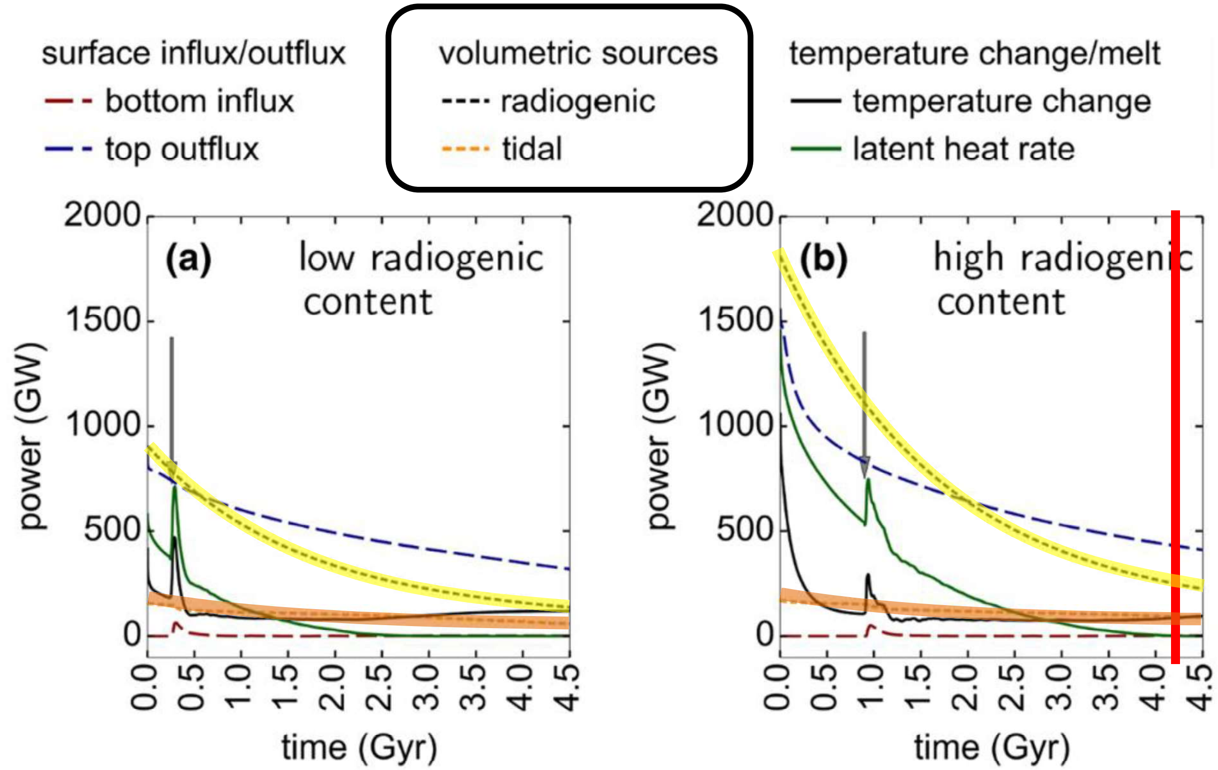

Tidal heating ~ 40% radiogenic heating in present era

Tidal heating – melting?

Běhounkova+ (2021): magmatism in Europa's mantle

- 3D modelling of heat production by tidal+radiogenic heating
- Model transfer of heat and melting

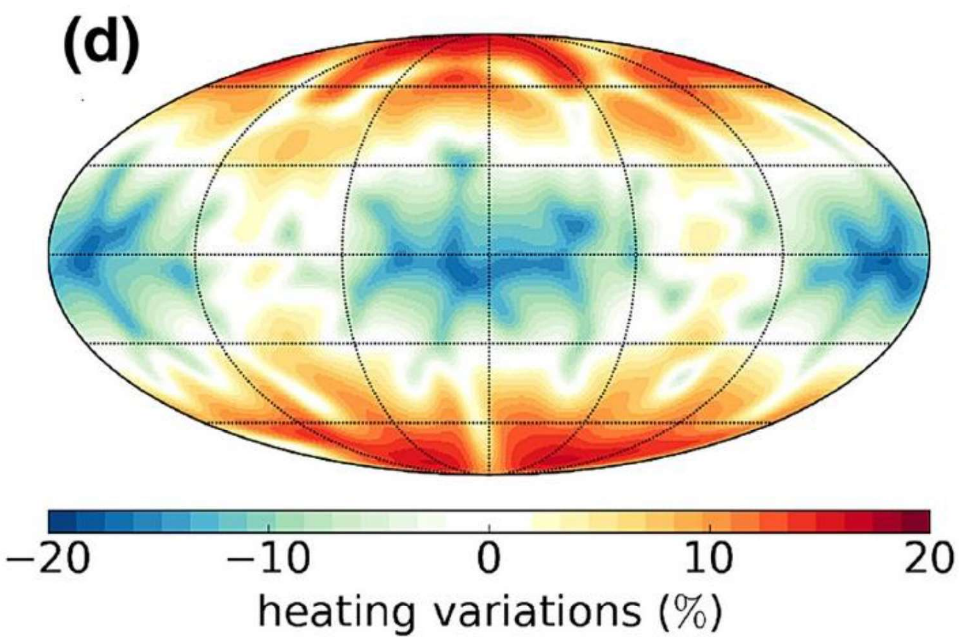

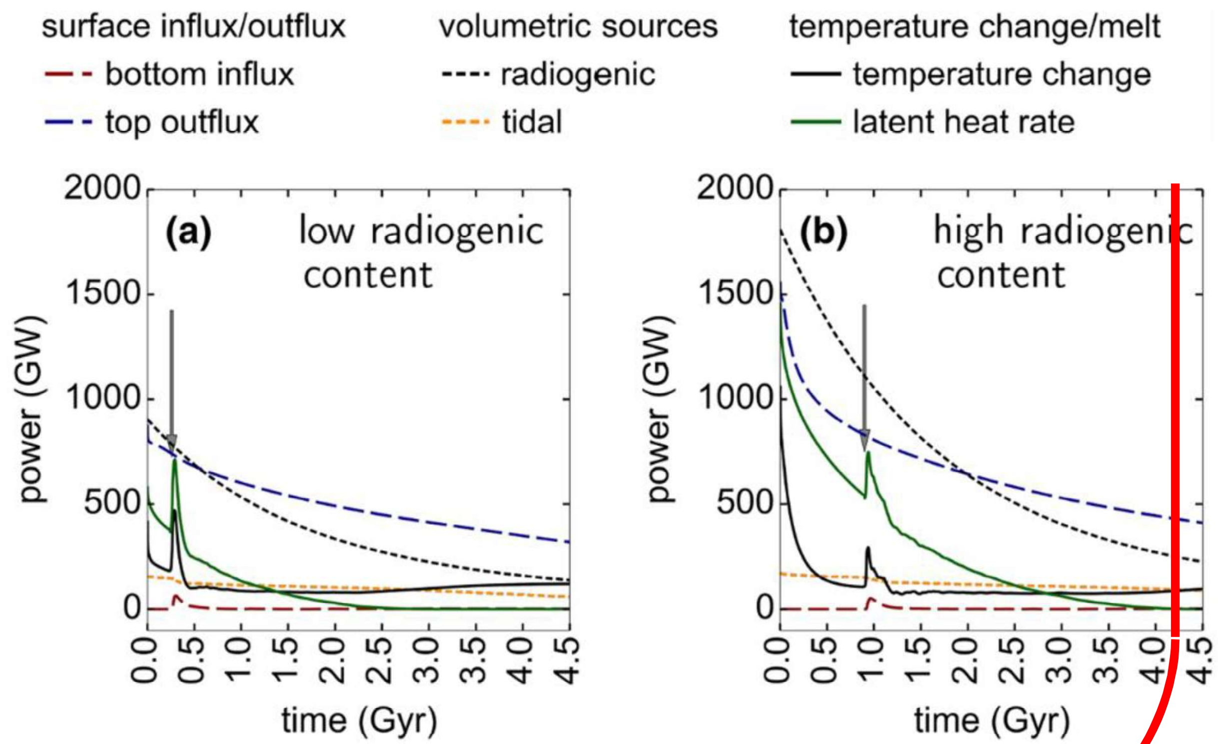

Tidal heating ~ 40% radiogenic heating in present era

Tidal heating – amplitude?

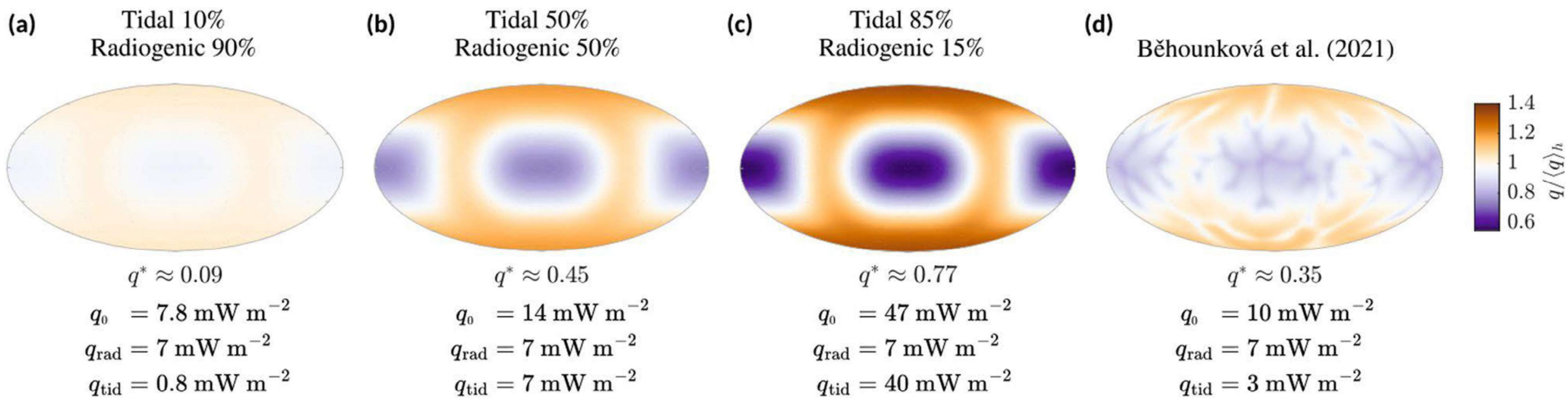

(1) What would be the impact of large-scale heating variations on Europa's ocean circulation?

(2) Can large-scale thermal anomalies from the seafloor be transposed up to the ice-ocean boundary?

(3) Would the resulting oceanic heat flux variations at the top of the ocean affect the ice crust equilibrium?

Previous studies with heterogenous Dirichlet/Neumann BC

Earth's outer core convection [e.g., Sahoo and Sreenivasan 2020, Mound et al., 2019, Davies and Mound 2019, Dietrich et al. 2016, Olson et al. 2015, Gubbins et al, 2011…].

Compositional and thermal heterogeneity in the D"-layer?

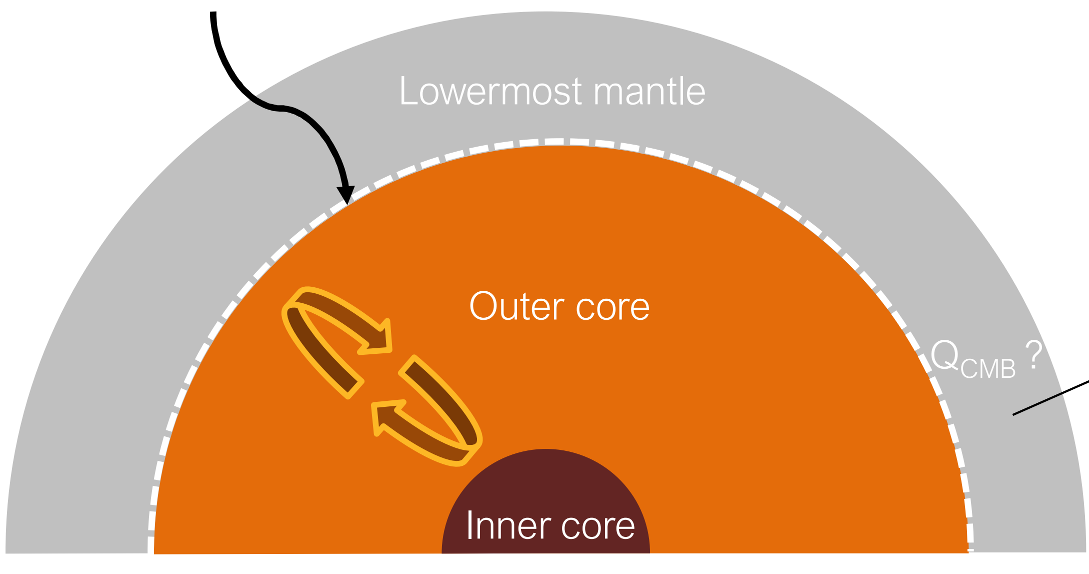

CMB heat flux considered in Mound et al., Nat Geo, 2019

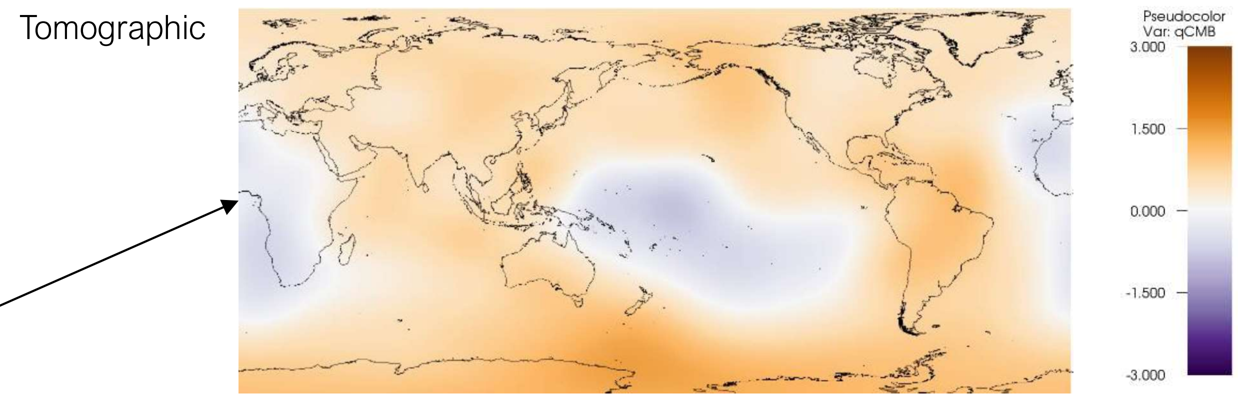

$$q^* = \frac{\Delta q}{q_0} \sim 1 \text{ to } 30!$$

Previous studies with heterogenous Dirichlet/Neumann BC

Dietrich, PEPI, 2016:

- Radial convection + heterogenous hemispherical heat flux

steady *no inertia* *inviscid*

$$\cancel{\frac{\partial \boldsymbol{u}}{\partial t}} + \cancel{\boldsymbol{u}\cdot\nabla\boldsymbol{u}} = -\nabla p - \frac{2}{E}\boldsymbol{e}_z \times \boldsymbol{u} + \frac{Ra_F}{\Pr}\frac{r}{r_o} T \boldsymbol{e}_r + \cancel{\nabla^2 \boldsymbol{u}}$$

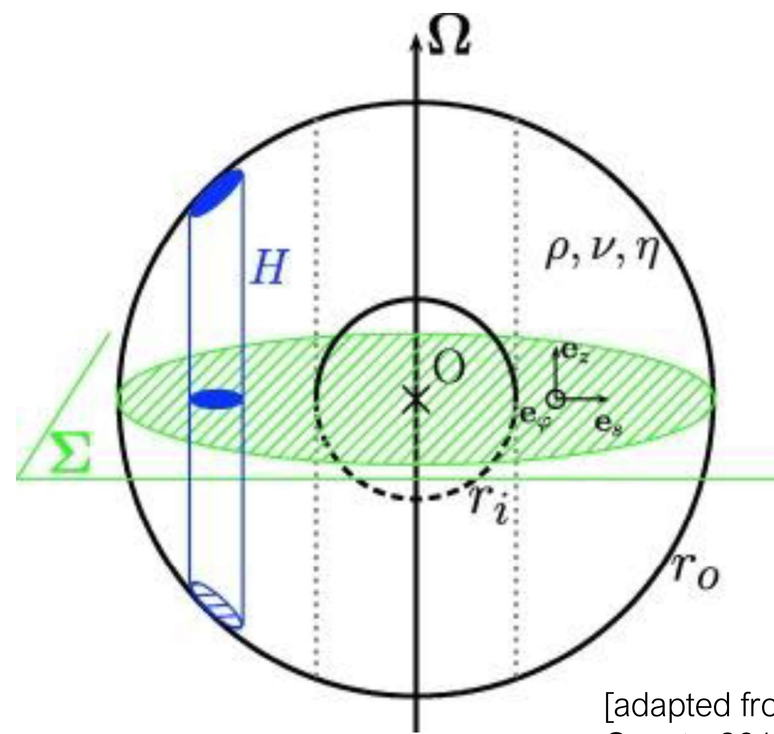

[adapted from Canet+ 2014]

Previous studies with heterogenous Dirichlet/Neumann BC

Dietrich, PEPI, 2016:

- Radial convection + heterogenous hemispherical heat flux

steady *no inertia* *inviscid*

$$\cancel{\frac{\partial \boldsymbol{u}}{\partial t}} + \cancel{\boldsymbol{u}\cdot\nabla\boldsymbol{u}} = -\nabla p - \frac{2}{E}\boldsymbol{e}_z \times \boldsymbol{u} + \frac{Ra_F}{\mathrm{Pr}}\frac{r}{r_o}T\boldsymbol{e}_r + \cancel{\nabla^2\boldsymbol{u}}$$

$\boldsymbol{\nabla} \times (\cdot)$

Vorticity equation

$$-\frac{2}{E}\nabla\times(\boldsymbol{e}_z\times\boldsymbol{u}) + \frac{Ra_F}{\mathrm{Pr}\ r_0}\nabla\times(T\boldsymbol{r}) = 0$$

Coriolis Buoyancy

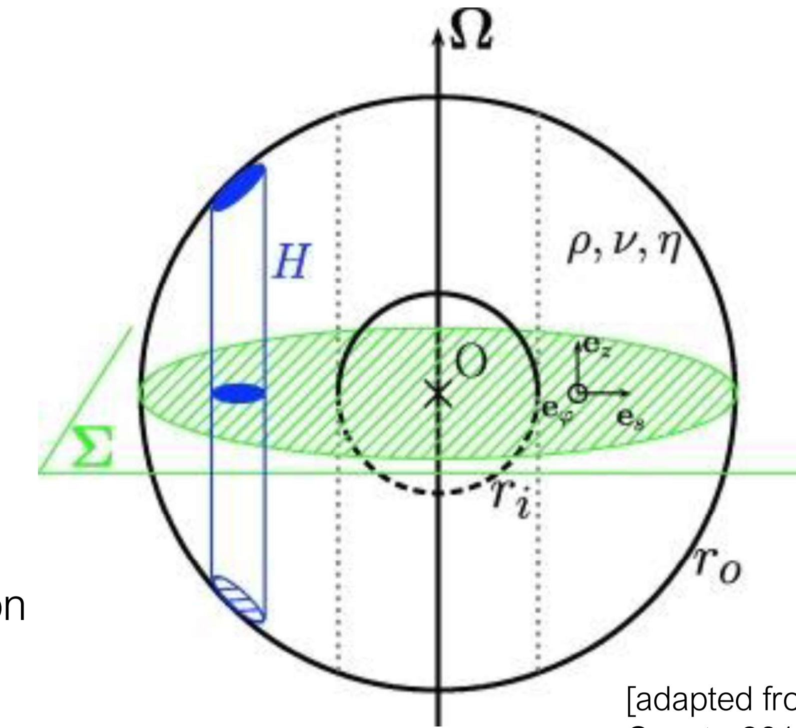

[adapted from Canet+ 2014]

Previous studies with heterogenous Dirichlet/Neumann BC

Dietrich, PEPI, 2016:

- Radial convection + heterogenous hemispherical heat flux

steady *no inertia* *inviscid*

$$\cancel{\frac{\partial \boldsymbol{u}}{\partial t}} + \cancel{\boldsymbol{u}\cdot\nabla\boldsymbol{u}} = -\nabla p - \frac{2}{E}\boldsymbol{e}_z \times \boldsymbol{u} + \frac{Ra_F}{\mathrm{Pr}}\frac{r}{r_o}T\boldsymbol{e}_r + \cancel{\nabla^2\boldsymbol{u}}$$

$\boldsymbol{\nabla} \times (\cdot)$

Vorticity equation

$$-\frac{2}{E}\nabla \times (\boldsymbol{e}_z \times \boldsymbol{u}) + \frac{Ra_F}{\mathrm{Pr}\ \ r_0}\nabla \times (T\boldsymbol{r}) = 0$$

Coriolis Buoyancy

Z-average (geostrophic flow) of z-component

$$\frac{2}{E}\left\langle \frac{\partial u_z}{\partial z} \right\rangle_z + \frac{Ra_F}{\mathrm{Pr}\ \ r_0}\langle \boldsymbol{e}_z \cdot (\nabla \times (T\boldsymbol{r}))\rangle_z = 0$$

$$\langle \cdot \rangle_z = \frac{1}{2H}\int_{-H}^{+H} \cdot \, \mathrm{d}z$$

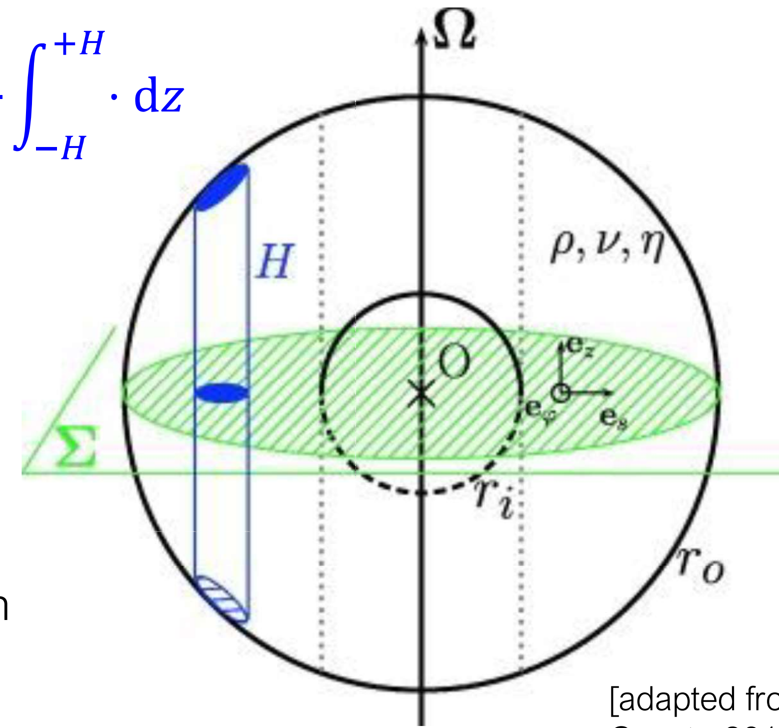

[adapted from Canet+ 2014]

Previous studies with heterogenous Dirichlet/Neumann BC

Dietrich, PEPI, 2016:

- Radial convection + heterogenous hemispherical heat flux

steady *no inertia* *inviscid*

$$\cancel{\frac{\partial \boldsymbol{u}}{\partial t}} + \cancel{\boldsymbol{u}\cdot\nabla\boldsymbol{u}} = -\nabla p - \frac{2}{E}\boldsymbol{e}_z \times \boldsymbol{u} + \frac{Ra_F}{\mathrm{Pr}}\frac{r}{r_o}T\boldsymbol{e}_r + \cancel{\nabla^2\boldsymbol{u}}$$

$\boldsymbol{\nabla}\times(\cdot)$

Vorticity equation

$$-\frac{2}{E}\nabla\times(\boldsymbol{e}_z\times\boldsymbol{u}) + \frac{Ra_F}{\mathrm{Pr}\ \ r_0}\nabla\times(T\boldsymbol{r}) = 0$$

Coriolis Buoyancy

Z-average (geostrophic flow) of z-component

$$\frac{2}{E}\left\langle\frac{\partial u_z}{\partial z}\right\rangle_z + \frac{Ra_F}{\mathrm{Pr}\ \ r_0}\langle\boldsymbol{e}_z\cdot(\nabla\times(T\boldsymbol{r}))\rangle_z = 0$$

Non-penetration of sloping boundaries:

$$\left\langle\frac{\partial u_z}{\partial z}\right\rangle_z = \frac{1}{2H}(u_z(H) - u_z(-H)) = -\langle u_s\rangle_z\frac{s}{H^2}$$

$$\boxed{\langle u_s\rangle_z = -\frac{Ra_F E}{\mathrm{Pr}}\left(\frac{r_o^2 - s^2}{2r_0 s}\right)\left\langle\frac{\partial T}{\partial\phi}\right\rangle_z}$$

$$\langle\cdot\rangle_z = \frac{1}{2H}\int_{-H}^{+H}\cdot\,\mathrm{d}z$$

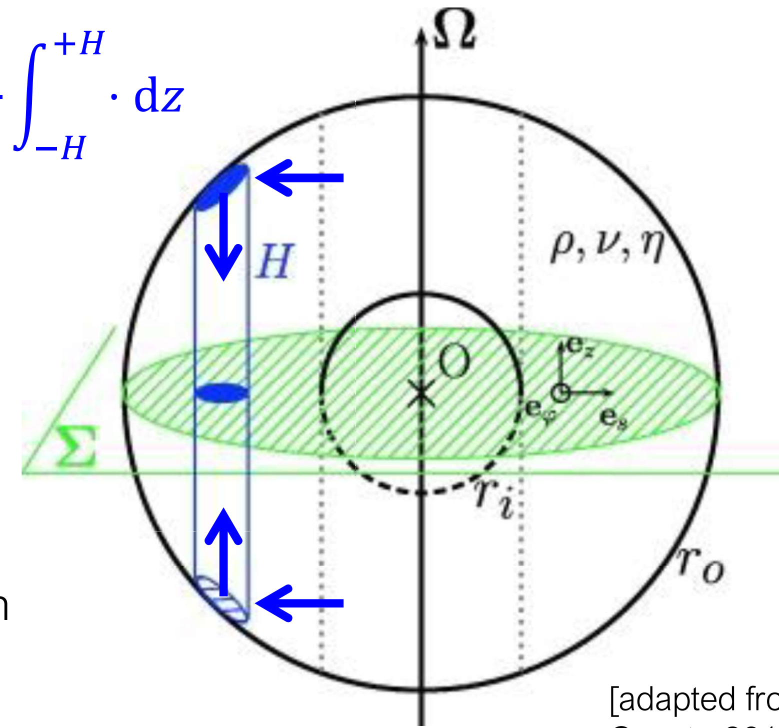

[adapted from Canet+ 2014]

Previous studies with heterogenous Dirichlet/Neumann BC

Dietrich, PEPI, 2016:

- Radial convection + heterogenous hemispherical heat flux

steady *no inertia* *inviscid*

$$\cancel{\frac{\partial \boldsymbol{u}}{\partial t}} + \cancel{\boldsymbol{u} \cdot \nabla \boldsymbol{u}} = -\nabla p - \frac{2}{E}\boldsymbol{e}_z \times \boldsymbol{u} + \frac{Ra_F}{\Pr}\frac{r}{r_o} T \boldsymbol{e}_r + \cancel{\nabla^2 \boldsymbol{u}}$$

$$-\frac{2}{E}\underbrace{\nabla \times (\boldsymbol{e}_z \times \boldsymbol{u})}_{\text{Coriolis}} + \underbrace{\frac{Ra_F}{\Pr\ r_0}\nabla \times (T\boldsymbol{r})}_{\text{Buoyancy}} = 0$$

$$\frac{2}{E}\left\langle \frac{\partial u_z}{\partial z} \right\rangle_z + \frac{Ra_F}{\Pr\ r_0}\langle \boldsymbol{e}_z \cdot (\nabla \times (T\boldsymbol{r}))\rangle_z = 0$$

$$\boxed{\langle u_s \rangle_z = -\frac{Ra_F E}{\Pr}\left(\frac{r_o^2 - s^2}{2 r_0 s}\right)\left\langle \frac{\partial T}{\partial \phi} \right\rangle_z}$$

Equatorial upwelling/downwelling where the boundary temperature <u>gradient</u> is the largest.

Previous studies with heterogenous Dirichlet/Neumann BC

Dietrich, PEPI, 2016:

- Radial convection + heterogenous hemispherical heat flux
- Max q*=2 (i.e. q small=0, q large= 2 q_0)
- From conductive to advective to largely super-critical

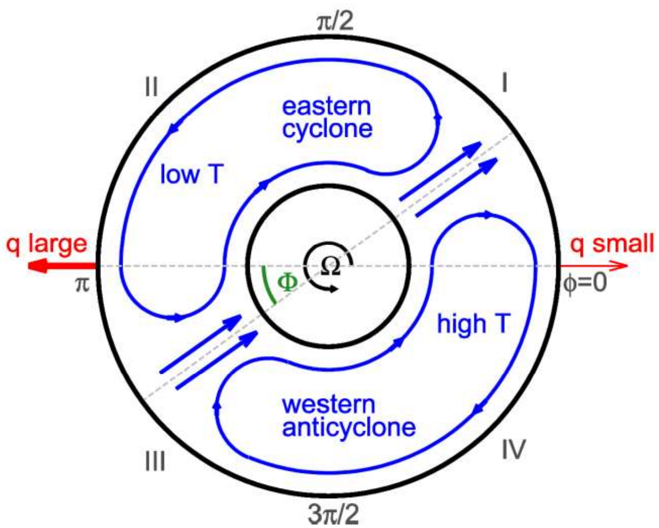

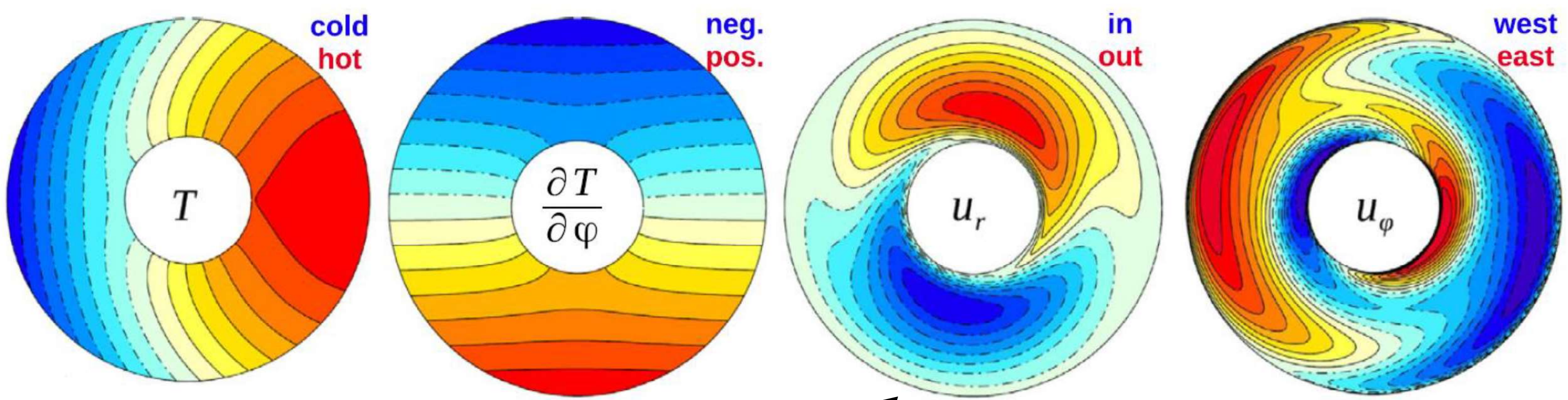

$$\langle u_s \rangle_z = -\frac{Ra_F\, E}{\Pr}\left(\frac{r_o^2 - s^2}{2r_0 s}\right)\left\langle \frac{\partial T}{\partial \phi} \right\rangle_z$$

Equatorial upwelling/downwelling where the boundary temperature <u>gradient</u> is the largest.

Previous studies with heterogenous Dirichlet/Neumann BC

Dietrich, PEPI, 2016:

- Radial convection + heterogenous hemispherical heat flux
- Max q*=2 (i.e. q small=0, q large= 2 q_0)
- From conductive to advective to largely super-critical

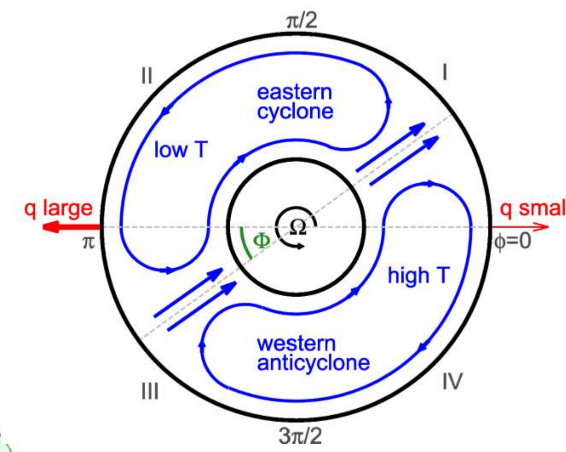

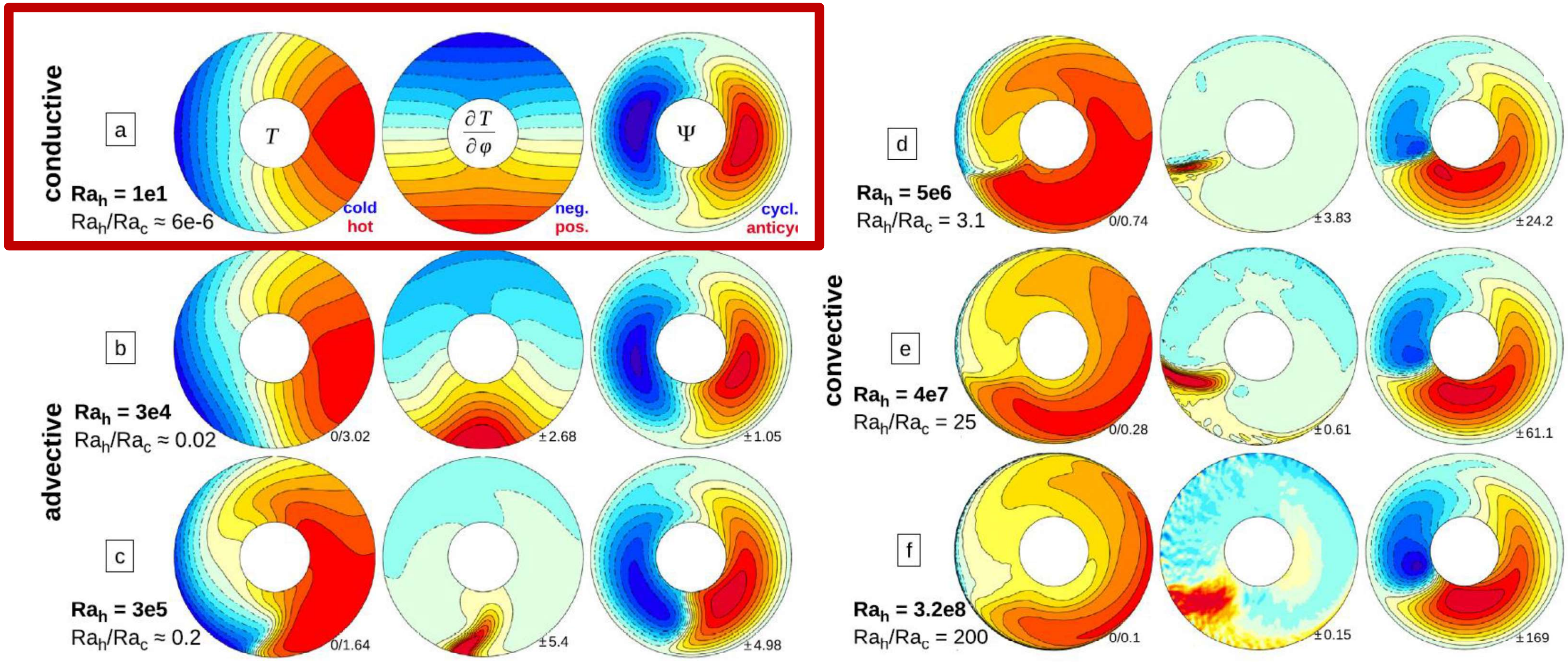

$$u_s = \frac{1}{s}\frac{\partial \Psi}{\partial \phi}$$

$$u_\phi = -\frac{\partial \Psi}{\partial s}$$

Previous studies with heterogenous Dirichlet/Neumann BC

Dietrich, PEPI, 2016:

- Radial convection + heterogenous hemispherical heat flux
- Max q*=2 (i.e. q small=0, q large= 2 q_0)
- From conductive to advective to largely super-critical

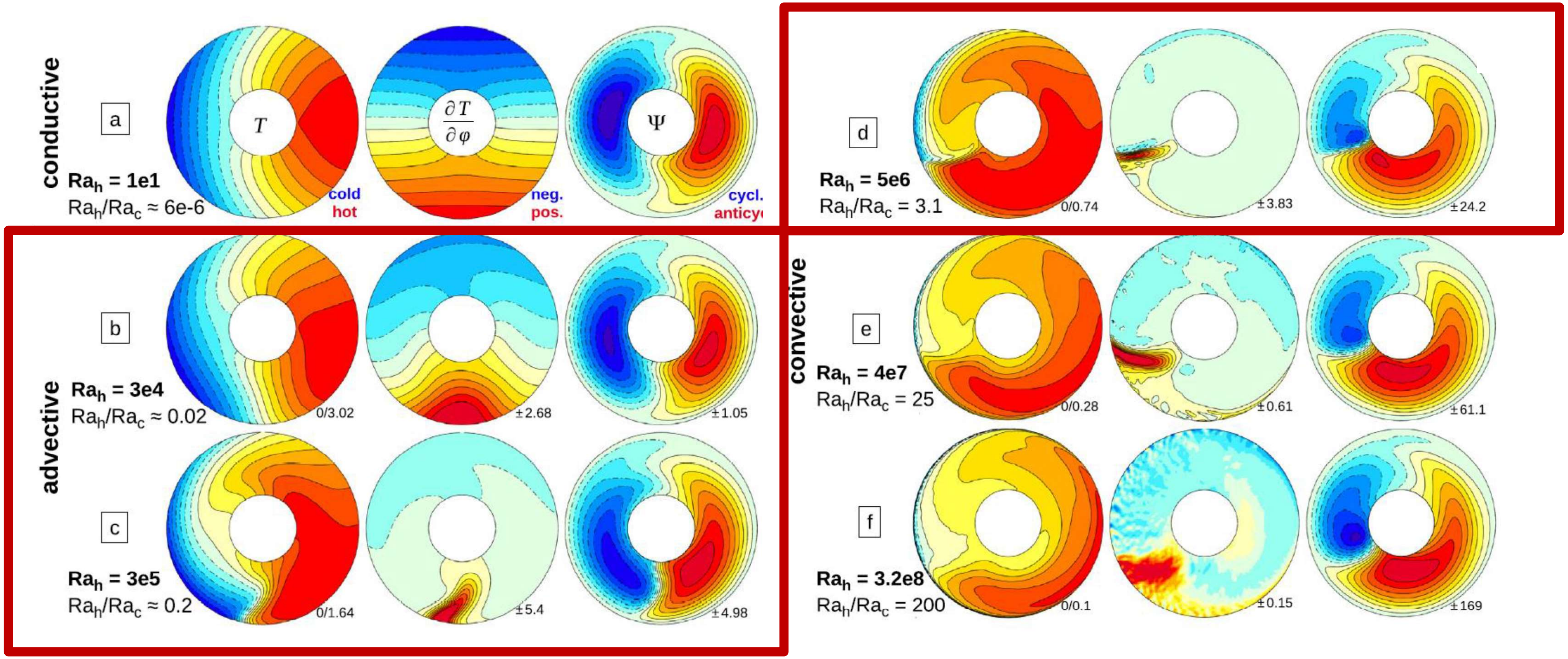

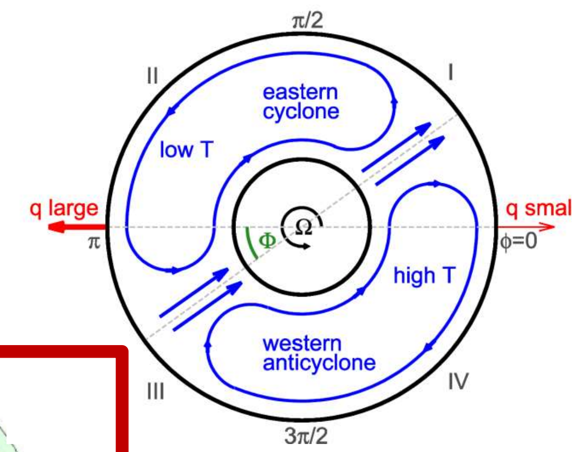

$$u_s = \frac{1}{s}\frac{\partial \Psi}{\partial \phi}$$

$$u_\phi = -\frac{\partial \Psi}{\partial s}$$

Previous studies with heterogenous Dirichlet/Neumann BC

Dietrich, PEPI, 2016:

- Radial convection + heterogenous hemispherical heat flux
- Max q*=2 (i.e. q small=0, q large= 2 q_0)
- From conductive to advective to largely super-critical

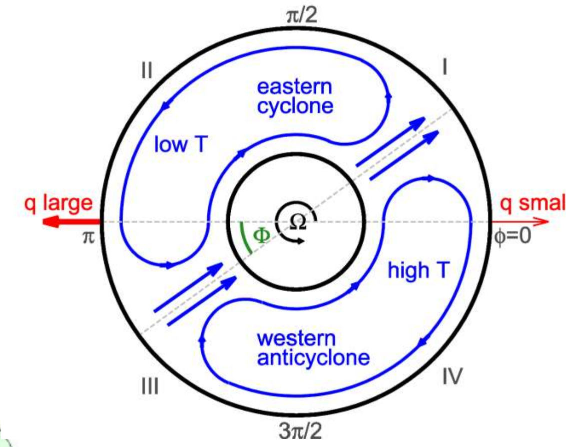

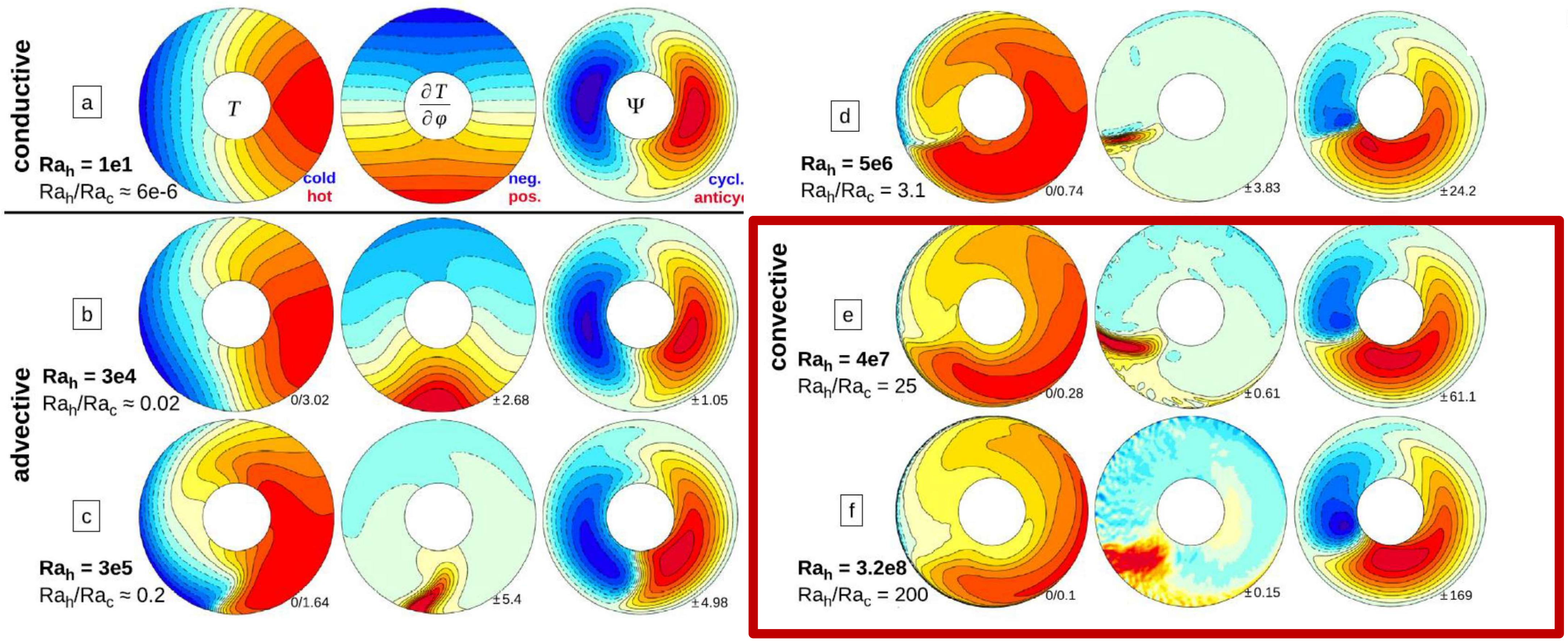

$$u_s = \frac{1}{s}\frac{\partial \Psi}{\partial \phi}$$

$$u_\phi = -\frac{\partial \Psi}{\partial s}$$

Previous studies with heterogenous Dirichlet/Neumann BC

Davies and Mound, GJI, 2019

- Systematic study with $10^{-4} \geq E \geq 10^{-6}$ and 1 < Ra/Rac < 800
- q* = 0, 2.3 and 5
- Hemispherical and tomographic patterns

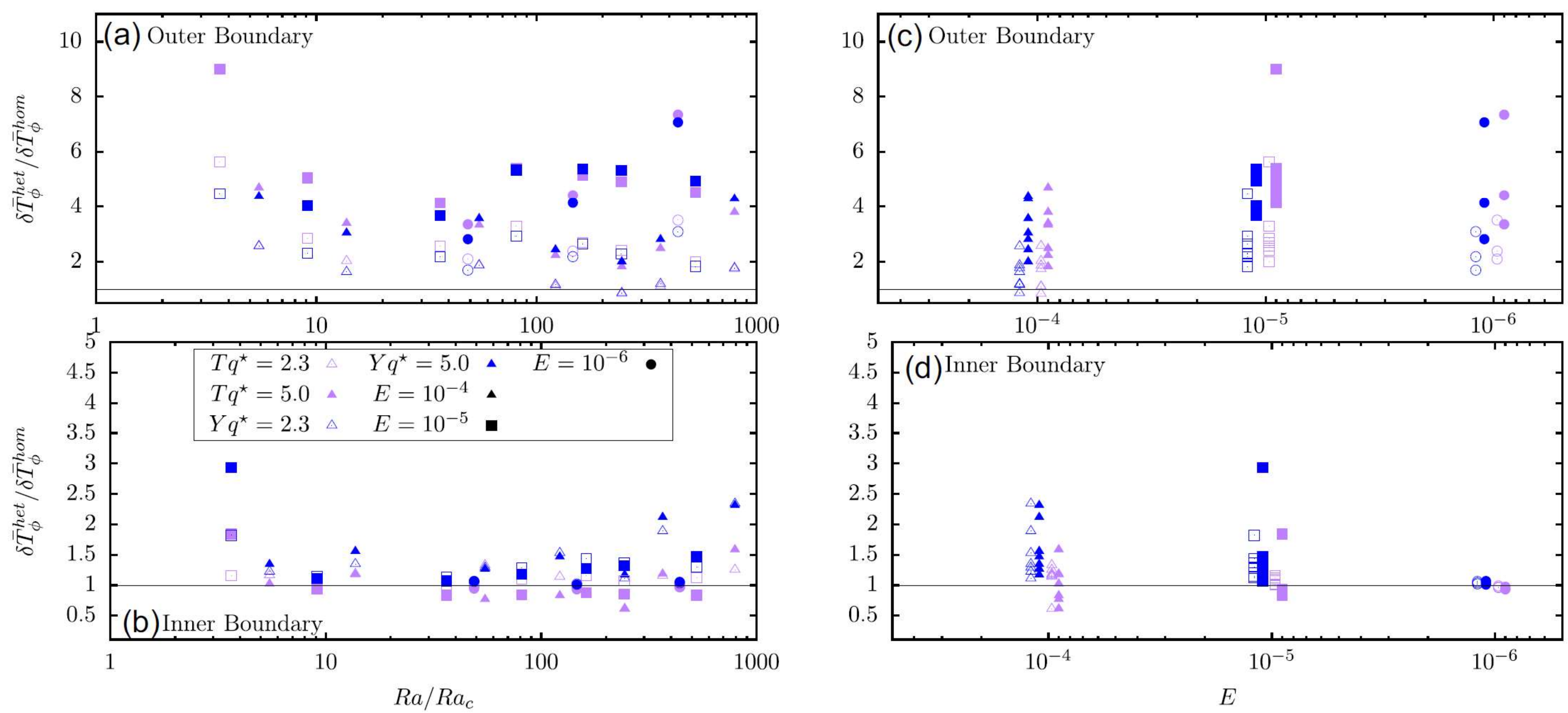

Previous studies with heterogenous Dirichlet/Neumann BC

Sumita and Olson [Science 1999, JGR Solid Earth 2002]

- Rapidly-rotating hemispherical shell
- Perturbed outer boundary heat flux with a **local** anomalous heat flux
- $E = 2.4 \times 10^{-6}, \frac{Ra_T}{Ra_c} \leq 62$ (strongly nonlinear), $\frac{q_{max}}{q_{ave}} \leq 95$

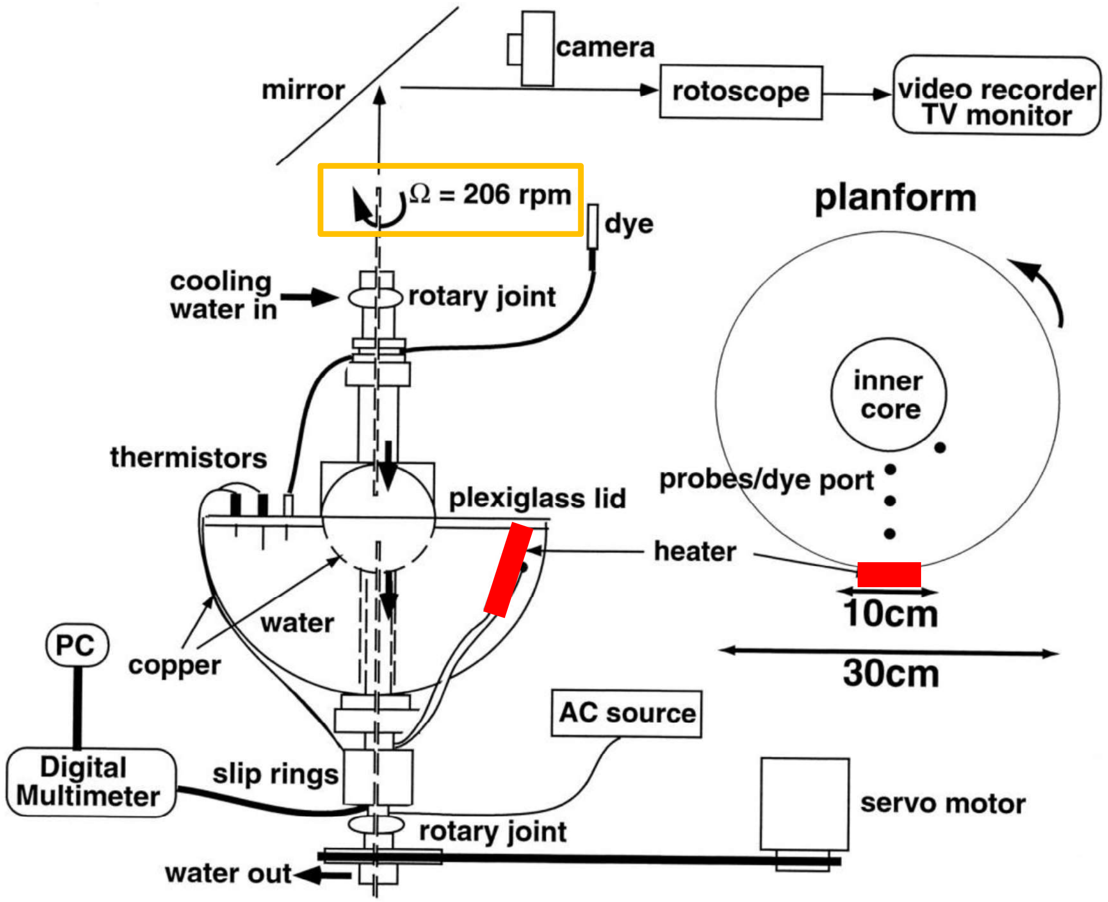

Previous studies with heterogenous Dirichlet/Neumann BC

Sumita and Olson [Science 1999, JGR Solid Earth 2002]
- Rapidly-rotating hemispherical shell
- Perturbed outer boundary heat flux with a **local** anomalous heat flux
- $E = 2.4 \times 10^{-6}, \frac{Ra_T}{Ra_c} \leq 62$ (strongly nonlinear), $\frac{q_{max}}{q_{ave}} \leq 95$

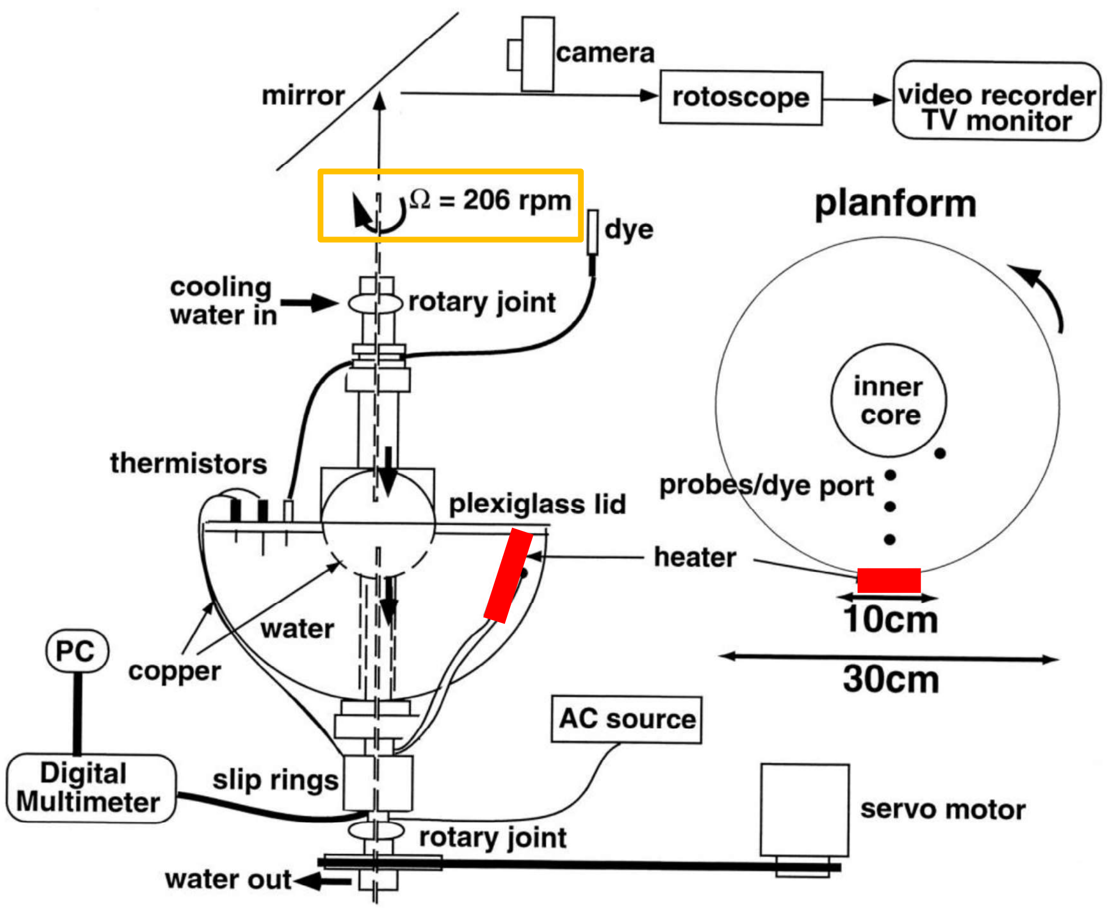

➔ Radial inflow deformed into a spiralling jet structure

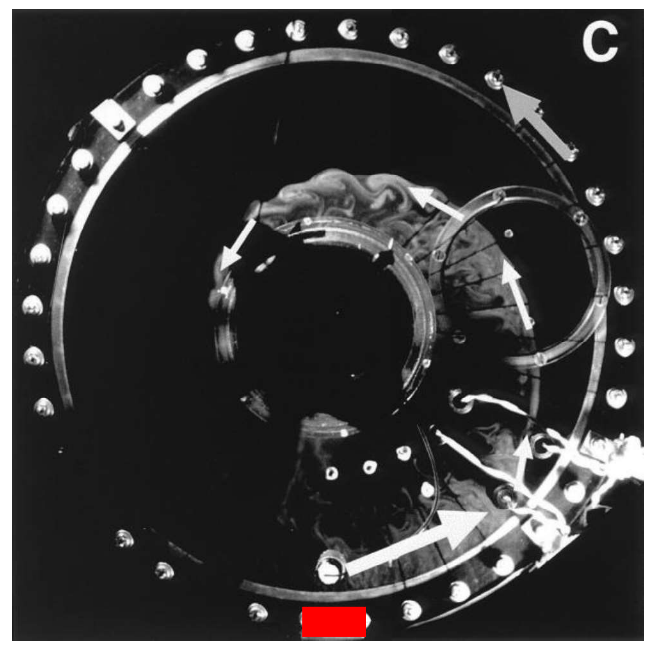

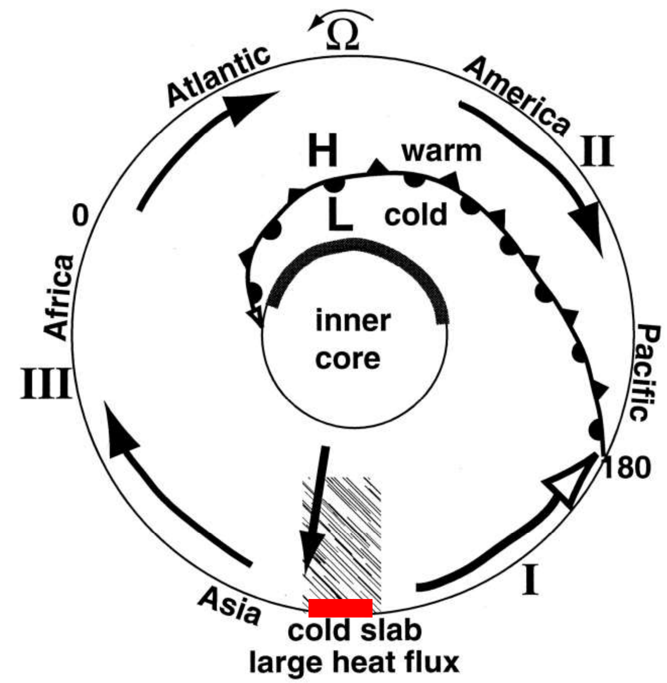

Previous studies with heterogenous Dirichlet/Neumann BC

Sumita and Olson [Science 1999, JGR Solid Earth 2002]

- Rapidly-rotating hemispherical shell
- Perturbed outer boundary heat flux with a **local** anomalous heat flux
- $E = 2.4 \times 10^{-6}, \frac{Ra_T}{Ra_c} \leq 62$ (strongly nonlinear), $\frac{q_{max}}{q_{ave}} \leq 95$

[Dietrich+ PEPI, 2016]

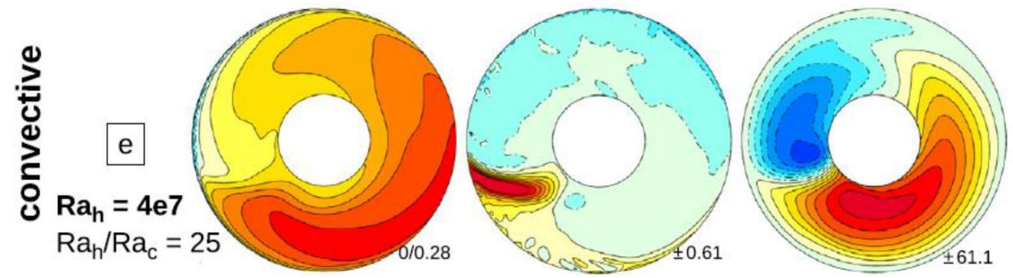

➔ Radial inflow deformed into a spiralling jet structure

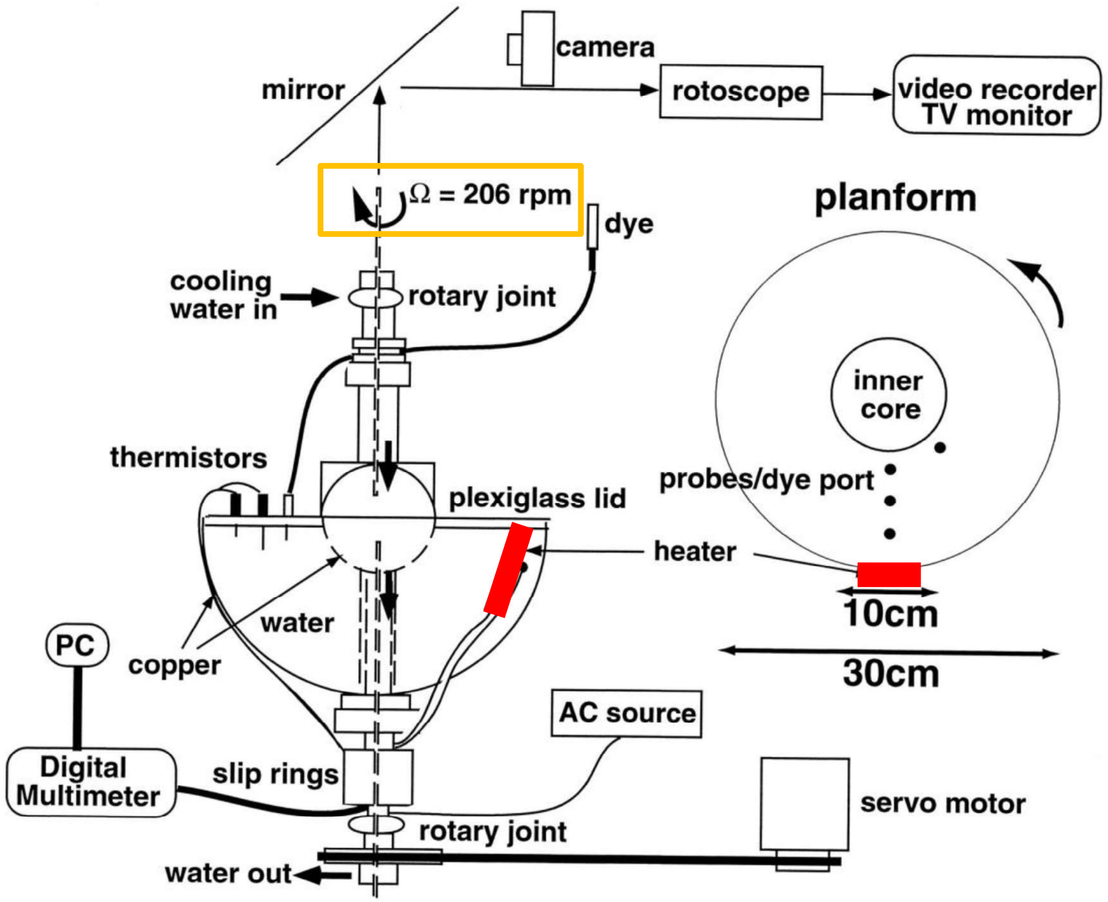

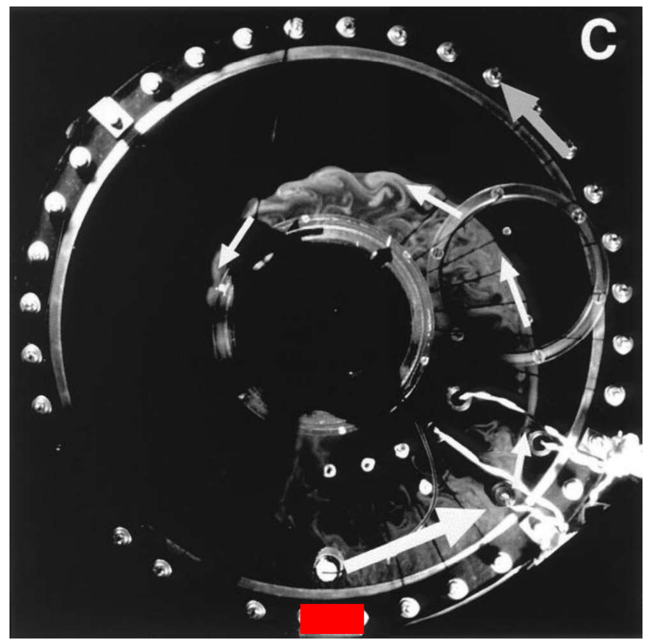

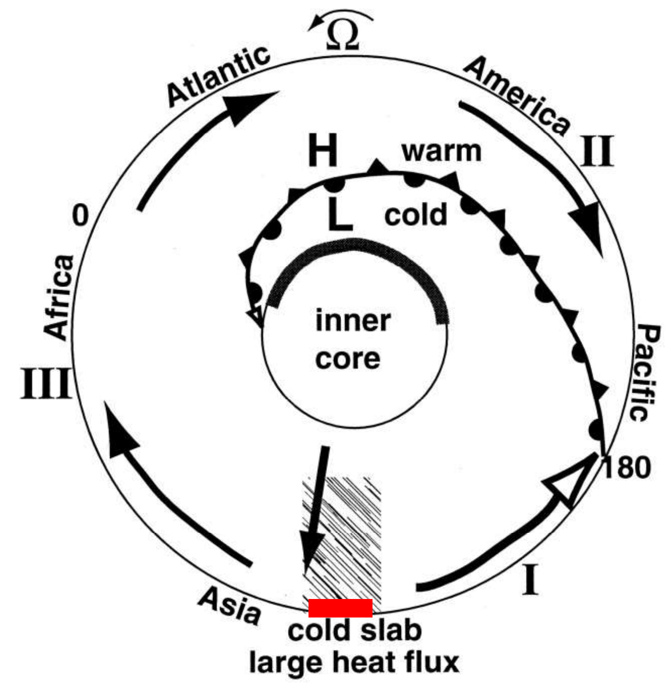

Previous studies with heterogenous Dirichlet/Neumann BC

Sahoo and Sreenivasan, JFM, 2019

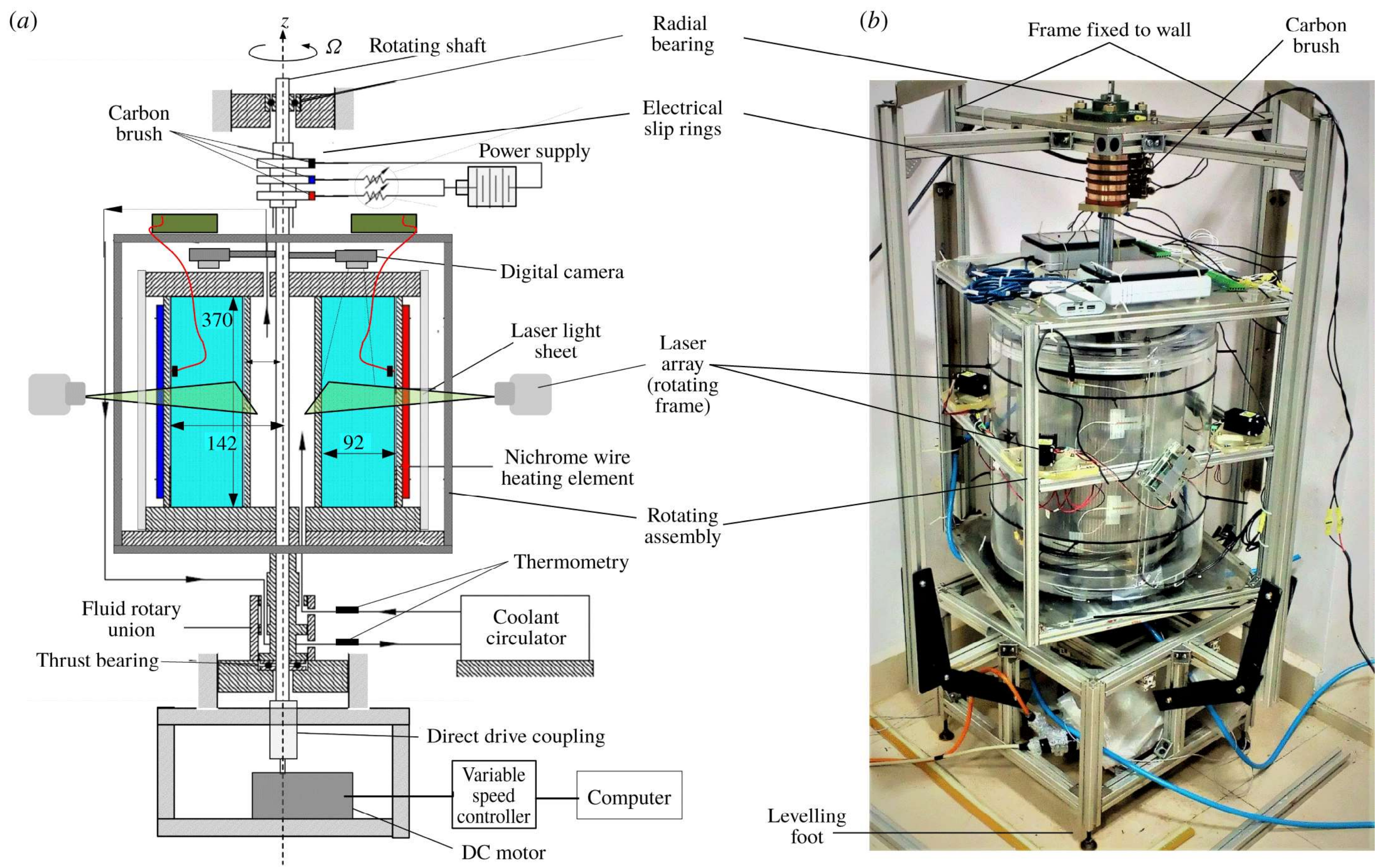

$\mathrm{E} = 1.8 \times 10^{-6}$ (300 rpm)

$\mathrm{Ra} = 0$ to $30\,Ra_c$

- From below onset of convection to super-critical states
- Heat flux heterogeneity q* in the range 0–2
- Inner cylinder maintained at 22 degC
- Heating on the sides via Nichrome wire heating element
- PIV visualisation

Previous studies with heterogenous Dirichlet/Neumann BC

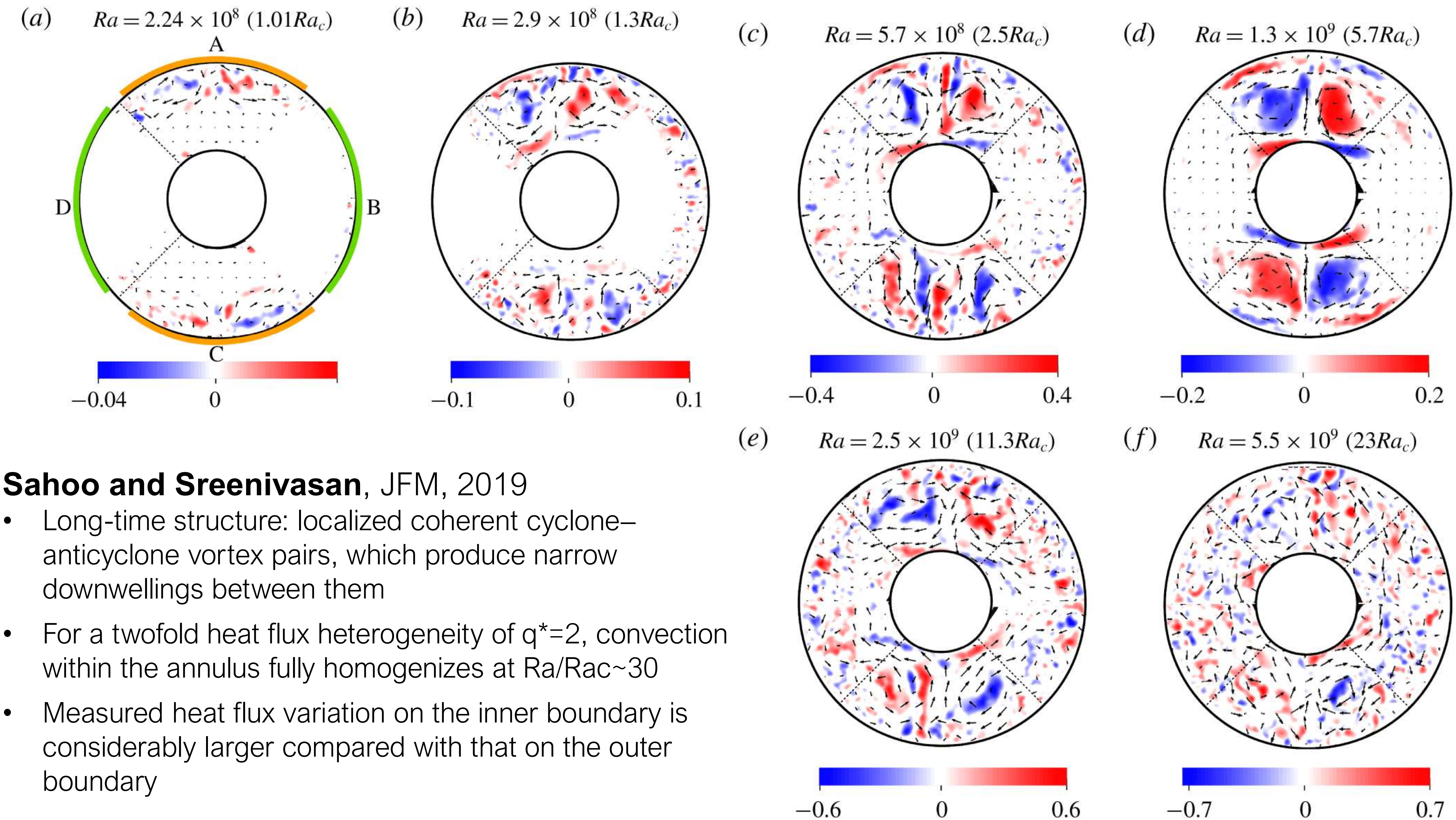

Sahoo and Sreenivasan, JFM, 2019

- Long-time structure: localized coherent cyclone–anticyclone vortex pairs, which produce narrow downwellings between them
- For a twofold heat flux heterogeneity of q*=2, convection within the annulus fully homogenizes at Ra/Rac~30
- Measured heat flux variation on the inner boundary is considerably larger compared with that on the outer boundary

Previous studies with heterogenous Dirichlet/Neumann BC

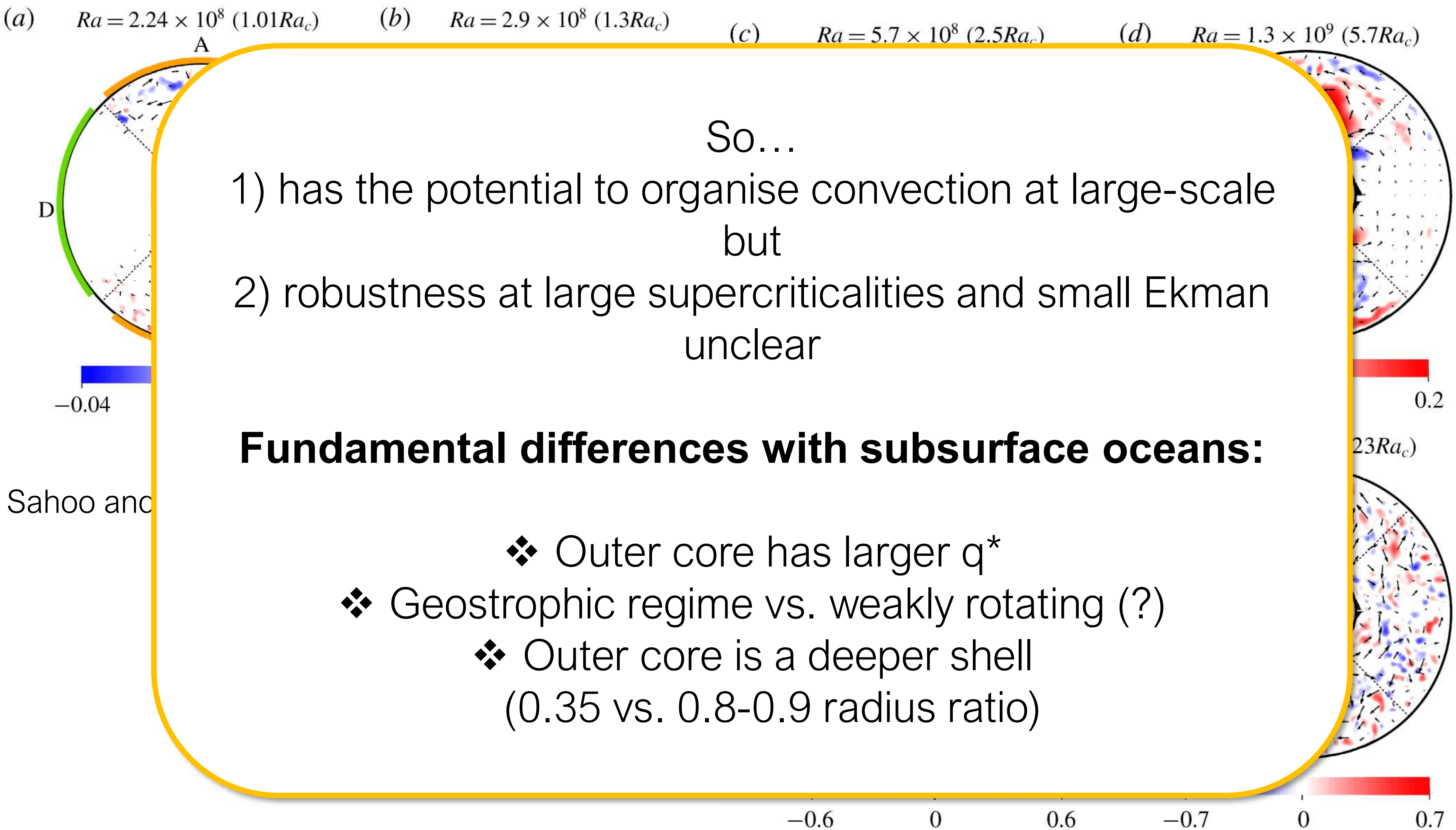

Sahoo and

So…
1) has the potential to organise convection at large-scale
but
2) robustness at large supercriticalities and small Ekman
unclear

Fundamental differences with subsurface oceans:

❖ Outer core has larger q*
❖ Geostrophic regime vs. weakly rotating (?)
❖ Outer core is a deeper shell
(0.35 vs. 0.8-0.9 radius ratio)

Previous studies with heterogenous Dirichlet/Neumann BC

Terra-Nova+ 2023: heating pattern from the high-pressure ice layer above the seafloor
(Titan, Ganymede)

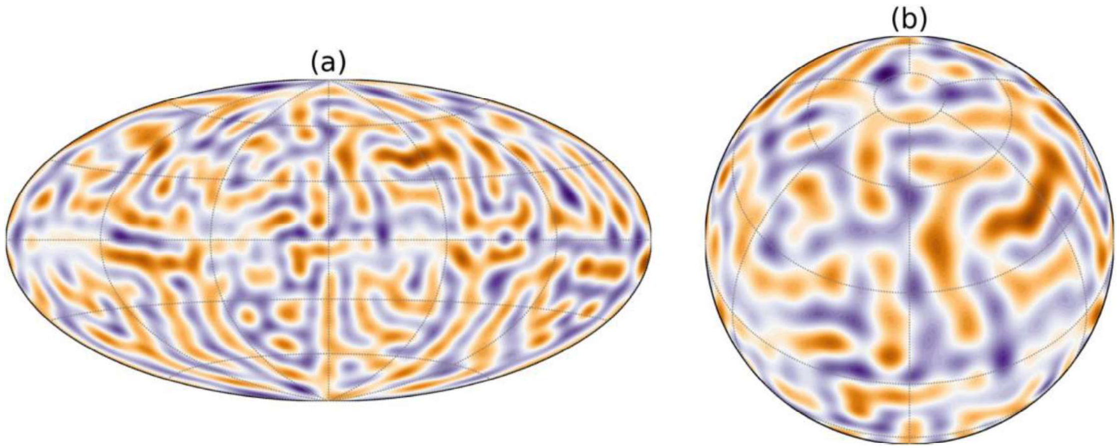

Imposed pattern of inner boundary heat flux taken from the output of a high-pressure ice convection simulation applied to Titan's mantle [Choblet+, 2017]

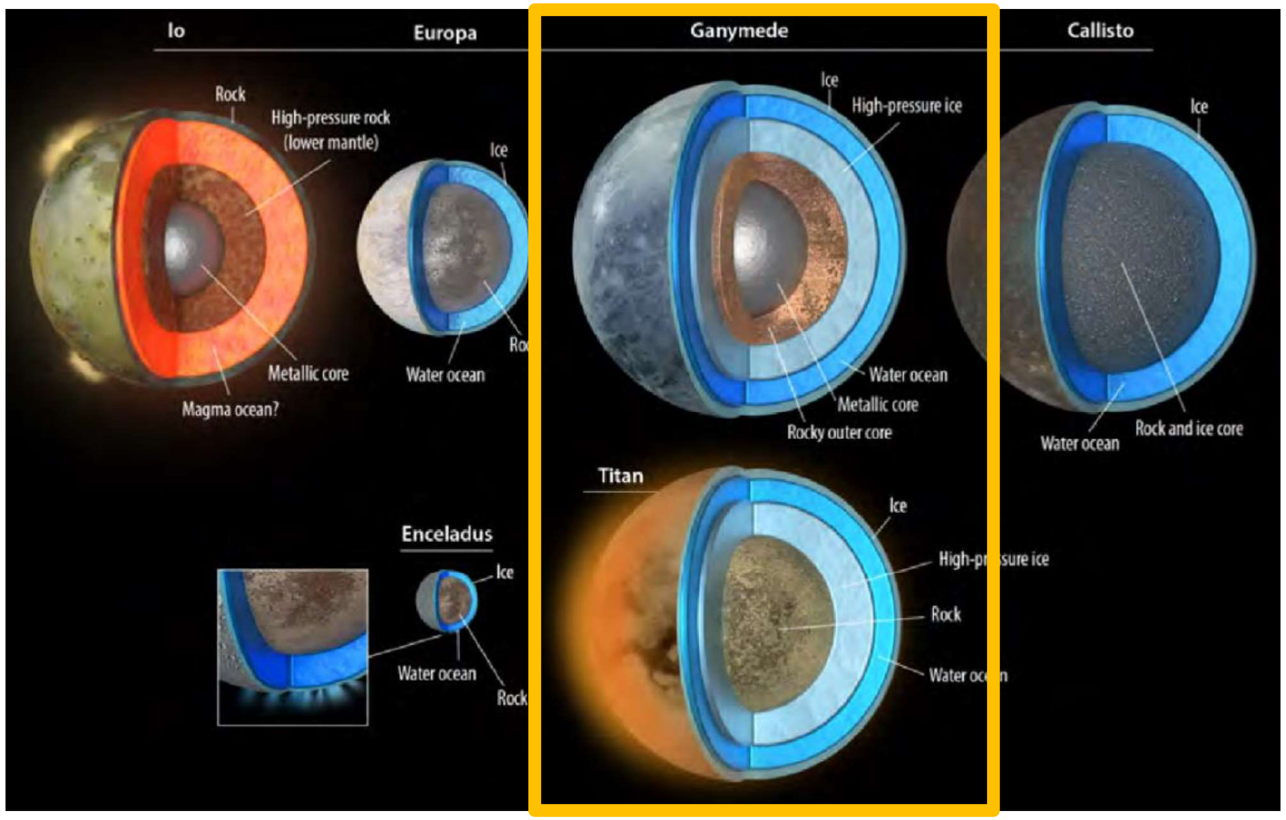

Key points:
- High correlation between persistent longitudes of inner/outer boundary heat fluxes.
- Bottom to top large-scale pattern amplification by the convection in the thin shell (order 2 pattern)
- Does not change equatorial vs polar cooling

Previous studies with heterogenous Dirichlet/Neumann BC

Enceladus: small-scale pattern as well due to convection in porous rocky core [Choblet+ 2017]

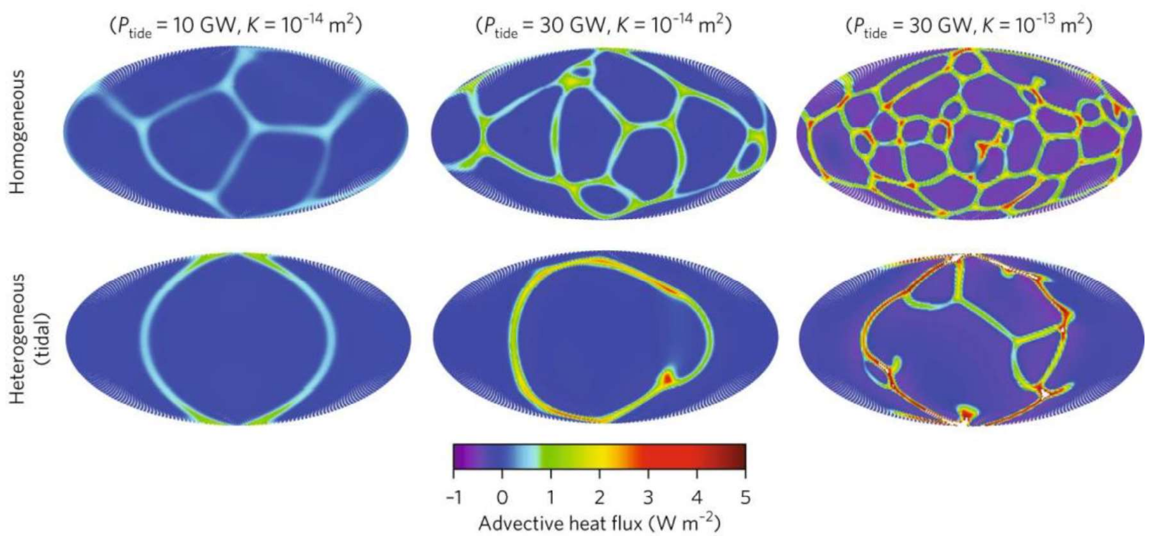

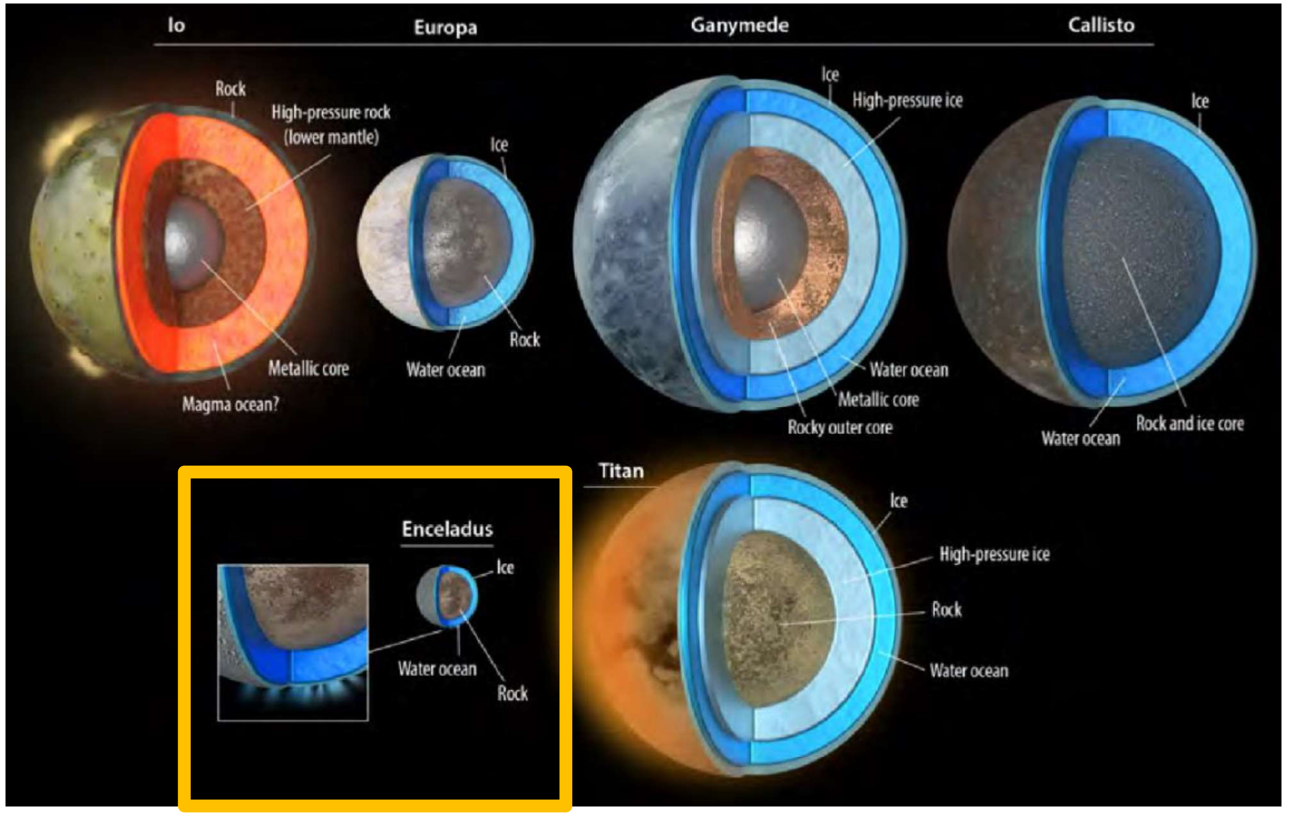

Previous studies with heterogenous Dirichlet/Neumann BC

Europa: conclusions likely different for a large-scale pattern

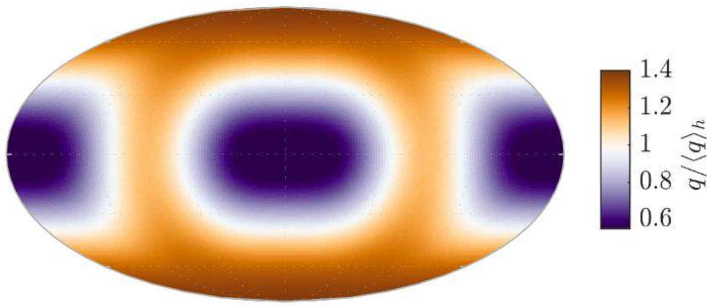

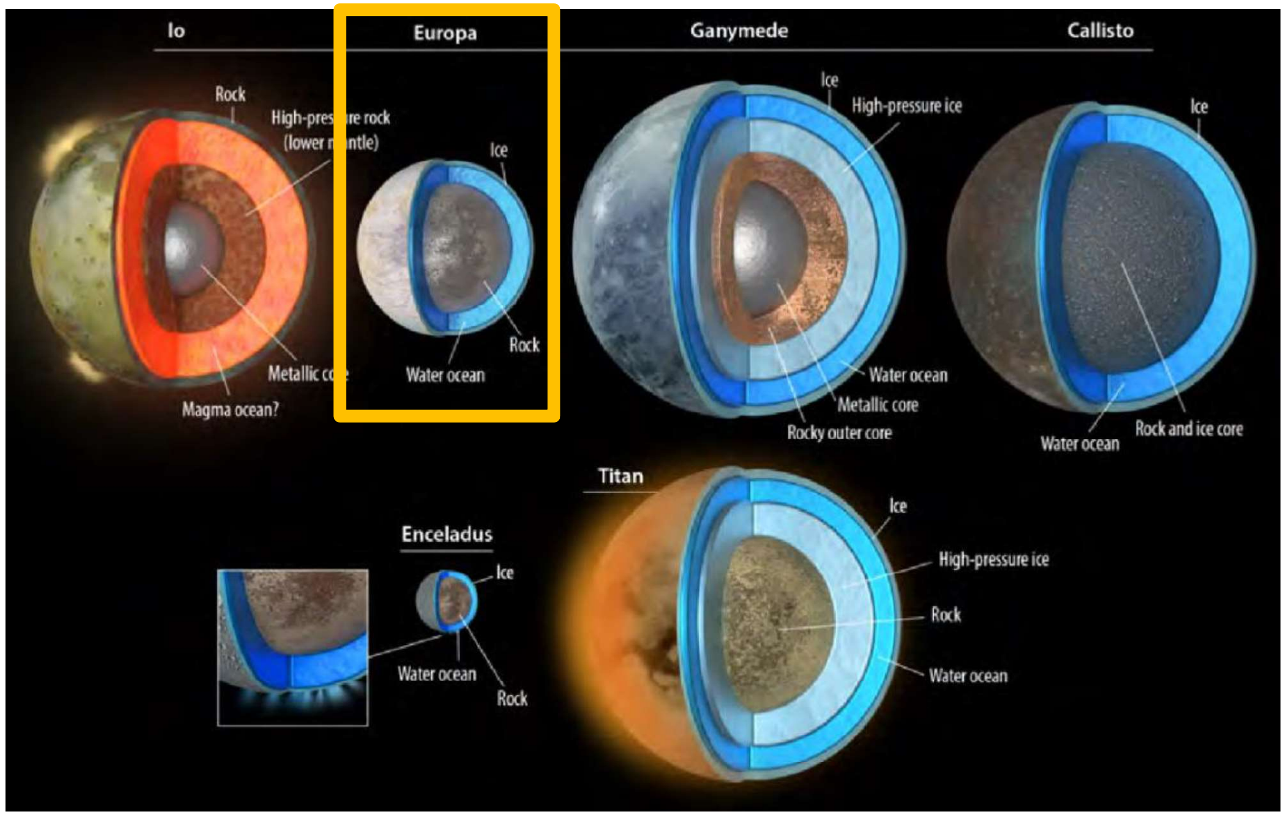

Global numerical model

Model: Rotating thermal convection in a spherical shell (open-source code **MagIC** [Wicht 2002, Gastine 2016])

Approximations/simplifications:
- Buoyancy-driven flow (no ocean tides, no libration)
- Salinity effect on buoyancy ignored
- Ice/ocean boundary = fixed T (no phase change)

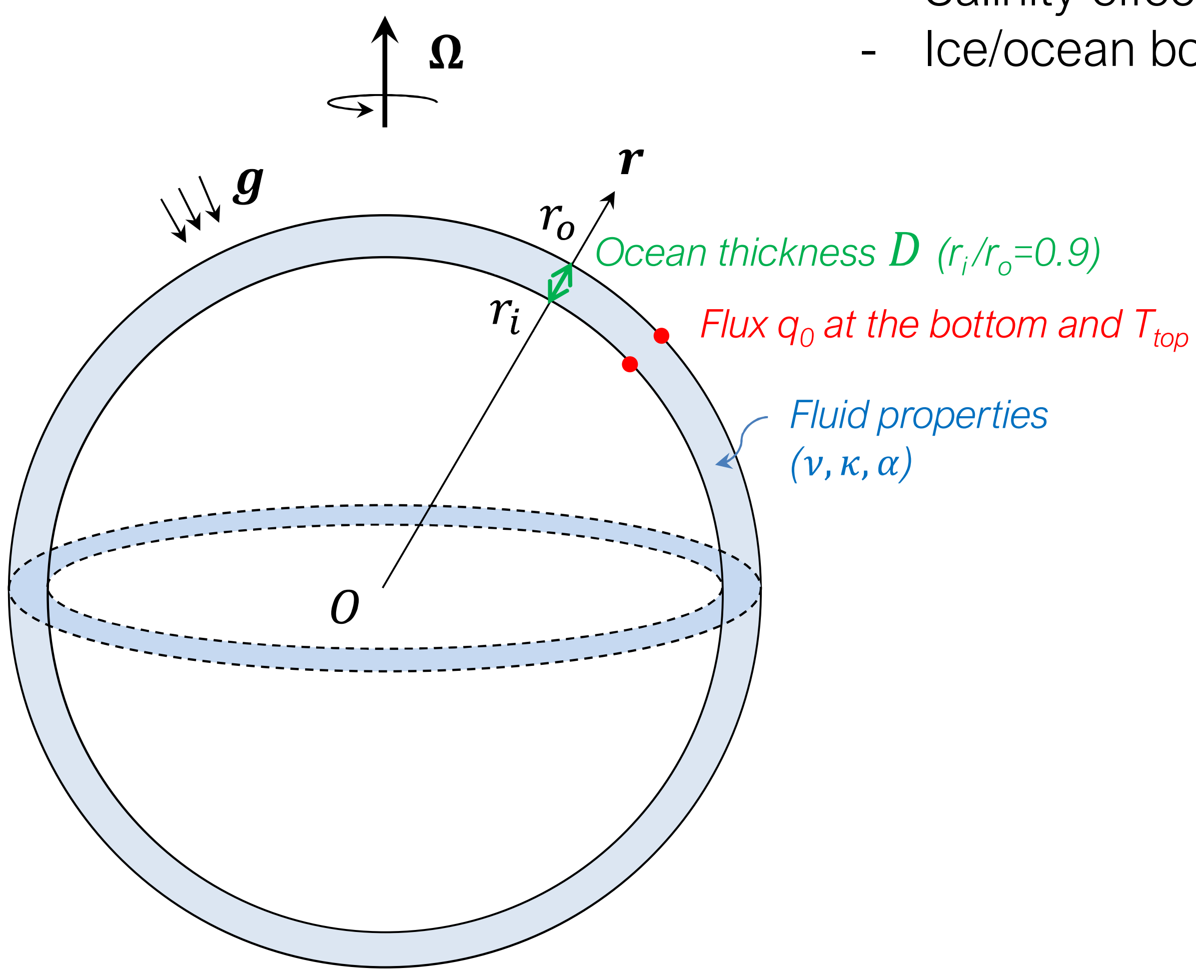

Global numerical model

Model: Rotating thermal convection in a spherical shell (open-source code **MagIC** [Wicht 2002, Gastine 2016])

Approximations/simplifications:
- Buoyancy-driven flow (no ocean tides, no libration)
- Salinity effect on buoyancy ignored
- Ice/ocean boundary = fixed T (no phase change)

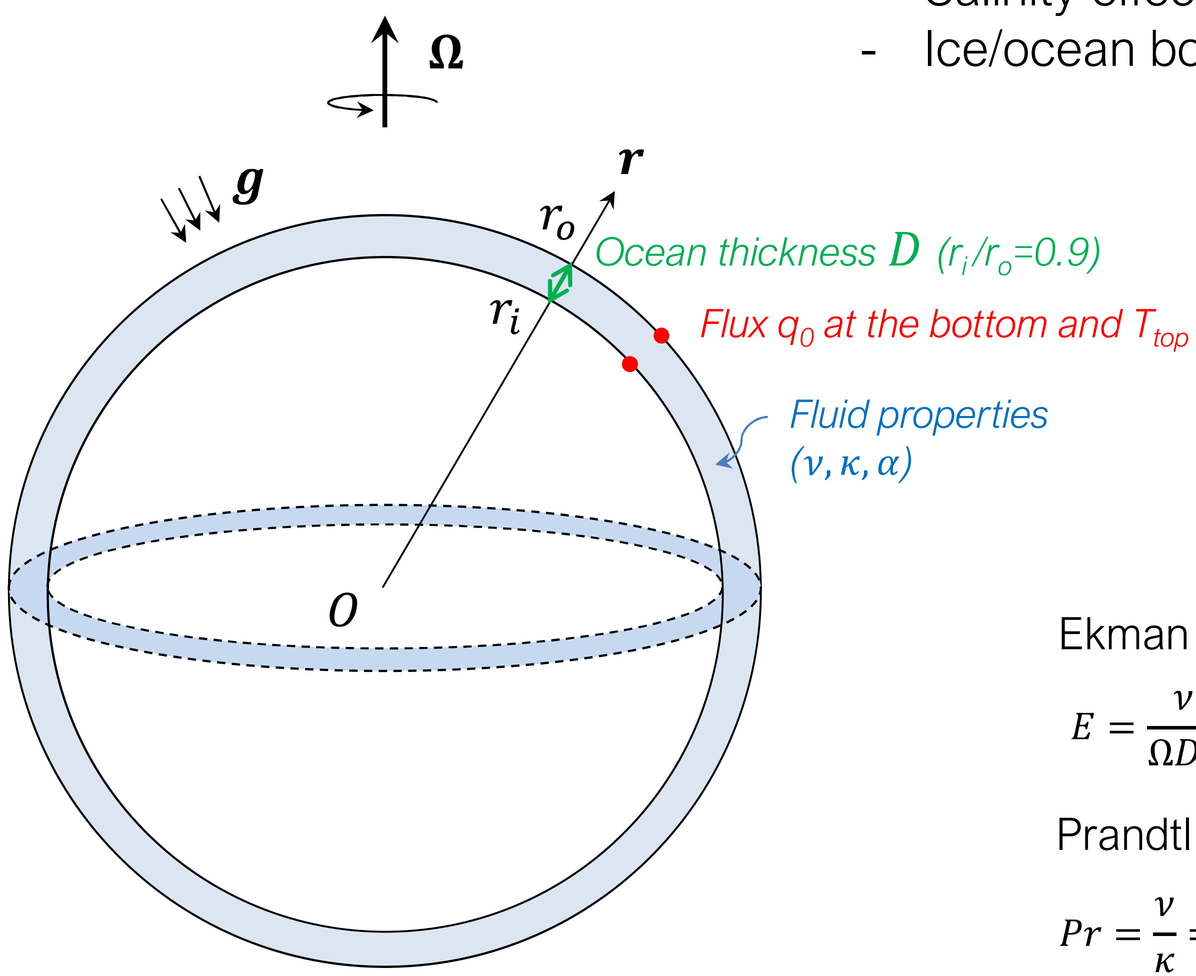

Governing equations

$$E\left(\frac{\partial \boldsymbol{u}}{\partial t} + \boldsymbol{u}\cdot\boldsymbol{\nabla}\boldsymbol{u}\right) = -\boldsymbol{\nabla}p - 2\boldsymbol{e}_z \times \boldsymbol{u} + \frac{Ra\ E}{Pr}\frac{r}{r_o}T\boldsymbol{e}_r + E\nabla^2\boldsymbol{u}$$

$$\frac{\partial T}{\partial t} + \boldsymbol{u}\cdot\boldsymbol{\nabla}T = \frac{1}{Pr}\nabla^2 T$$

$$\boldsymbol{\nabla}\cdot\boldsymbol{u} = 0$$

Ekman

$$E = \frac{\nu}{\Omega D^2} = \frac{\text{viscous effects}}{\text{rotation effects}}$$

Prandtl

$$Pr = \frac{\nu}{\kappa} = \frac{\text{viscous diffusion}}{\text{thermal diffusion}}$$

Rayleigh

$$Ra = \frac{\alpha g_0 q_0 D^4}{\nu k \kappa} = \frac{\text{buoyancy force}}{\text{diffusive effects}}$$

Relative amplitude of the bottom anomaly

$$q^* = \frac{\Delta q}{q_0}$$

Global numerical model

Model: Rotating thermal convection in a spherical shell (open-source code **MagIC** [Wicht 2002, Gastine 2016])

Approximations/simplifications:
- Buoyancy-driven flow (no ocean tides, no libration)
- Salinity effect on buoyancy ignored
- Ice/ocean boundary = fixed T (no phase change)

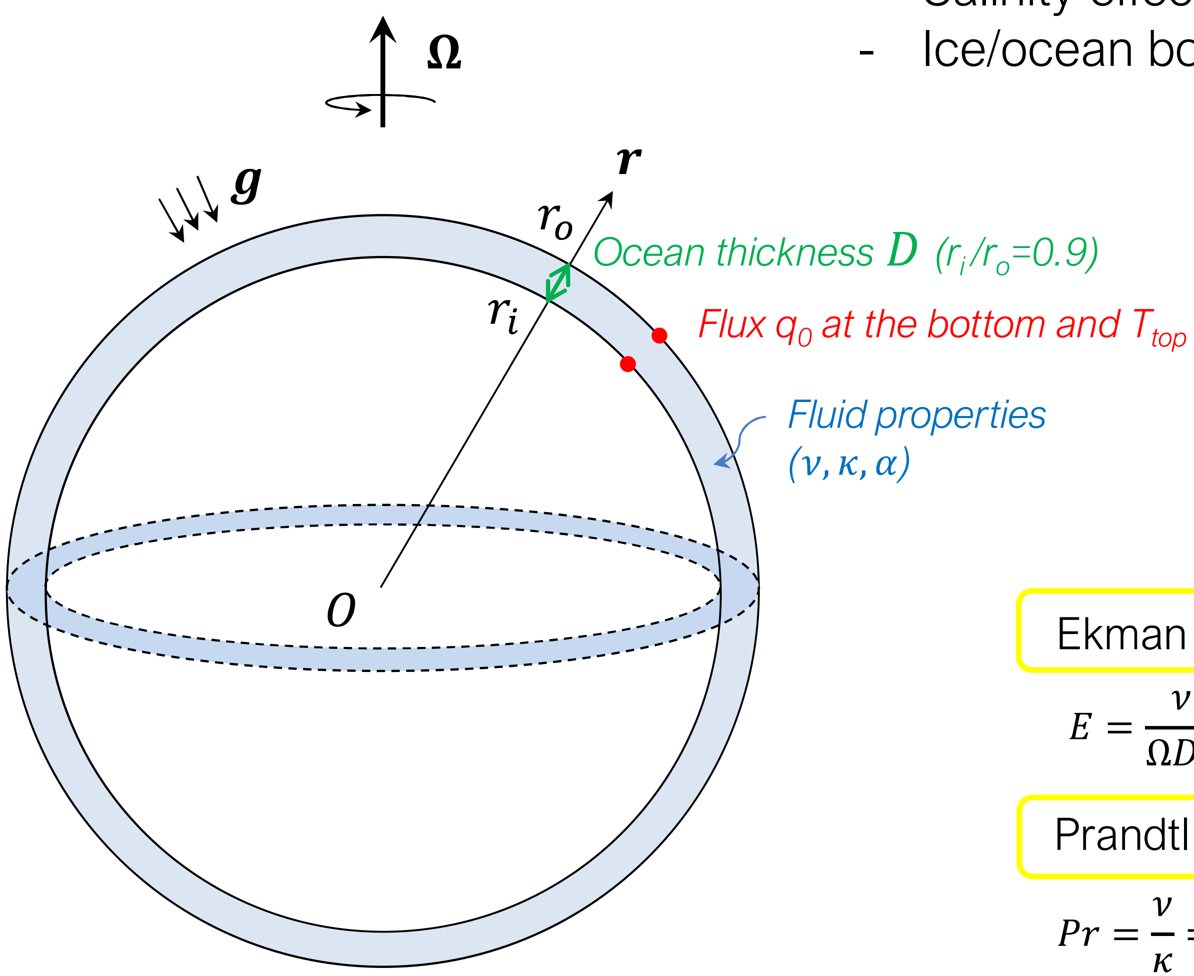

Governing equations

$$E\left(\frac{\partial \boldsymbol{u}}{\partial t} + \boldsymbol{u}\cdot\boldsymbol{\nabla}\boldsymbol{u}\right) = -\boldsymbol{\nabla}p - 2\boldsymbol{e}_z \times \boldsymbol{u} + \frac{Ra\ E}{Pr}\frac{r}{r_o}T\boldsymbol{e}_r + E\nabla^2\boldsymbol{u}$$

$$\frac{\partial T}{\partial t} + \boldsymbol{u}\cdot\boldsymbol{\nabla}T = \frac{1}{Pr}\nabla^2 T$$

$$\boldsymbol{\nabla}\cdot\boldsymbol{u} = 0$$

Ekman

$$E = \frac{\nu}{\Omega D^2} = \frac{\text{viscous effects}}{\text{rotation effects}}$$

Prandtl

$$Pr = \frac{\nu}{\kappa} = \frac{\text{viscous diffusion}}{\text{thermal diffusion}}$$

Rayleigh

$$Ra = \frac{\alpha g_0 q_0 D^4}{\nu k \kappa} = \frac{\text{buoyancy force}}{\text{diffusive effects}}$$

Relative amplitude of the bottom anomaly

$$q^* = \frac{\Delta q}{q_0}$$

Parameters space and convective regimes

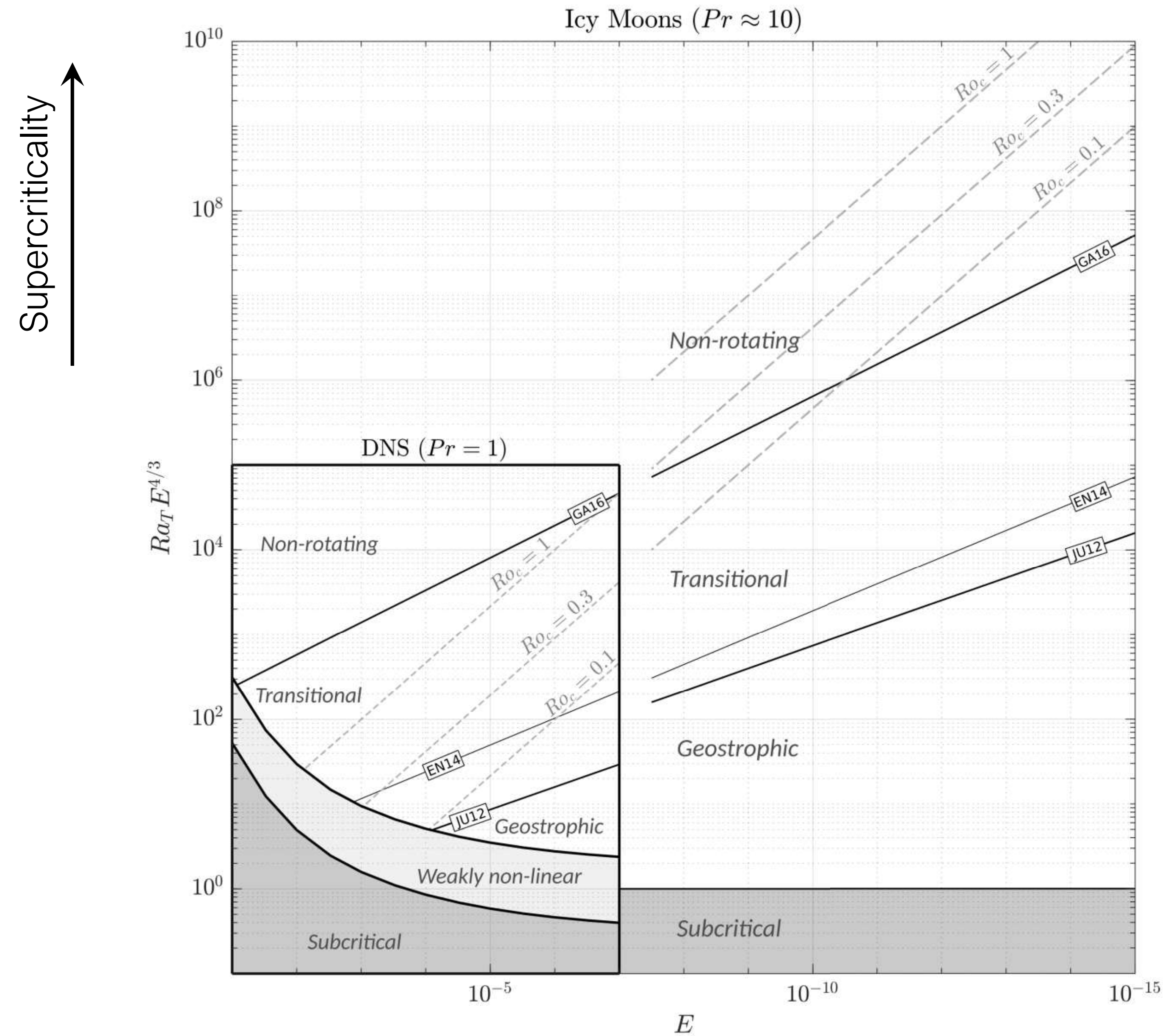

[Lemasquerier+ 2023, Cheng+, 2015; 2018; Gastine, 2016; Soderlund 2019; Kvorka and Cadek, 2022]

Decreasing Ekman

$$E = \frac{\nu}{\Omega D^2} = \frac{\text{viscous effects}}{\text{rotation effects}}$$

Parameters space and convective regimes

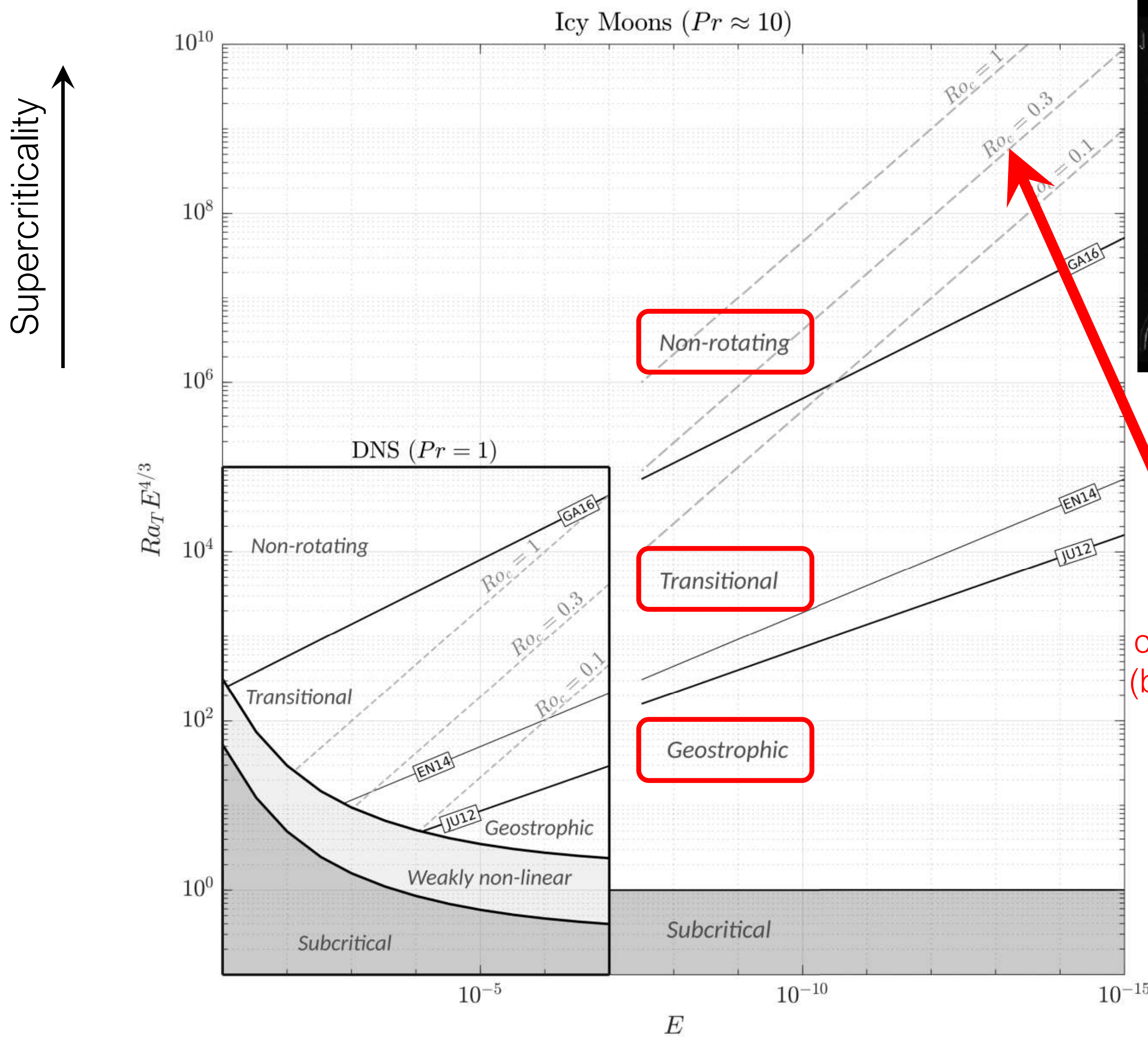

Increasing convective Rossby (buoyancy/Coriolis)
➔ **Decreasing geostrophy**

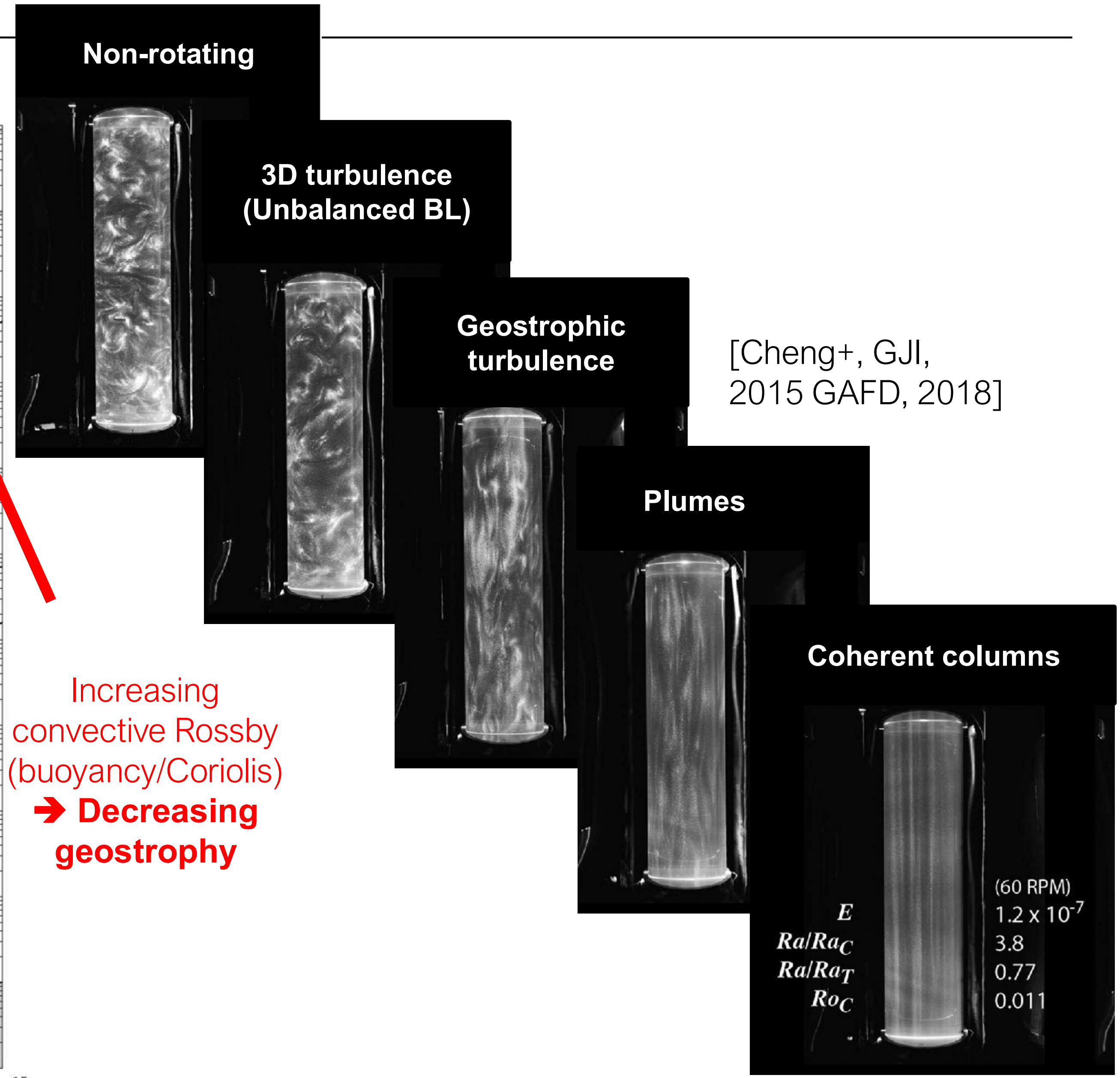

[Cheng+, GJI, 2015 GAFD, 2018]

[Lemasquerier+ 2023, Cheng+, 2015; 2018; Gastine, 2016; Soderlund 2019; Kvorka and Cadek, 2022]

Decreasing Ekman

$$E = \frac{\nu}{\Omega D^2} = \frac{\text{viscous effects}}{\text{rotation effects}}$$

Parameters space and convective regimes

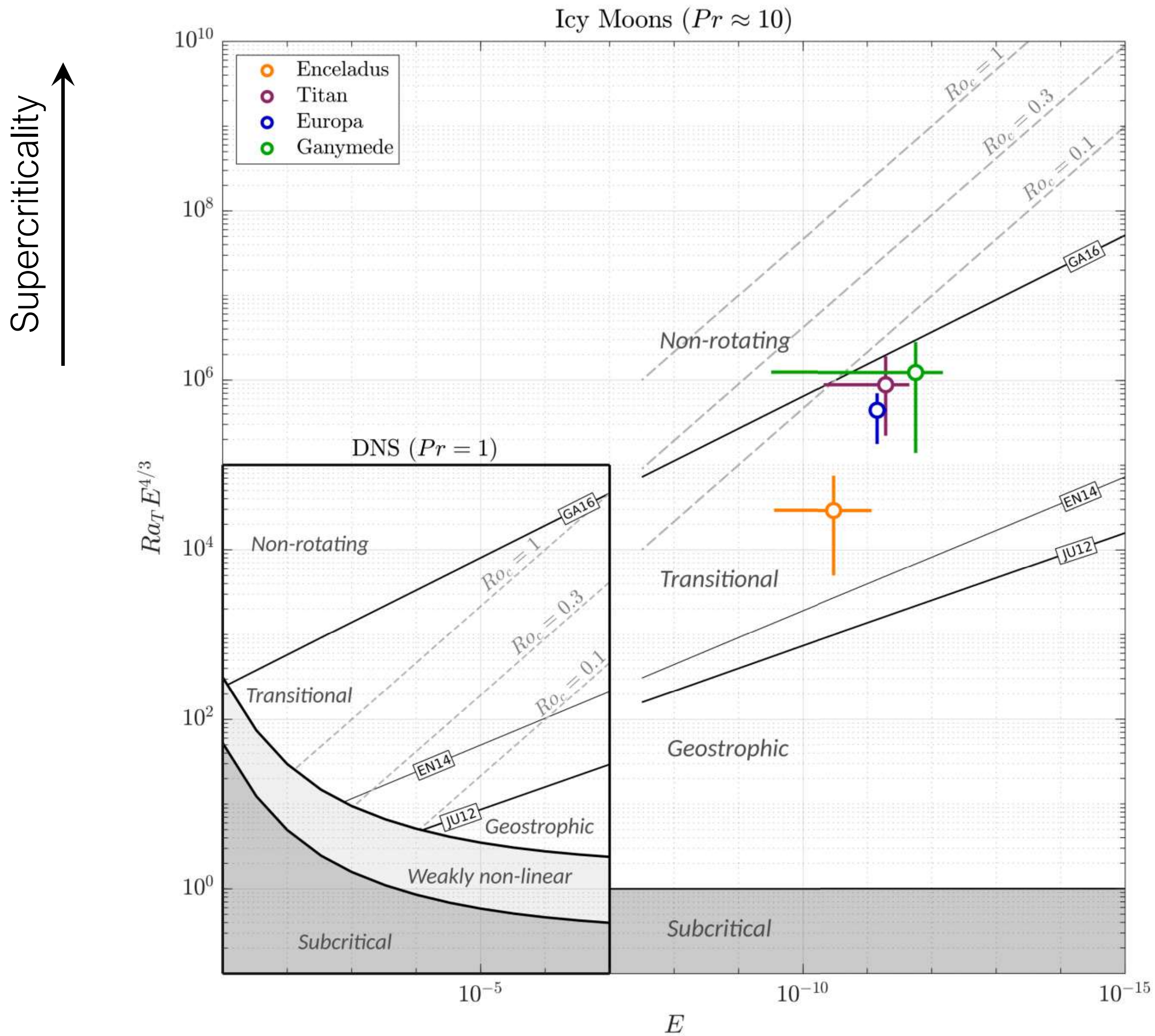

[Lemasquerier+ 2023, Cheng+, 2015; 2018; Gastine, 2016; Soderlund 2019; Kvorka and Cadek, 2022]

Decreasing Ekman

$$E = \frac{\nu}{\Omega D^2} = \frac{\text{viscous effects}}{\text{rotation effects}}$$

Parameters space and convective regimes

Supercriticality

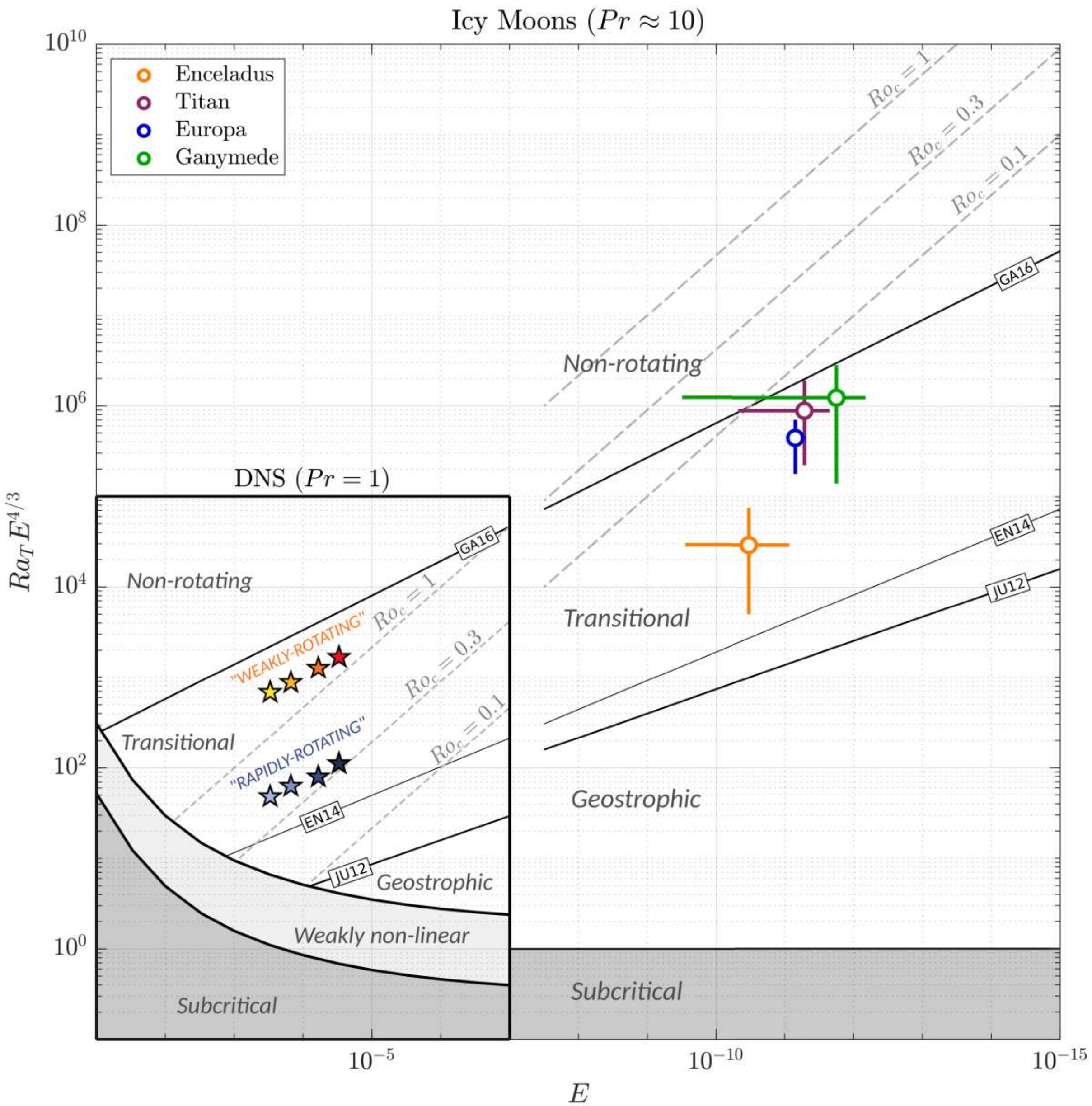

[Lemasquerier+ 2023, Cheng+, 2015; 2018; Gastine, 2016; Soderlund 2019; Kvorka and Cadek, 2022]

Decreasing Ekman

$$E = \frac{\nu}{\Omega D^2} = \frac{\text{viscous effects}}{\text{rotation effects}}$$

Global numerical model

Model: Rotating thermal convection in a sp

Approximations/simplifications:

- B
- Sa
- Ic

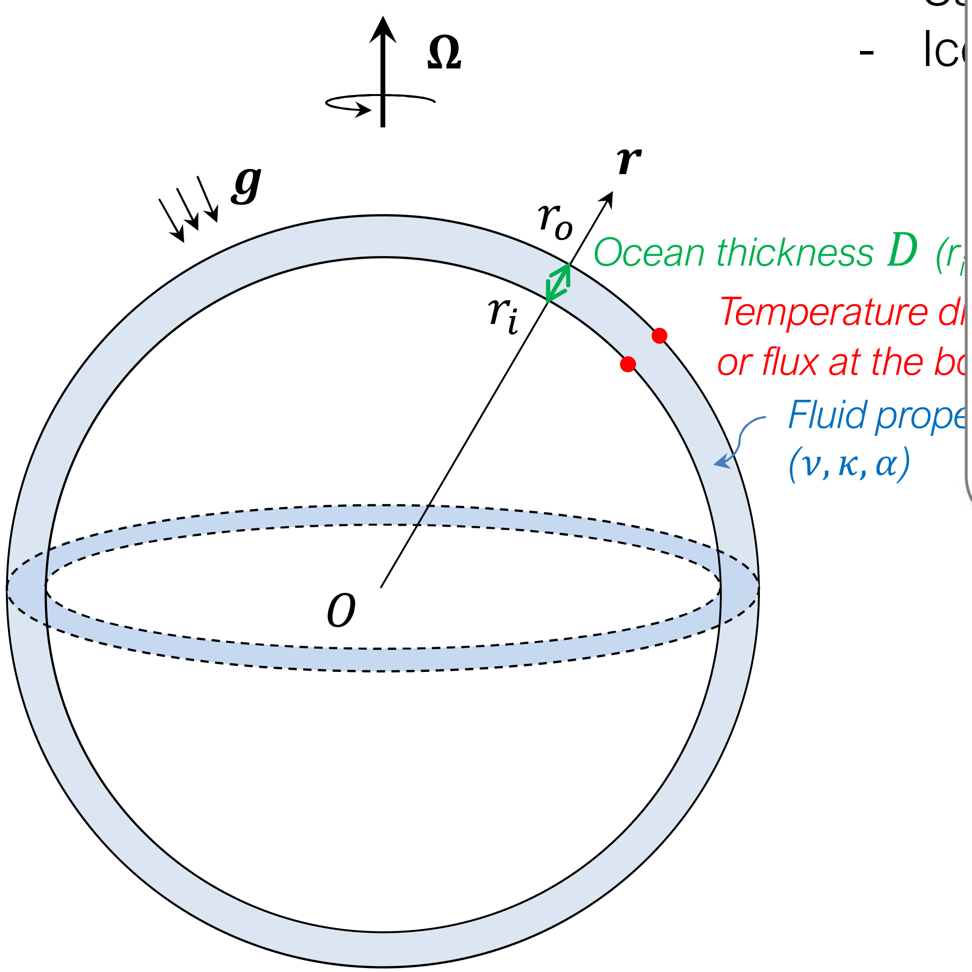

Relative amplitude of the bottom anomaly:

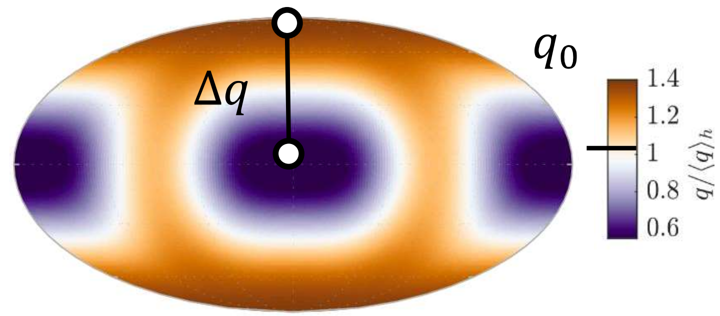

$$q^* = \frac{\Delta q}{q_0} \in [0,2]$$

Ekman

$$E = \frac{\nu}{\Omega D^2} = \frac{\text{viscous effects}}{\text{rotation effects}}$$

Prandtl

$$Pr = \frac{\nu}{\kappa} = \frac{\text{viscous diffusion}}{\text{thermal diffusion}}$$

Rayleigh

$$Ra = \frac{\alpha g_0 q_0 D^4}{\nu k \kappa} = \frac{\text{buoyancy force}}{\text{diffusive effects}}$$

Relative amplitude of the bottom anomaly

$$q^* = \frac{\Delta q}{q_0}$$

Results

Homogeneous forcing

Inhomogeneous forcing *following the tidal pattern (progressively larger bottom anomaly)*

$q^* = \frac{\Delta q}{q_0}$

$q^* = 0.0$ $q^* = 0.46$ $q^* = 0.87$ $q^* = 1.30$ $q^* = 1.72$ $q^* = 2.16$

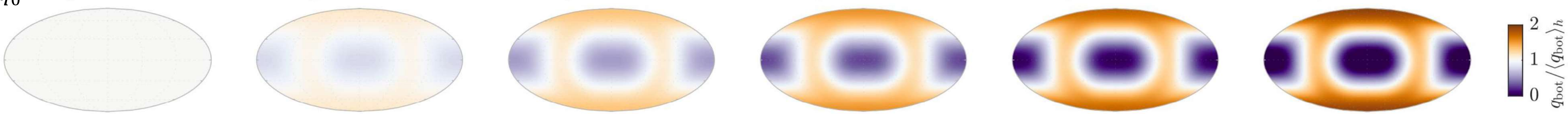

Results

Homogeneous forcing

Inhomogeneous forcing *following the tidal pattern (progressively larger bottom anomaly)*

$q^* = \frac{\Delta q}{q_0}$

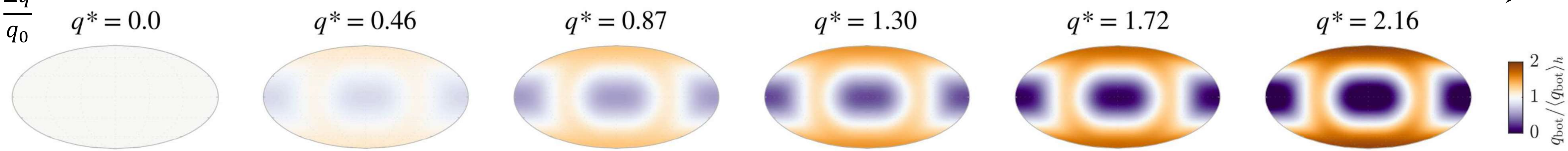

PURE
RADIOGENIC
HEATING
(Homogeneous)

PURE TIDAL HEATING
(Heterogeneous with
q*~1)

Results

Homogeneous forcing

Inhomogeneous forcing *following the tidal pattern (progressively larger bottom anomaly)*

$q^* = \frac{\Delta q}{q_0}$

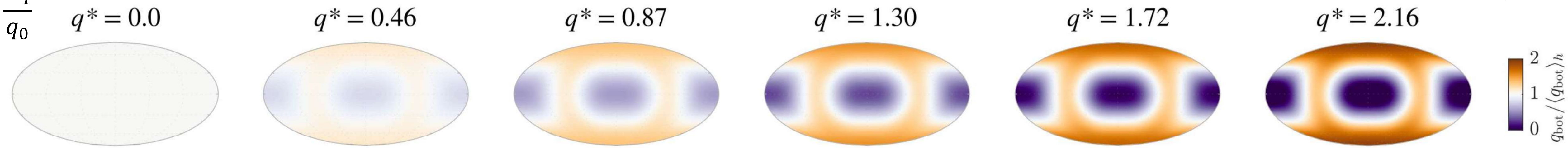

Two mechanical boundary conditions considered:

- ✓ Both boundaries **stress-free** [No Ekman boundary layers, strong zonal flows]
- ✓ Both boundaries **no-slip** [Ekman boundary layers develop, Ekman pumping, reduced zonal flows]

Results

Homogeneous forcing

Inhomogeneous forcing *following the tidal pattern (progressively larger bottom anomaly)*

$q^* = \frac{\Delta q}{q_0}$

$q* = 0.0$ $q* = 0.46$ $q* = 0.87$ $q* = 1.30$ $q* = 1.72$ $q* = 2.16$

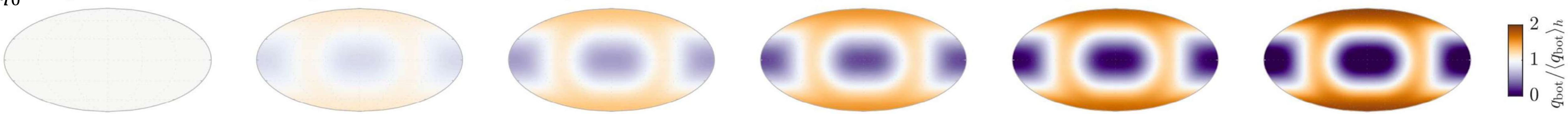

Stress-Free cases

Results: mean circulation

Stress Free

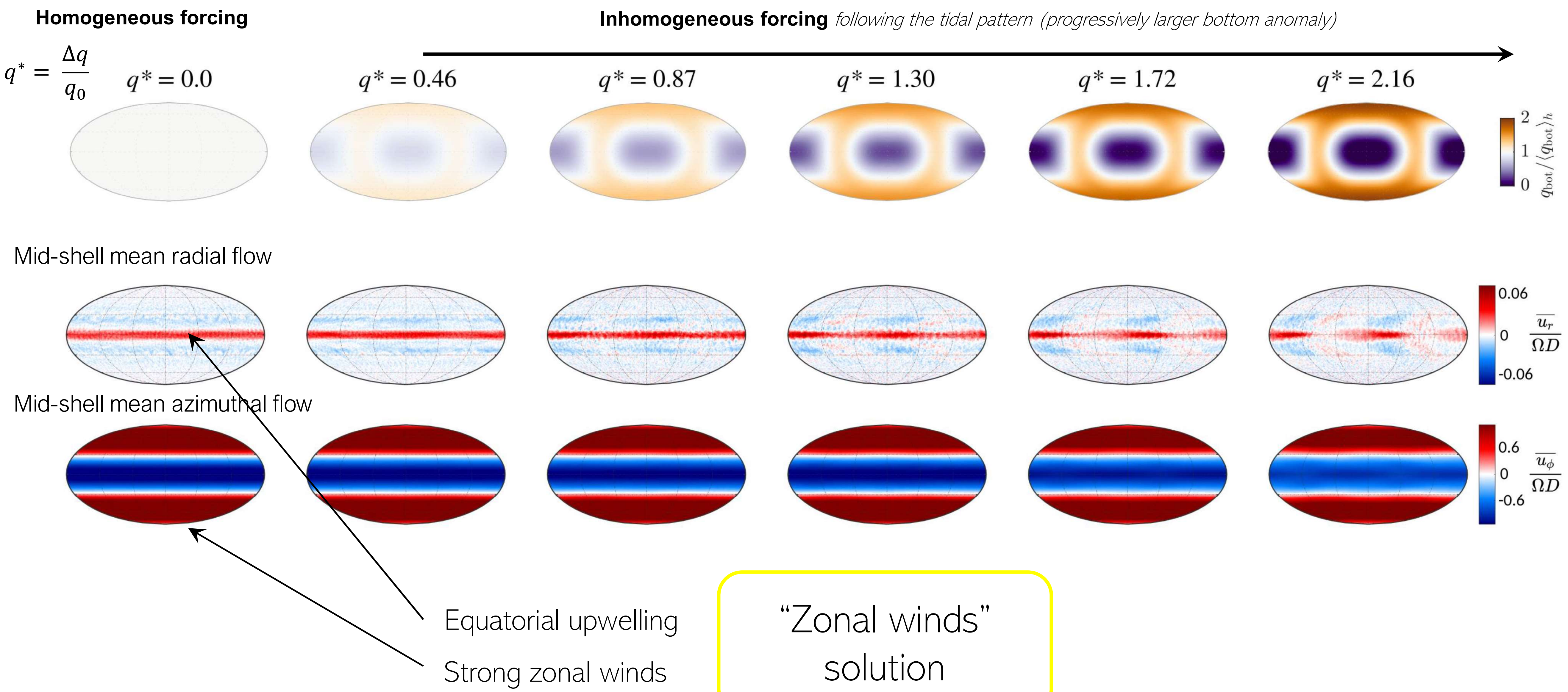

"Zonal winds" solution

[Lemasquerier+ 2023]

Results: mean circulation

Homogeneous forcing **Inhomogeneous forcing** *following the tidal pattern (progressively larger bottom anomaly)*

$q^* = \frac{\Delta q}{q_0}$

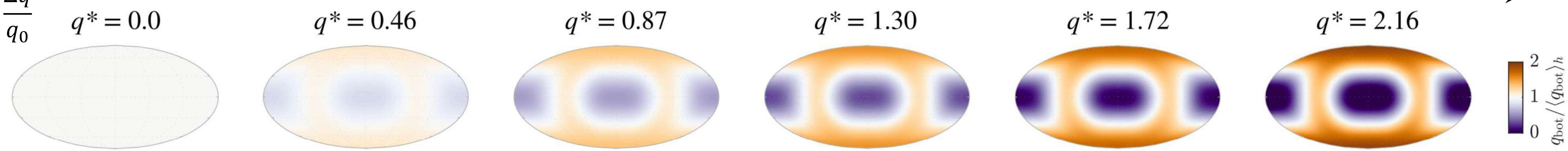

No slip cases

[Lemasquerier+ 2023]

Results: mean circulation

No slip

Homogeneous forcing **Inhomogeneous forcing** *following the tidal pattern (progressively larger bottom anomaly)*

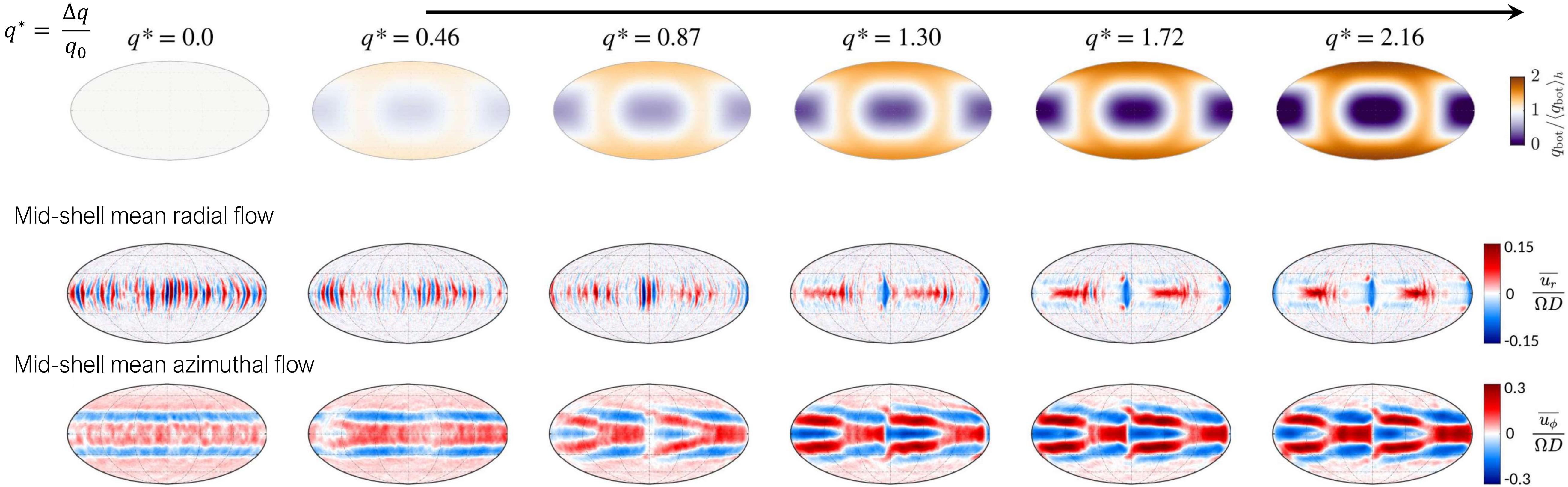

[Lemasquerier+ 2023]

Results: mean circulation

No slip

Homogeneous forcing

Inhomogeneous forcing *following the tidal pattern (progressively larger bottom anomaly)*

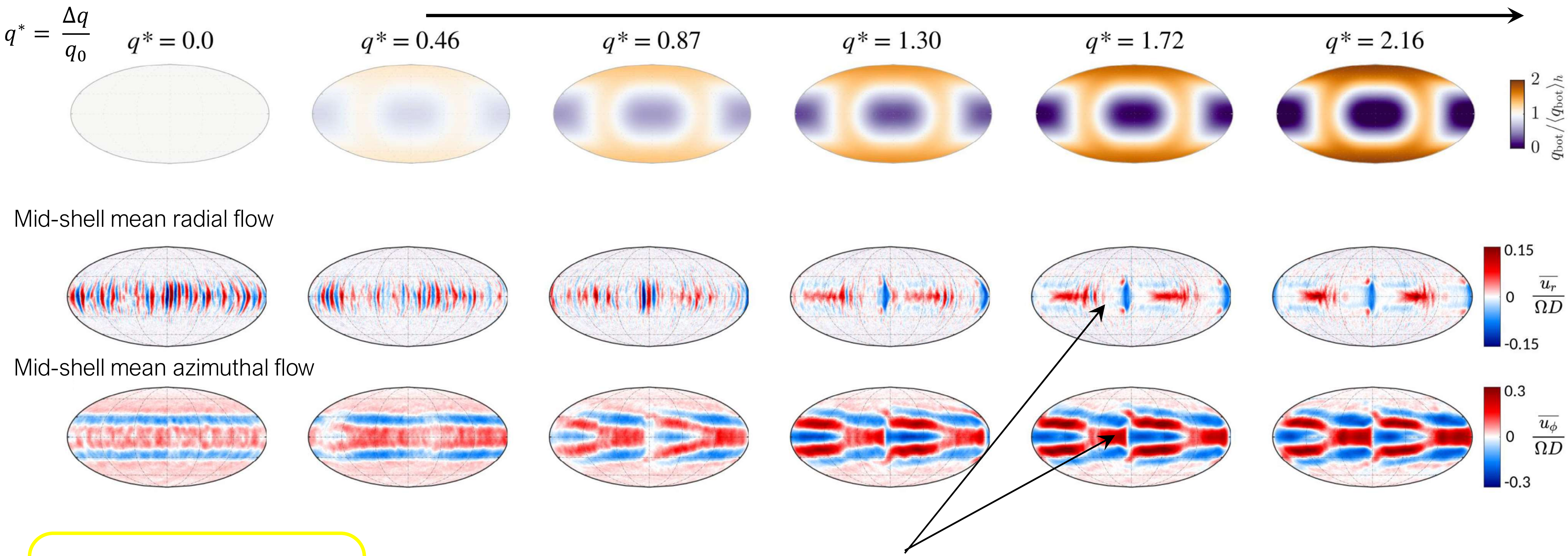

“Thermal winds” solution

Localized downwellings, spead upwellings

Non-axisymmetric thermal winds

[Lemasquerier+ 2023]

Results: mean circulation

No slip

Homogeneo ... **homogeneous forcing** *following the tidal pattern (progressively larger bottom anomaly)*

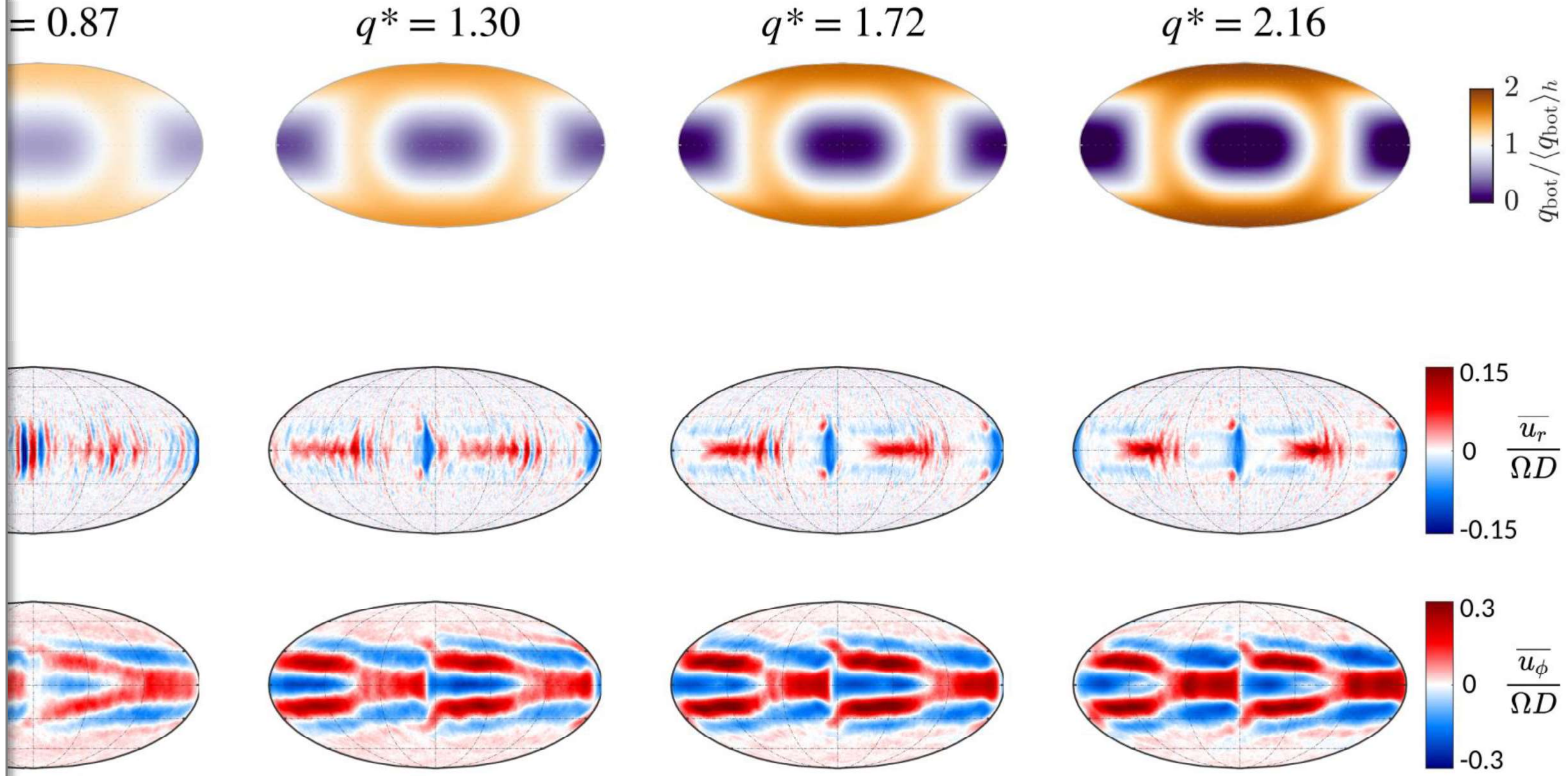

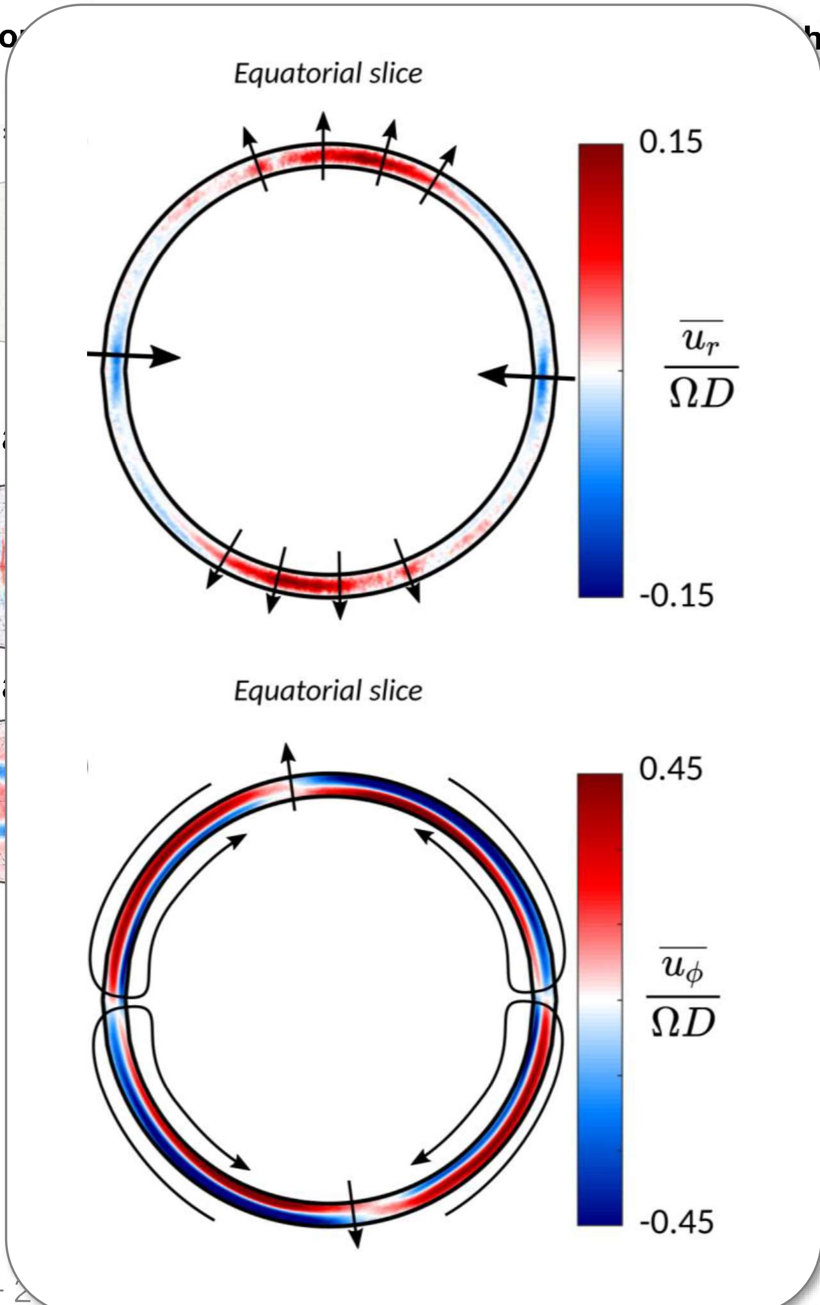

Thermal-wind balance
Buoyancy~Coriolis
(steady, no-inertia, inviscid)

$$u^g_{s,r} = -\frac{r_o^2 - s^2}{2 r_o s^2} \frac{RaE}{Pr} \left\langle \frac{\partial T}{\partial \phi} \right\rangle_z$$

[Dietrich, PEPI 2016]

[Lemasquerier+ 2

Results

Homogeneous forcing

Inhomogeneous forcing *following the tidal pattern (progressively larger bottom anomaly)*

$q^* = \frac{\Delta q}{q_0}$

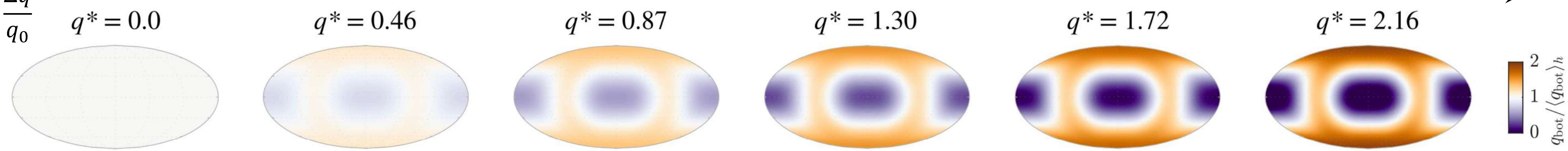

➔ How is the bottom heat flux anomaly transposed up the ice-ocean boundary in each solution?

Results: Heat anomaly at the top of the ocean

Latitudinal profiles (longitudinal average)

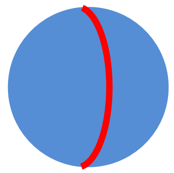

Longitudinal profiles (latitudinal average)

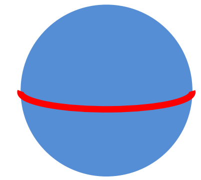

"Zonal winds" solution (Stress-free)

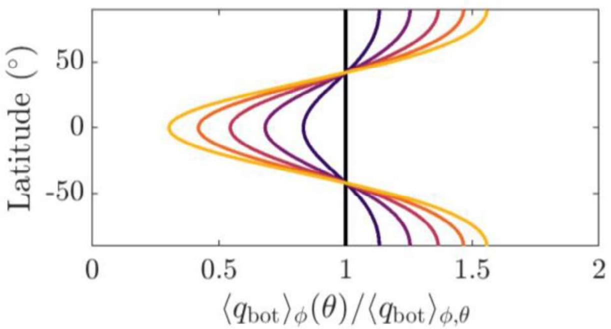

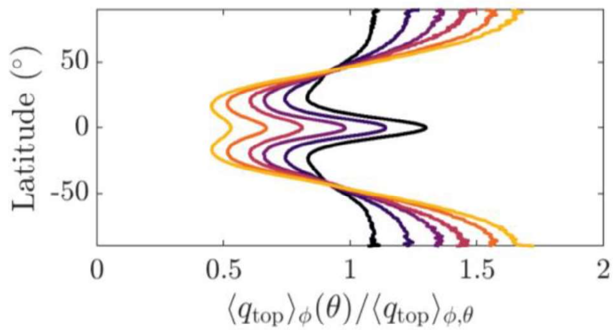

"Thermal winds" solution (No-slip)

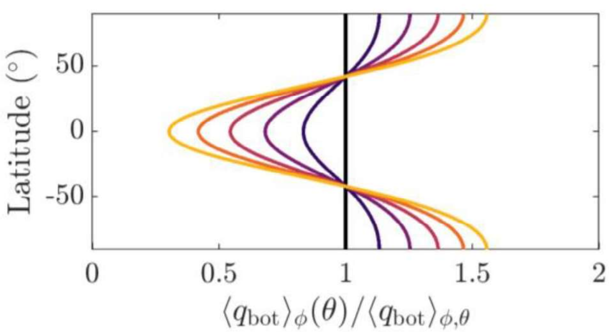

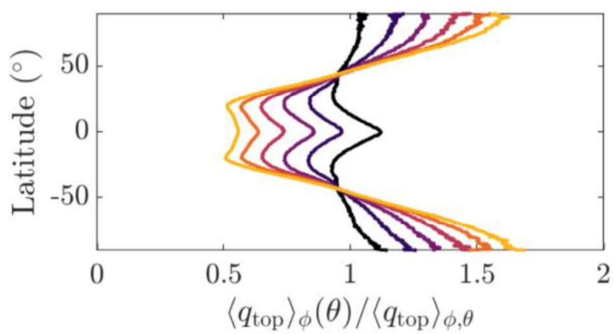

Bottom (seafloor) **Top (ocean-ice)** **Bottom (seafloor)** **Top (ocean-ice)**

[Lemasquerier+ 2023]

Results: Heat anomaly at the top of the ocean

Latitudinal profiles (longitudinal average)

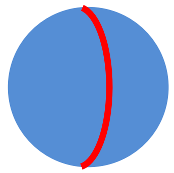

Longitudinal profiles (latitudinal average)

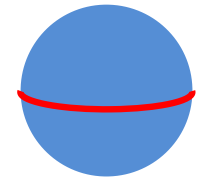

"Zonal winds" solution (Stress-free)

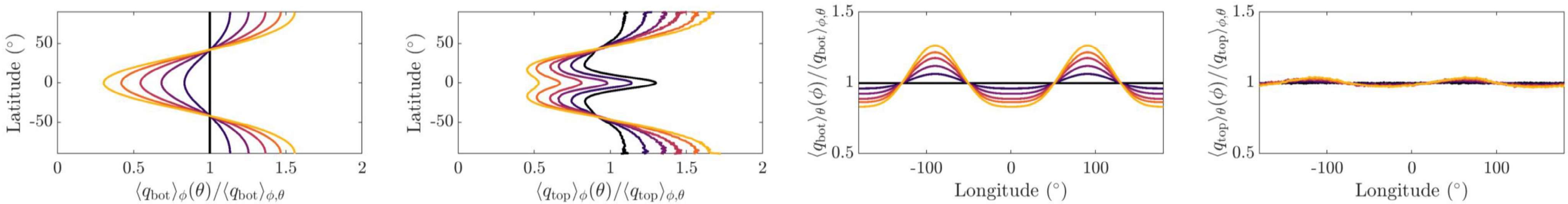

"Thermal winds" solution (No-slip)

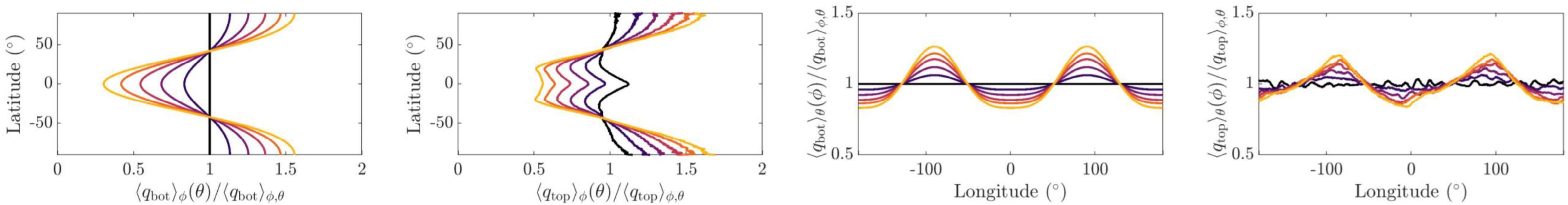

Bottom (seafloor) **Top (ocean-ice)** **Bottom (seafloor)** **Top (ocean-ice)**

[Lemasqu

Results: Heat anomaly at the top of the ocean

Relative anomalies in latitude, longitude, at the bottom and at the top of the ocean:

$$K_{top}^{lat} = \left[(\langle q\rangle_{\phi}^{\max} - \langle q\rangle_{\phi}^{\min})/\langle q\rangle_{\phi,\theta}\right]_{\mathrm{TOP}}$$
$$K_{bot}^{lat} = \left[(\langle q\rangle_{\phi}^{\max} - \langle q\rangle_{\phi}^{\min})/\langle q\rangle_{\phi,\theta}\right]_{\mathrm{BOTTOM}}$$
$$K_{top}^{lon} = \left[(\langle q\rangle_{\theta}^{\max} - \langle q\rangle_{\theta}^{\min})/\langle q\rangle_{\phi,\theta}\right]_{\mathrm{TOP}}$$
$$K_{bot}^{lon} = \left[(\langle q\rangle_{\theta}^{\max} - \langle q\rangle_{\theta}^{\min})/\langle q\rangle_{\phi,\theta}\right]_{\mathrm{BOTTOM}}$$

"Zonal winds" solution (Stress-free)

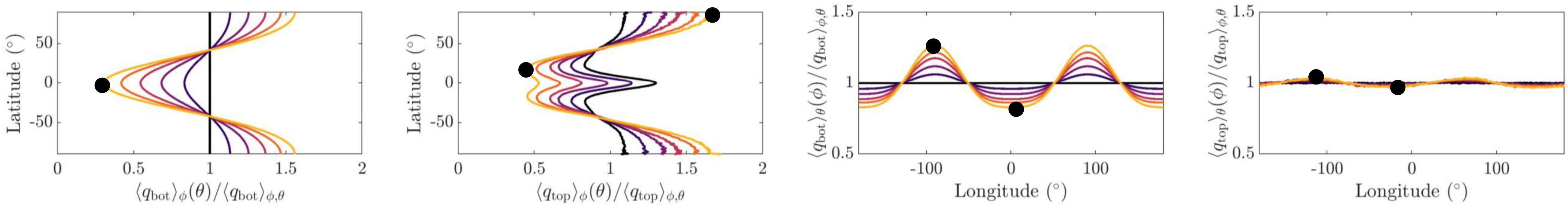

"Thermal winds" solution (No-slip)

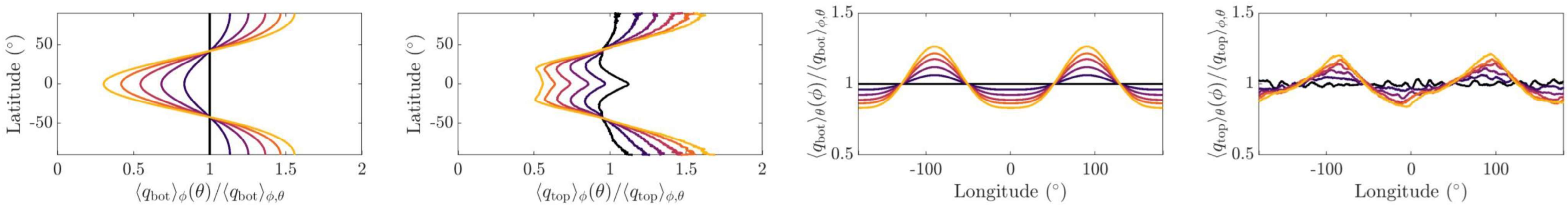

Bottom (seafloor) **Top (ocean-ice)** **Bottom (seafloor)** **Top (ocean-ice)**

[Lemasqu

Results: Heat anomaly at the top of the ocean

$$K^{lat}_{top} = \left[(\langle q\rangle^{\max}_{\phi} - \langle q\rangle^{\min}_{\phi})/\langle q\rangle_{\phi,\theta}\right]_{\mathrm{TOP}}$$
$$K^{lat}_{bot} = \left[(\langle q\rangle^{\max}_{\phi} - \langle q\rangle^{\min}_{\phi})/\langle q\rangle_{\phi,\theta}\right]_{\mathrm{BOTTOM}}$$
$$K^{lon}_{top} = \left[(\langle q\rangle^{\max}_{\theta} - \langle q\rangle^{\min}_{\theta})/\langle q\rangle_{\phi,\theta}\right]_{\mathrm{TOP}}$$
$$K^{lon}_{bot} = \left[(\langle q\rangle^{\max}_{\theta} - \langle q\rangle^{\min}_{\theta})/\langle q\rangle_{\phi,\theta}\right]_{\mathrm{BOTTOM}}$$

Latitudinal relative anomaly

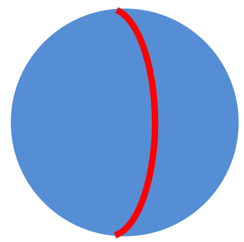

Longitudinal relative anomaly

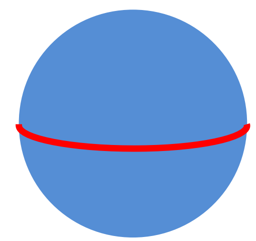

Top of the ocean

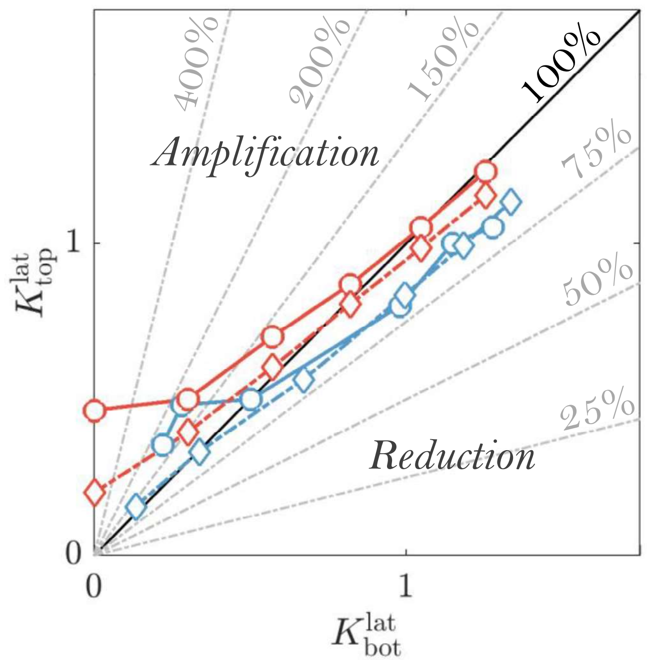

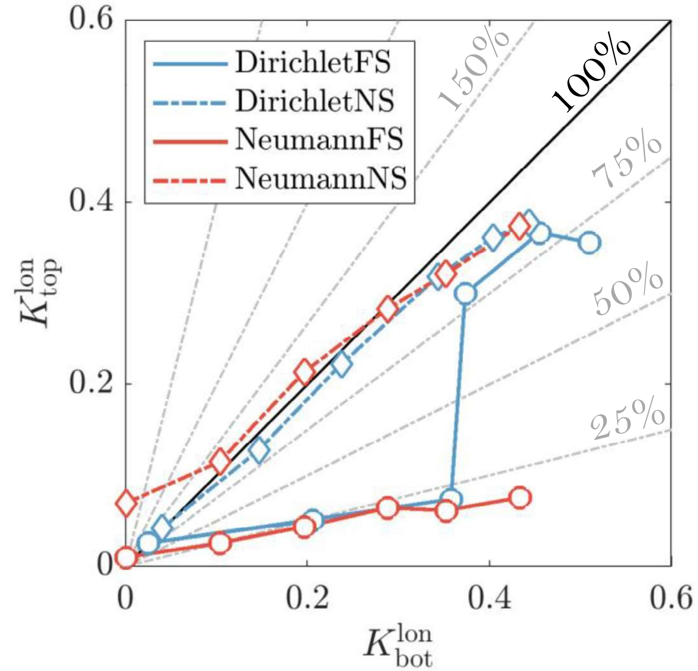

Bottom of the ocean

Increasing q*

[Lemasquerier+ 2023]

Results: Heat anomaly at the top of the ocean

$$K_{top}^{lat} = \left[(\langle q\rangle_\phi^{\max} - \langle q\rangle_\phi^{\min})/\langle q\rangle_{\phi,\theta}\right]_{\mathrm{TOP}}$$
$$K_{bot}^{lat} = \left[(\langle q\rangle_\phi^{\max} - \langle q\rangle_\phi^{\min})/\langle q\rangle_{\phi,\theta}\right]_{\mathrm{BOTTOM}}$$
$$K_{top}^{lon} = \left[(\langle q\rangle_\theta^{\max} - \langle q\rangle_\theta^{\min})/\langle q\rangle_{\phi,\theta}\right]_{\mathrm{TOP}}$$
$$K_{bot}^{lon} = \left[(\langle q\rangle_\theta^{\max} - \langle q\rangle_\theta^{\min})/\langle q\rangle_{\phi,\theta}\right]_{\mathrm{BOTTOM}}$$

Latitudinal relative anomaly

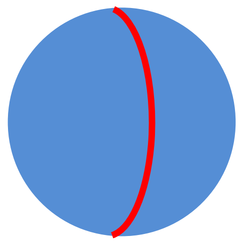

Top of the ocean

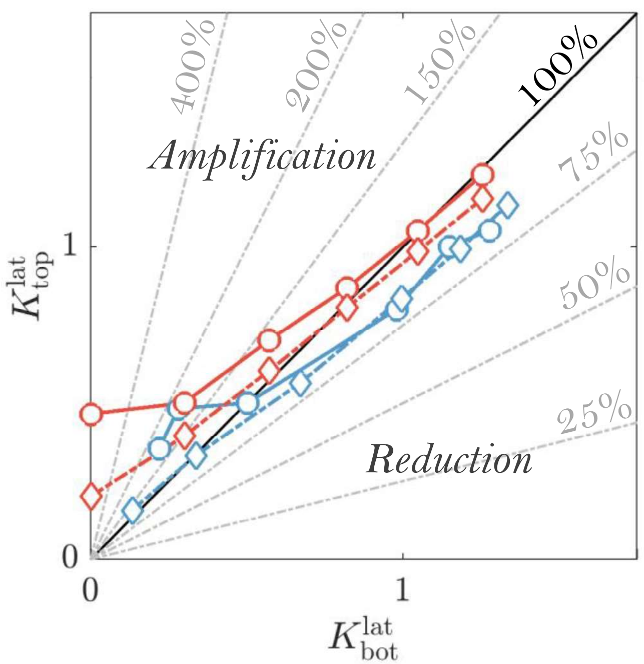

Bottom of the ocean

Longitudinal relative anomaly

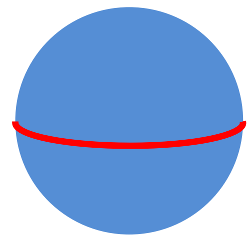

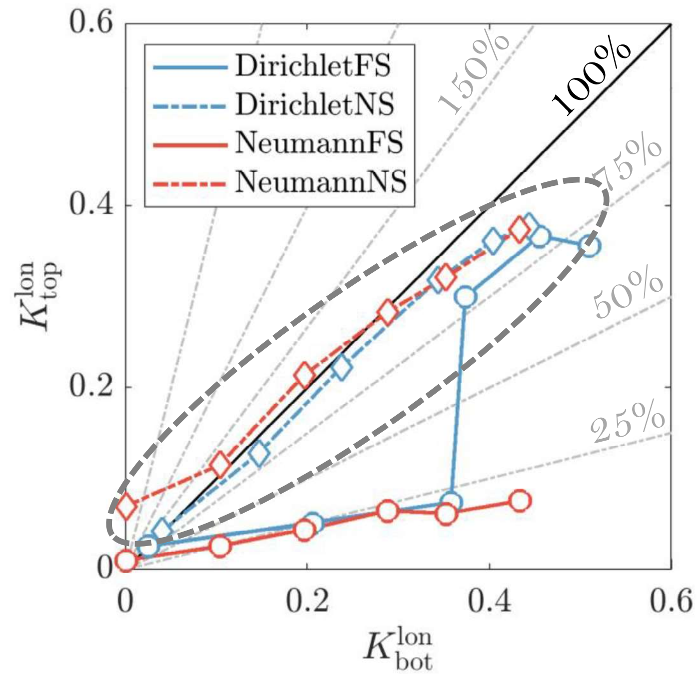

Increasing q*

“Thermal winds” solution

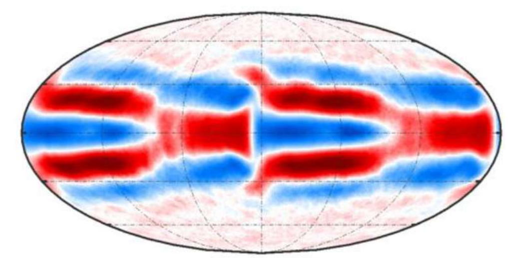

[Lemasquerier+ 2023]

Results: Heat anomaly at the top of the ocean

$$K^{lat}_{top} = \left[(\langle q\rangle^{\max}_{\phi} - \langle q\rangle^{\min}_{\phi})/\langle q\rangle_{\phi,\theta}\right]_{\mathrm{TOP}}$$
$$K^{lat}_{bot} = \left[(\langle q\rangle^{\max}_{\phi} - \langle q\rangle^{\min}_{\phi})/\langle q\rangle_{\phi,\theta}\right]_{\mathrm{BOTTOM}}$$
$$K^{lon}_{top} = \left[(\langle q\rangle^{\max}_{\theta} - \langle q\rangle^{\min}_{\theta})/\langle q\rangle_{\phi,\theta}\right]_{\mathrm{TOP}}$$
$$K^{lon}_{bot} = \left[(\langle q\rangle^{\max}_{\theta} - \langle q\rangle^{\min}_{\theta})/\langle q\rangle_{\phi,\theta}\right]_{\mathrm{BOTTOM}}$$

Latitudinal relative anomaly

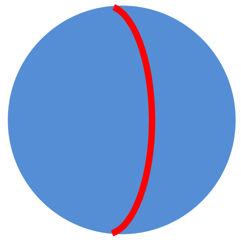

Longitudinal relative anomaly

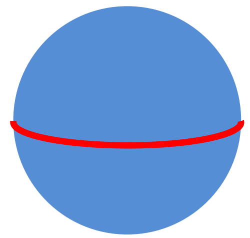

Top of the ocean

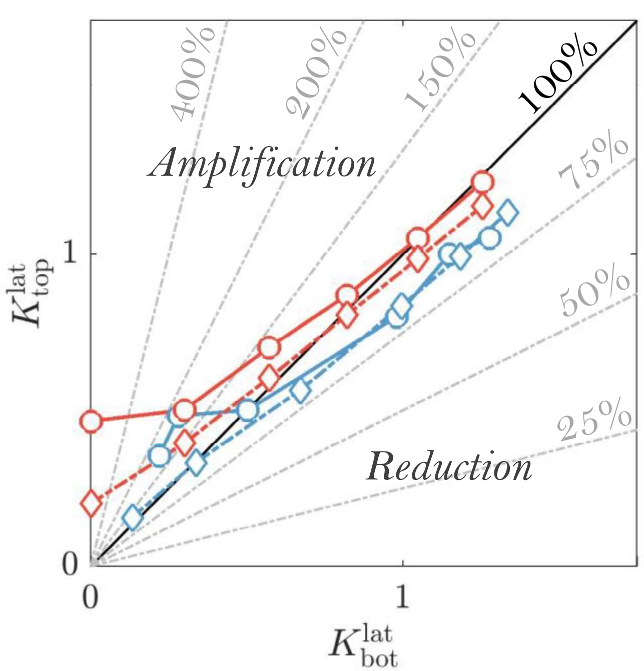

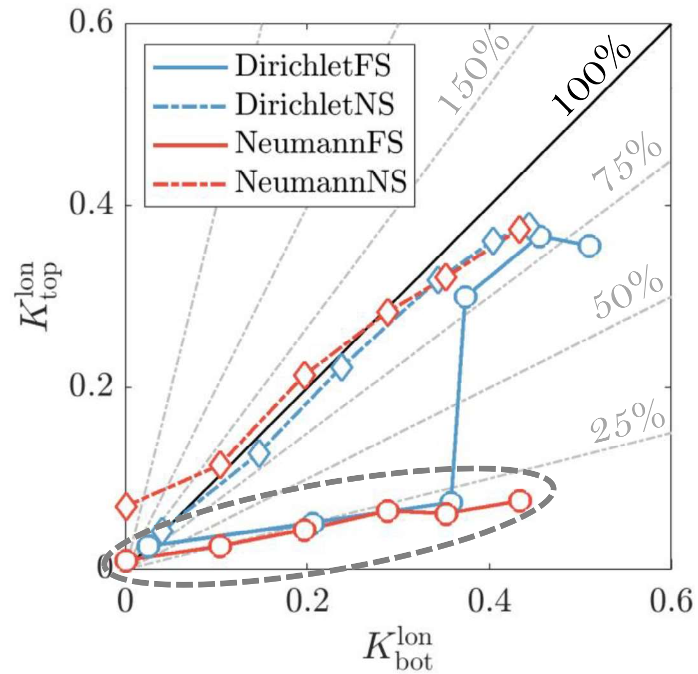

"Zonal winds" solution

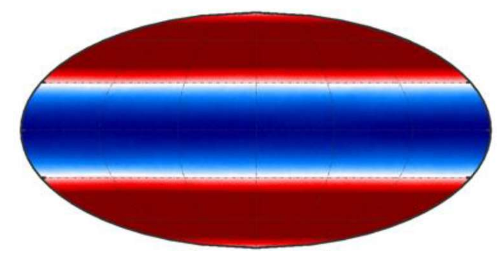

Bottom of the ocean

Increasing q*

[Lemasquerier+ 2023]

Results: Heat anomaly at the top of the ocean

Latitudinal relative anomaly

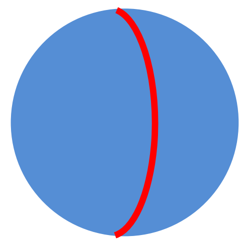

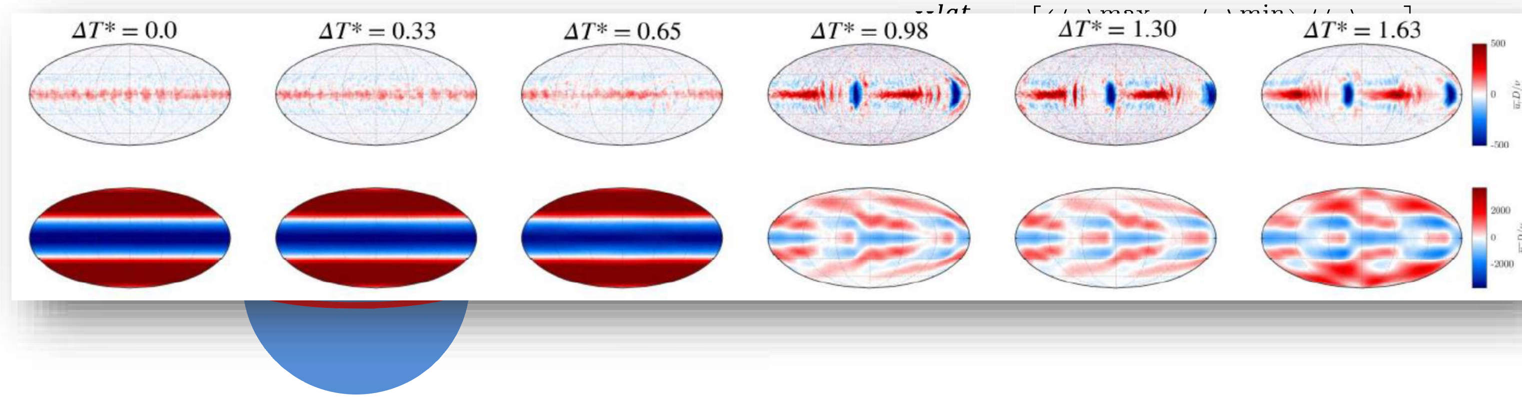

Top of the ocean

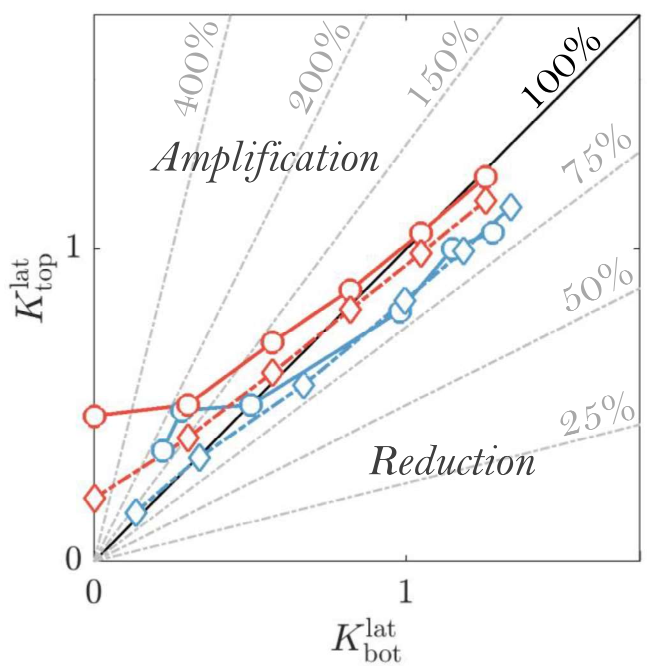

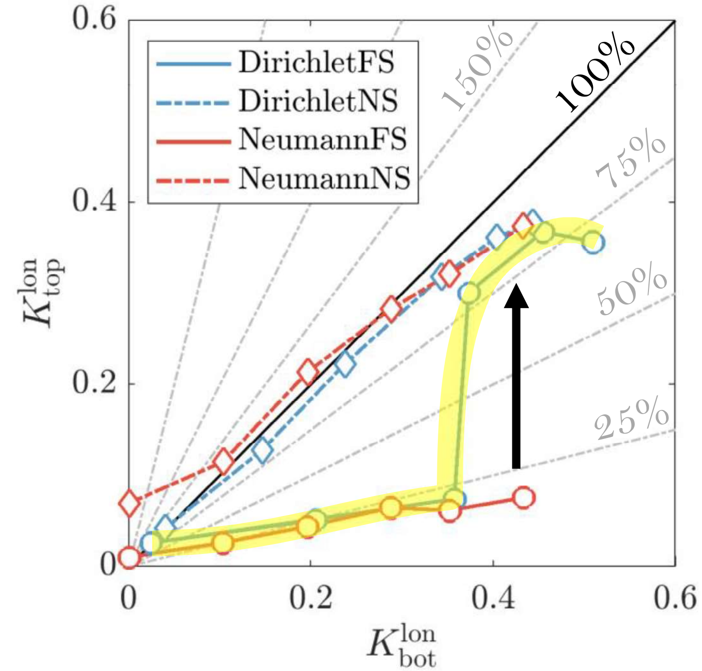

Note: Dirichlet + Stress-free → abrupt transition to thermal winds solution!
In the weakly rotating regime only…..

Bottom of the ocean

Increasing q*

[Lemasquerier+ 2023]

Caveat: behaviour at smaller Ekman

Weakly rotating

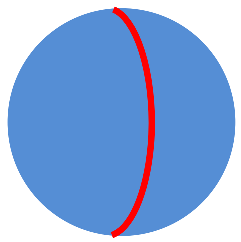

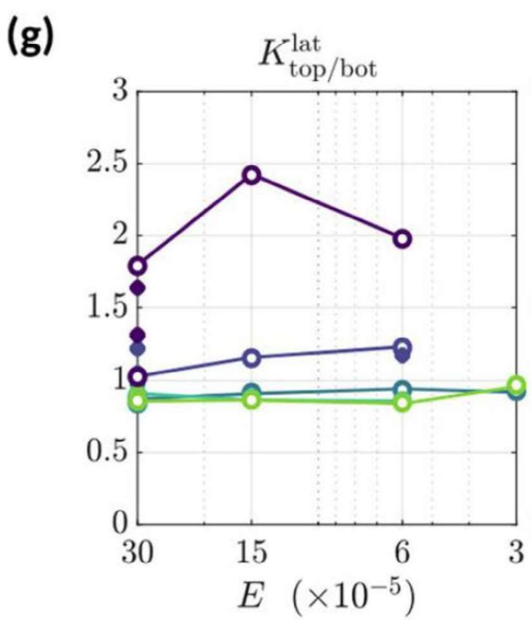

Moderately rotating

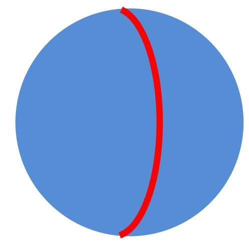

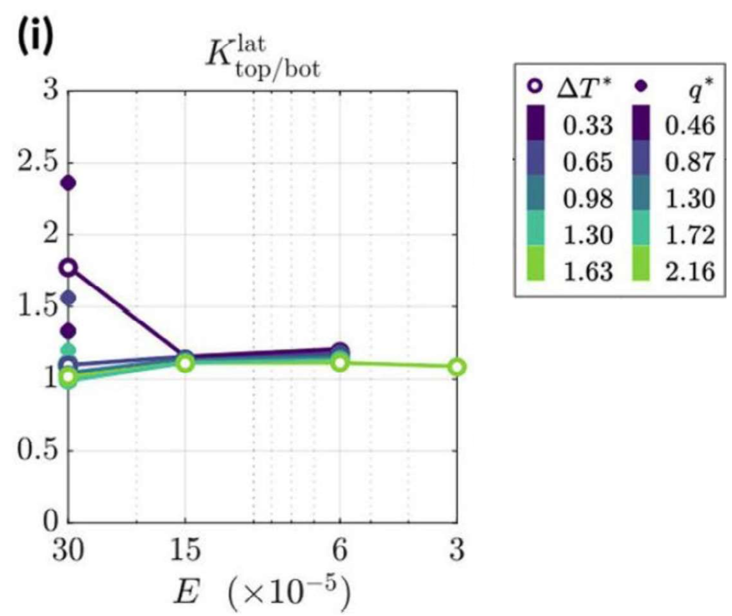

Caveat: behaviour at smaller Ekman

Weakly rotating

Moderately rotating

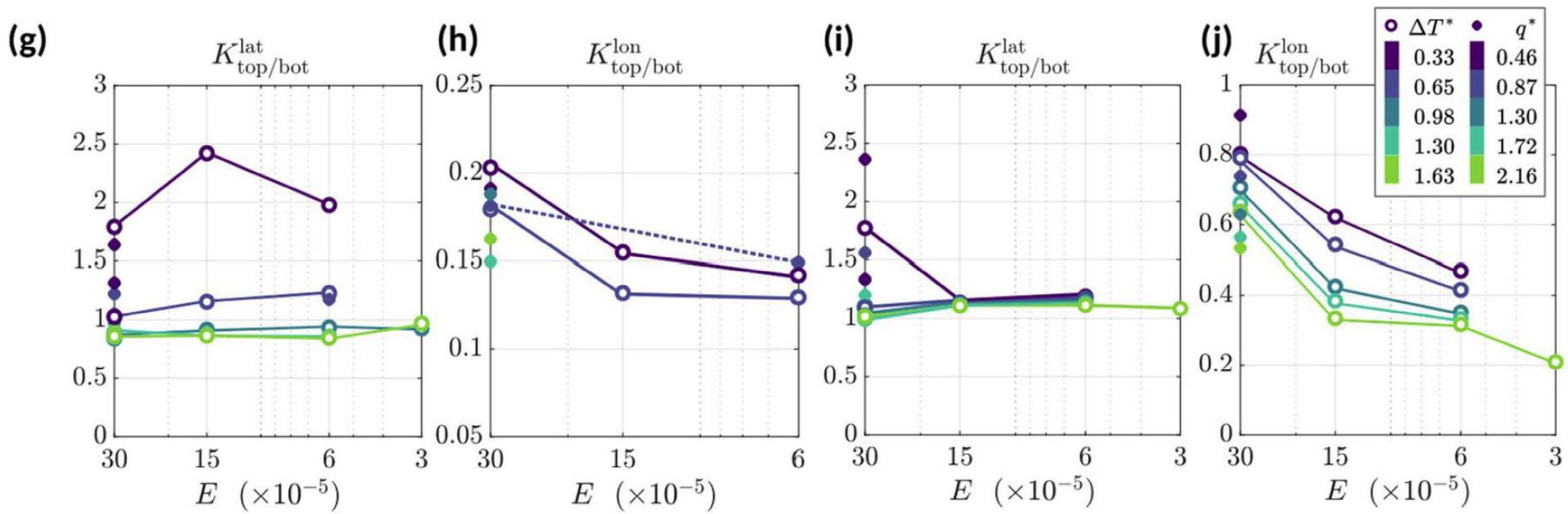

→ Longitudinal anomaly erased in planetary regime?

Link with observations?

TITAN

ENCELADUS

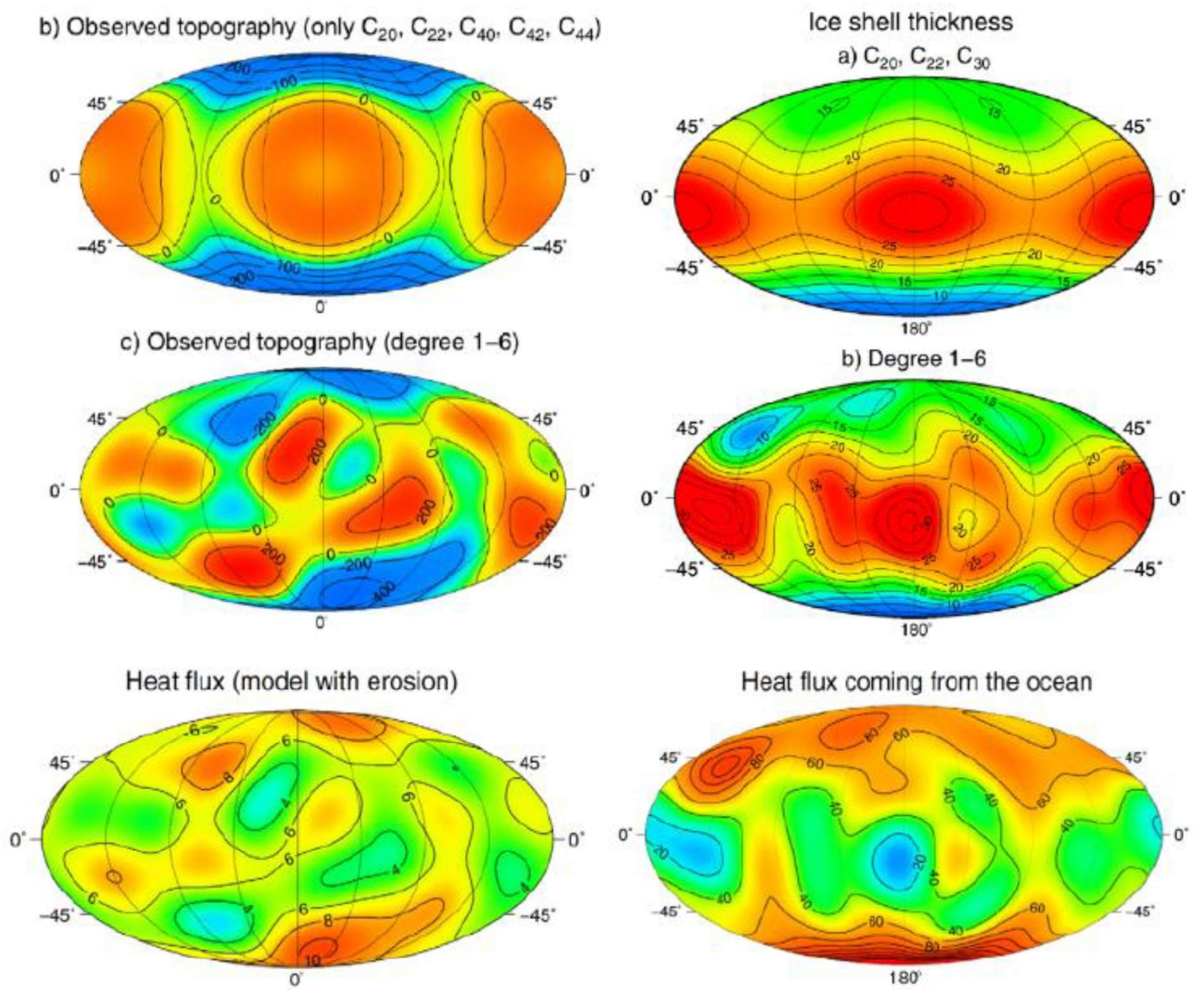

[Kvorka et al., 2018, Cadek et al., 2019]

- ❖ Ice thickness estimates for Titan and Enceladus
- ❖ Europa Clipper likely to provide such estimates for Europa (radar instrument)

➔ What we can do: **provide predictive ice thickness models**

Link with observations?

Radar for Europa Assessment and Sounding: Ocean to Near-surface (REASON)

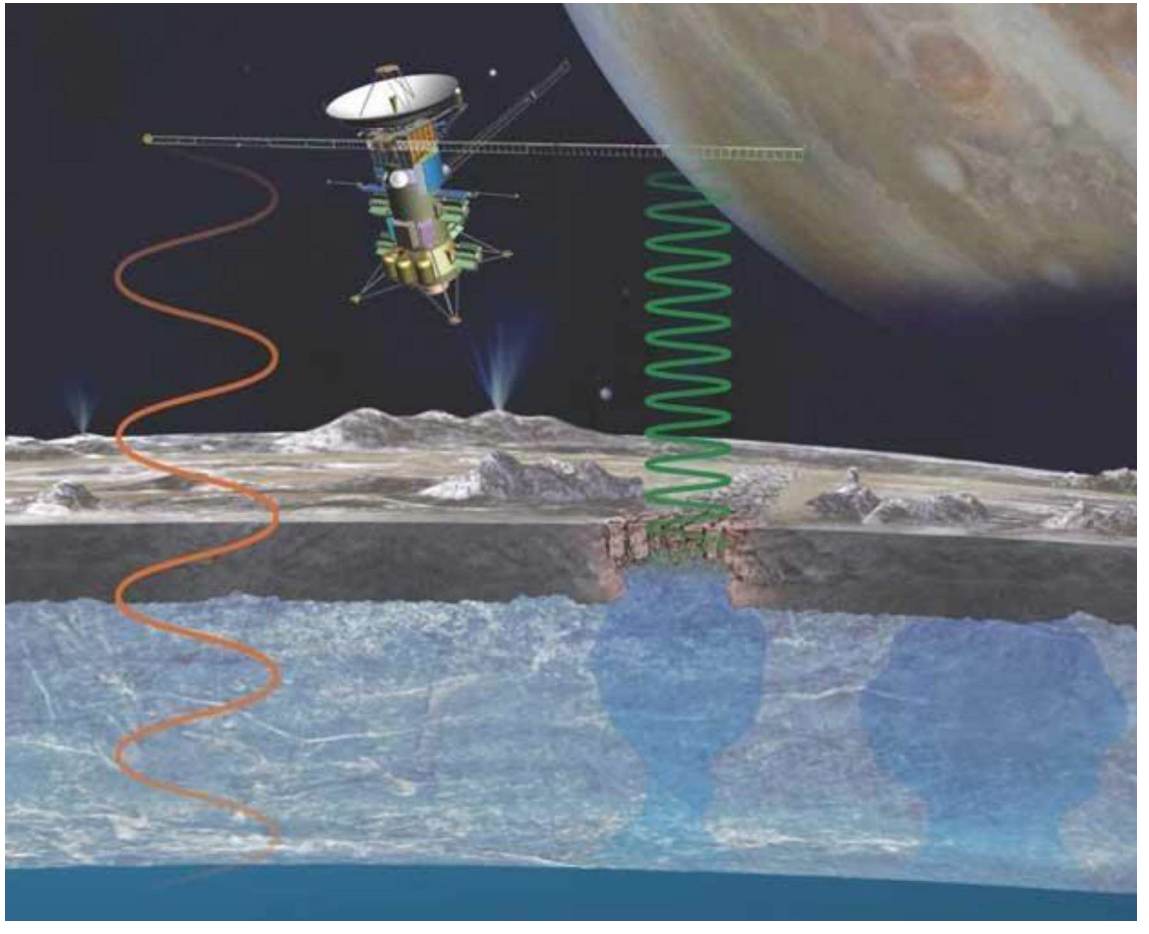

- ❖ Ice thickness estimates for Titan and Enceladus
- ❖ Europa Clipper likely to provide such estimates for Europa (radar instrument)

➔ What we can do: **provide predictive ice thickness models**

Implication for the ice crust

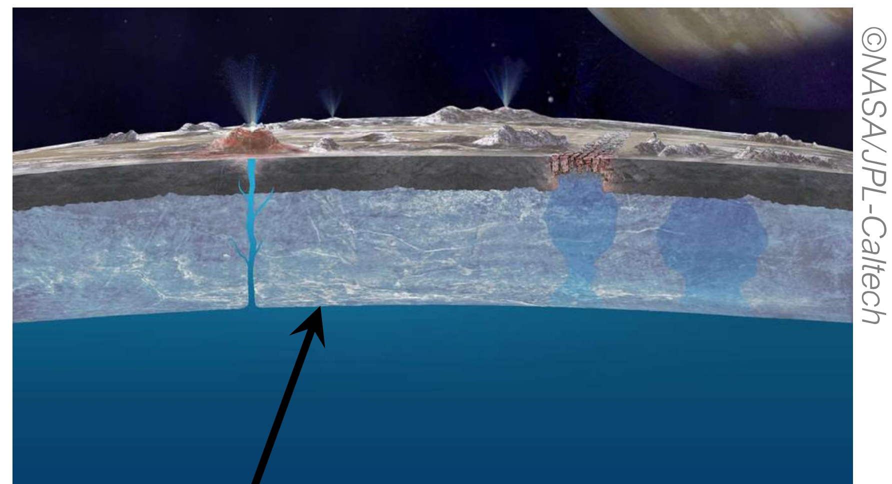

$T_b = T_m = 273$ K melting temperature

$-k\frac{dT}{dz} = q$ oceanic heat flux

Oceanic heat flux

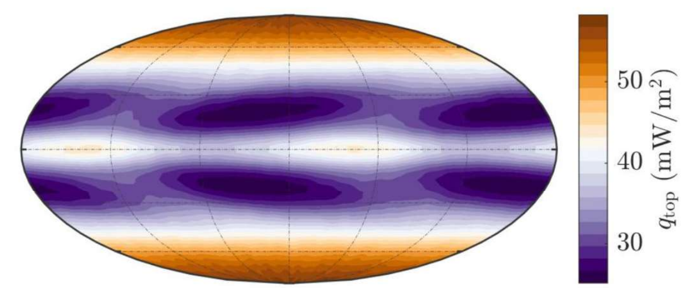

Implication for the ice crust

Surface temperature

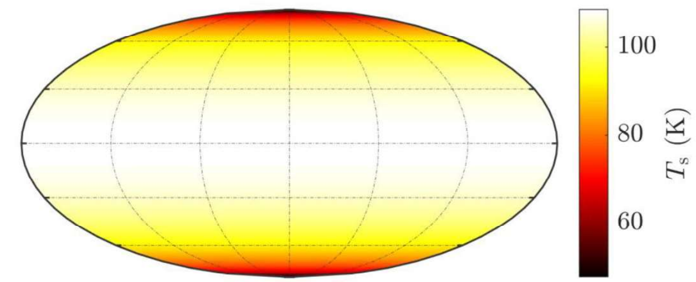

[Ojakangas and Stevenson, 1989]

$T_s = T_s(\theta)$ radiative equilibrium

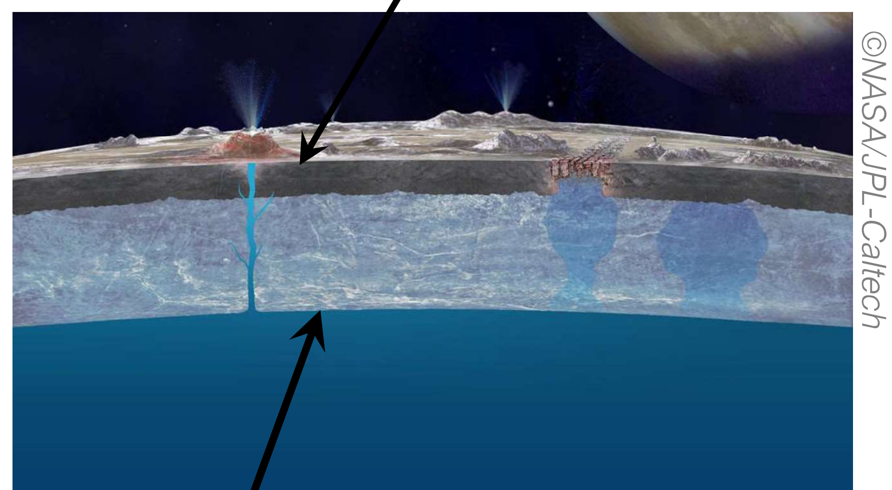

$T_b = T_m = 273$ K melting temperature

$-k\frac{dT}{dz} = q$ oceanic heat flux

Oceanic heat flux

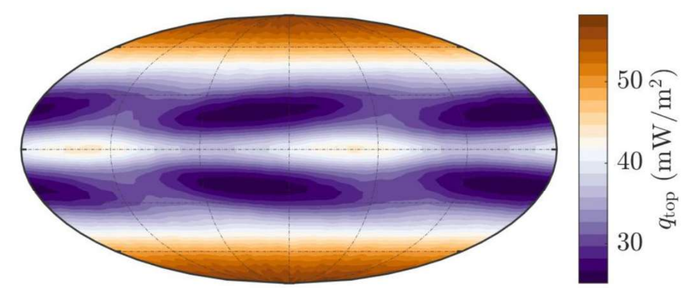

Implication for the ice crust

Surface temperature

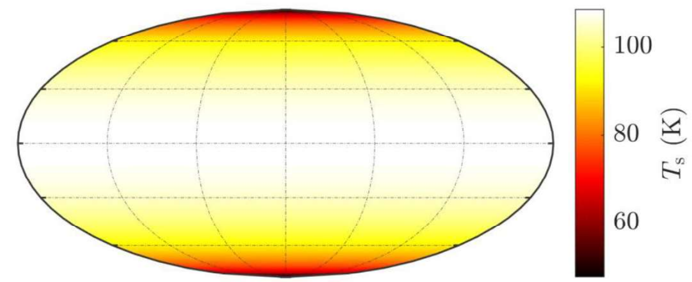

[Ojakangas and Stevenson, 1989]

Internal ice tidal heating *h*

$$h(T) = \frac{2\mu\overline{\dot{\epsilon}_{ij}}^2}{\omega}\left[\frac{\omega\tau_m}{1+(\omega\tau_m)^2}\right]$$

$$\begin{cases} \tau_m(T) = \dfrac{\eta(T)}{\mu} & \textit{Maxwell time} \\ \eta(T) = \eta_b \exp(-\gamma(T - T_b)) \end{cases}$$

Temperature-dependent viscosity

[Nimmo+ 2007]

$T_s = T_s(\theta)$ radiative equilibrium

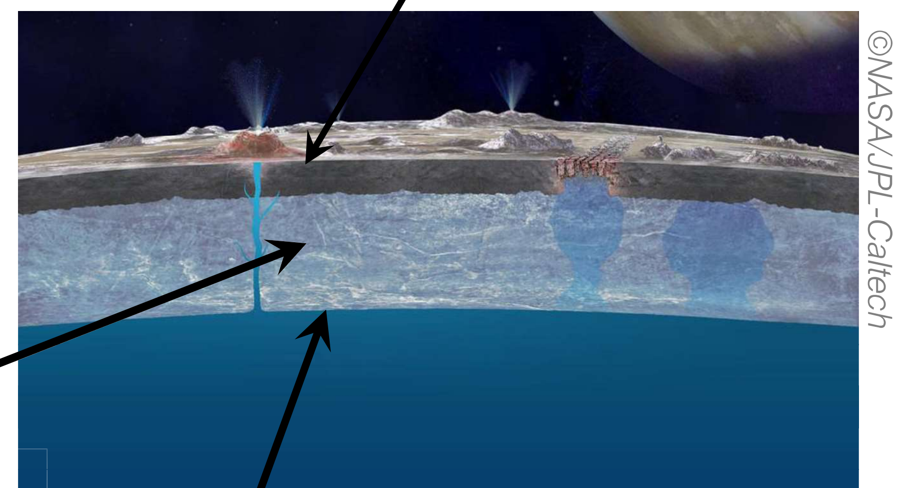

Strain rate $\overline{\dot{\epsilon}_{ij}}^2$

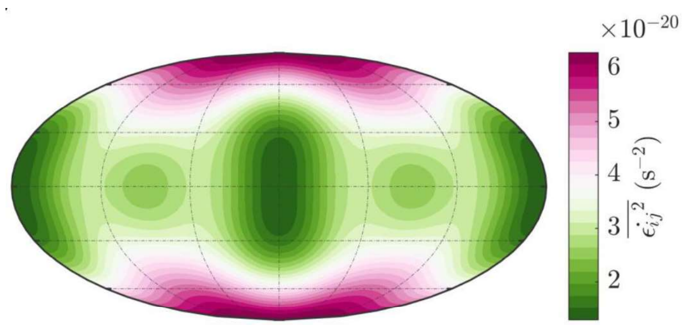

$T_b = T_m = 273$ K melting temperature

$-k\dfrac{dT}{dz} = q$ oceanic heat flux

Oceanic heat flux

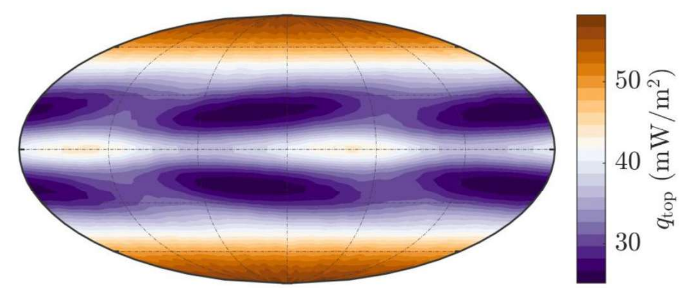

Implication for the ice crust

Solve one dimensional (steady) heat equation with internal tidal heating h *for each* (θ, φ) to find the ice thickness

$$-\frac{d}{dz}\left(k\frac{dT}{dz}\right) = h(T)$$

[Ojakangas and Stevenson, 1989]
[Nimmo et al., 2007]

Surface temperature

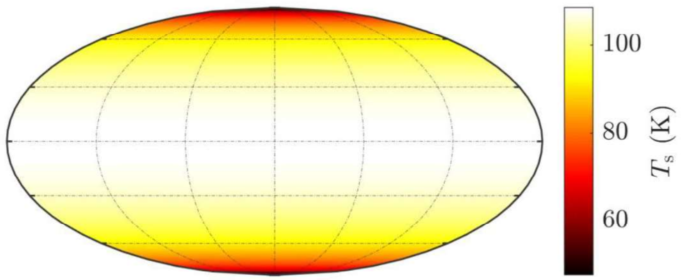

[Ojakangas and Stevenson, 1989]

$T_s = T_s(\theta)$ radiative equilibrium

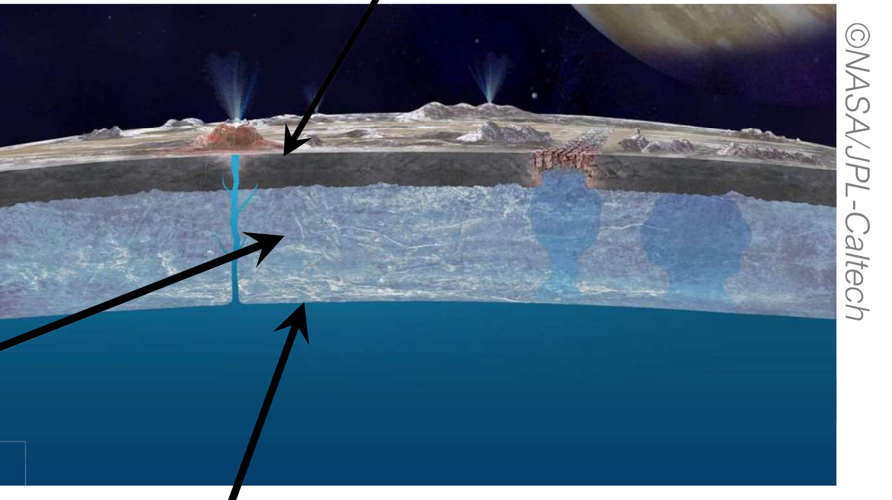

Strain rate $\overline{\dot{\epsilon}_{ij}}^2$

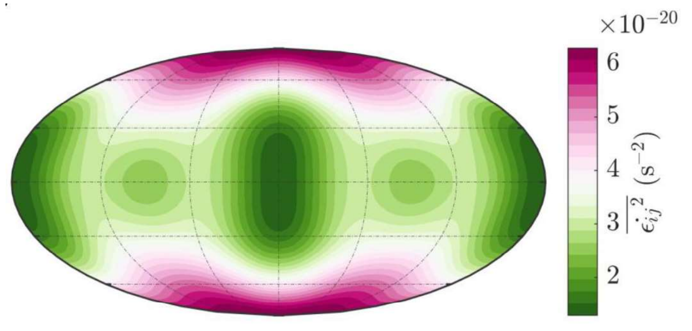

$T_b = T_m = 273$ K melting temperature

$-k\frac{dT}{dz} = q$ oceanic heat flux

Oceanic heat flux

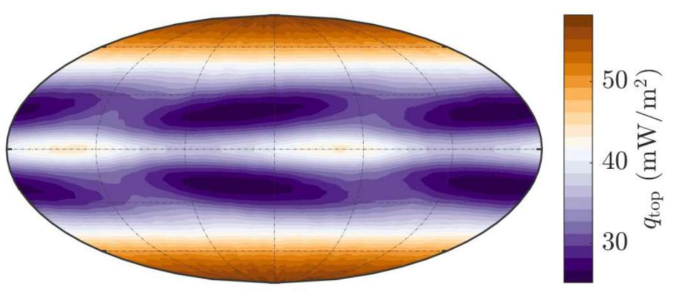

Implication for the ice crust

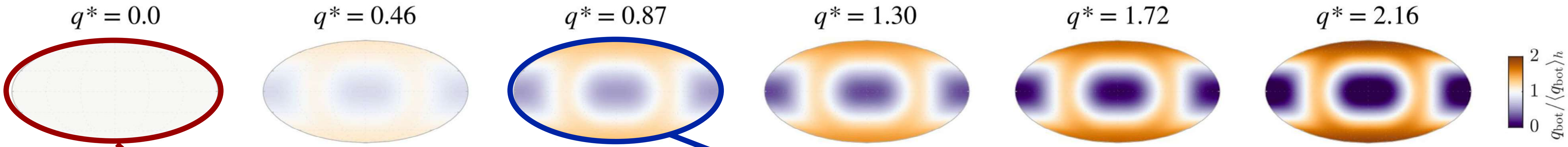

100% Radiogenic Heating

100% Tidal Heating

Implication for the ice crust

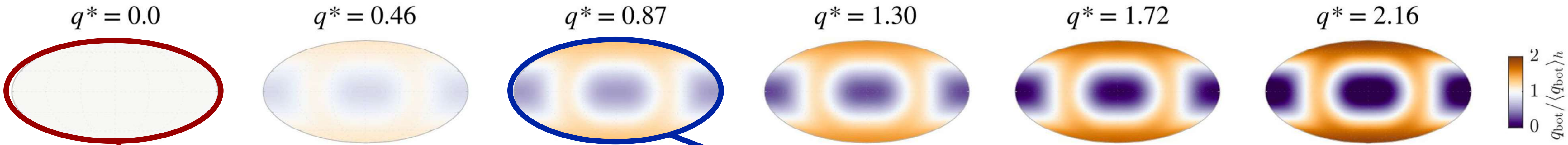

100% Radiogenic Heating

Top heat flux variations

Ice thickness variations ***(ocean heating only)***

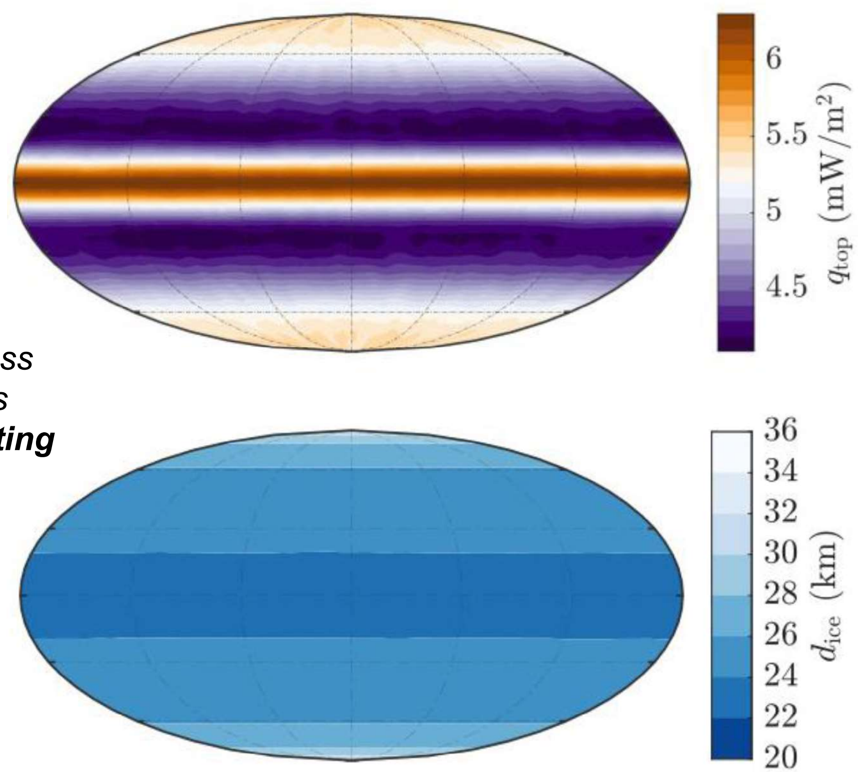

100% Tidal Heating

Top heat flux variations

Ice thickness variations ***(ocean heating only)***

[Lemasquerier+ 2023]

Implication for the ice crust

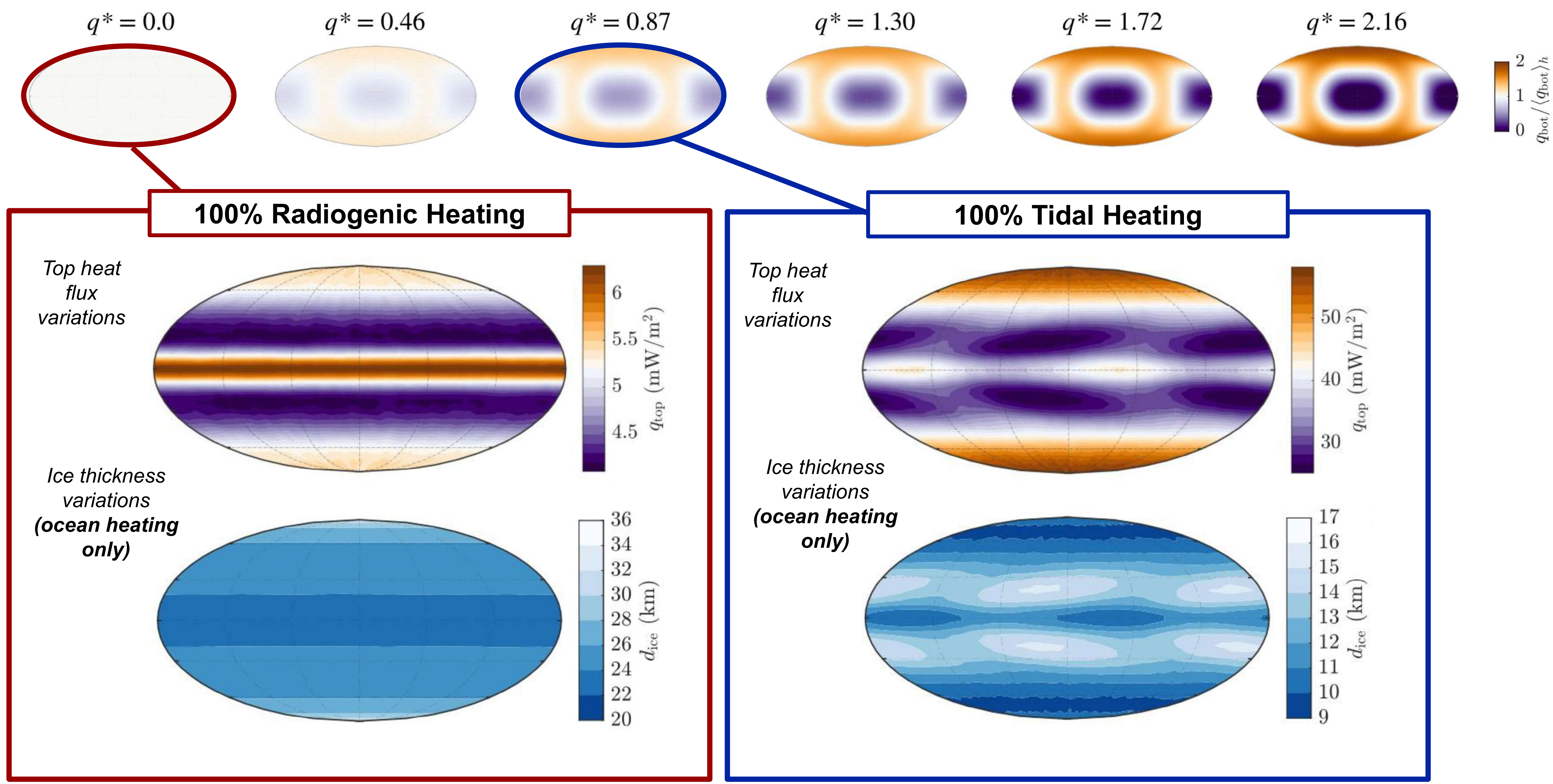

[Lemasquerier+ 2023]

Implication for the ice crust

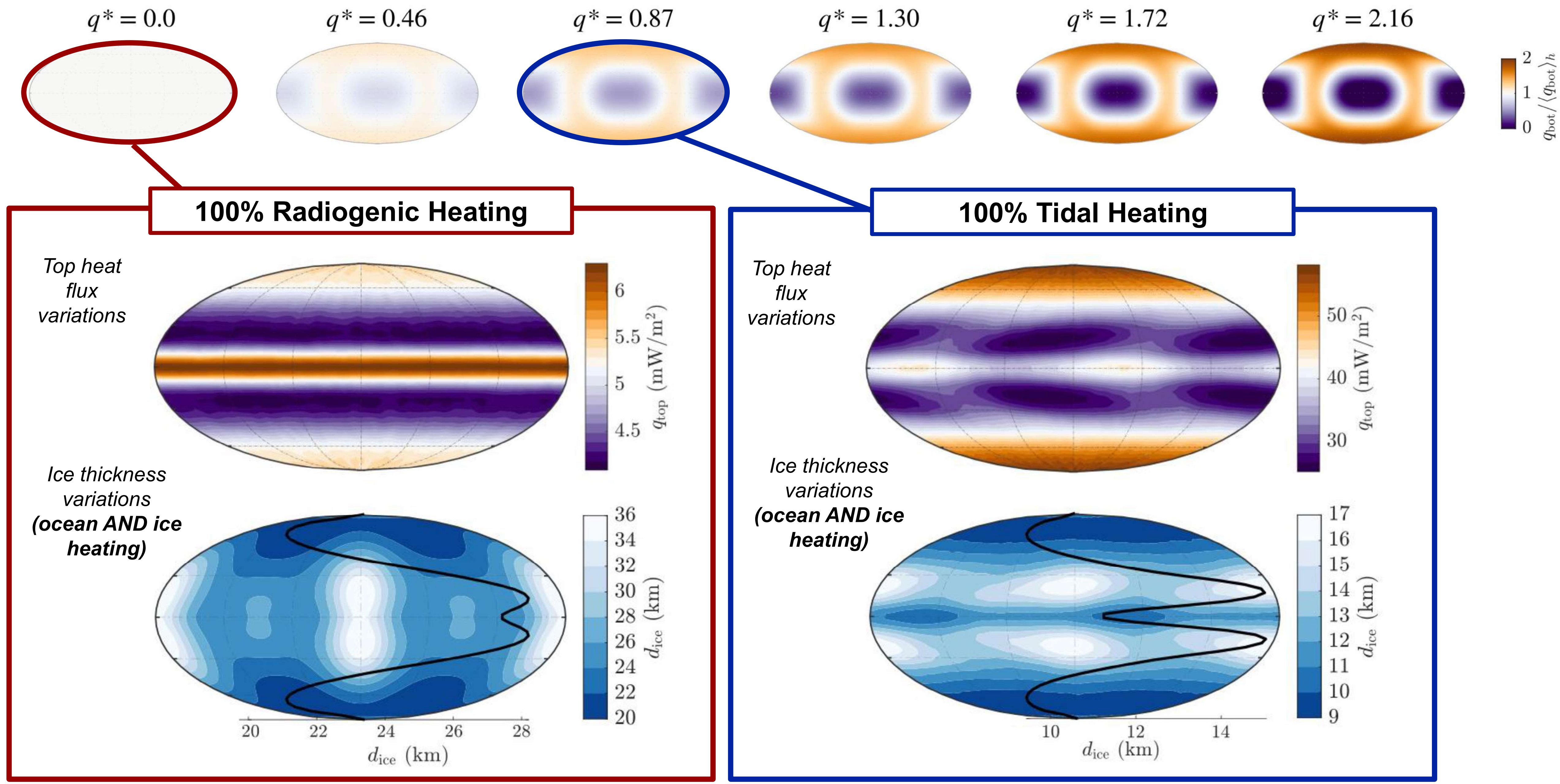

[Lemasquerier+ 2023]

Implication for the ice crust

Underlying hypothesis: **ice shell thickness anti-correlated with the heat flux at the top of the ocean**

CAVEATS

Implication for the ice crust

Underlying hypothesis: **ice shell thickness anti-correlated with the heat flux at the top of the ocean**

CAVEATS

Melting point depression with pressure

- 20-km latitudinal ice thickness variation on Enceladus → **0.2 K difference** at the base of the ice crust
- Thermal gradient could drive **large-scale baroclinic flows** and hamper the convective transport in the polar regions [Kang, MNRAS 2023]

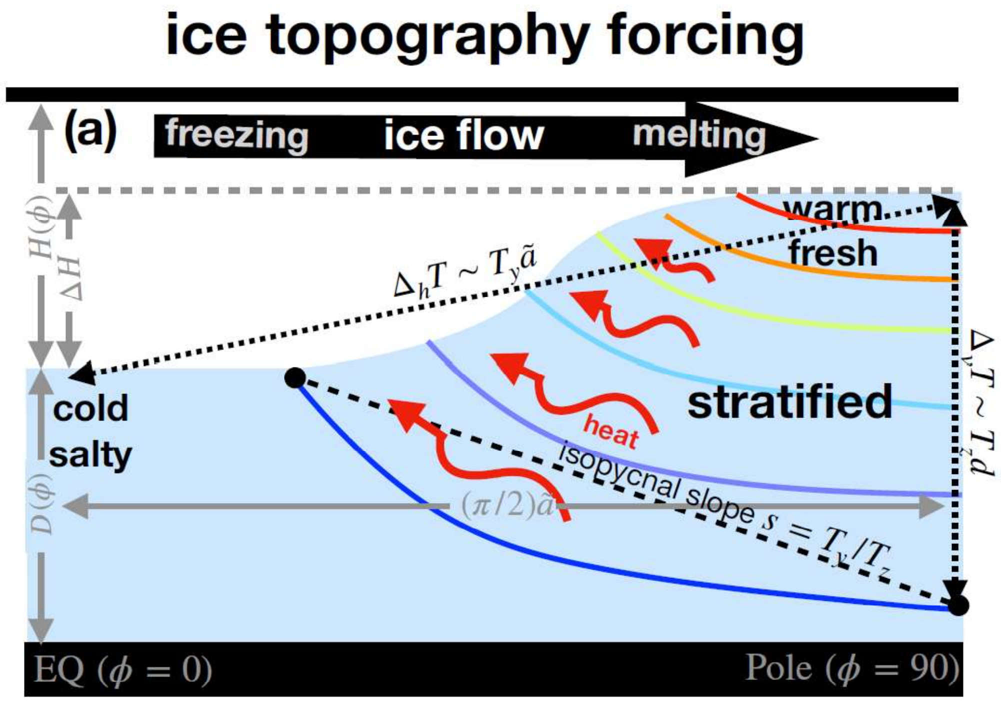

[Kang, MNRAS 2023]

Implication for the ice crust

Underlying hypothesis: **ice shell thickness anti-correlated with the heat flux at the top of the ocean**

CAVEATS

Melting point depression with pressure

- 20-km latitudinal ice thickness variation on Enceladus → **0.2 K difference** at the base of the ice crust
- Thermal gradient could drive **large-scale baroclinic flows** and hamper the convective transport in the polar regions [Kang, MNRAS 2023]

Variations in salinity due to melting/freezing

Double-diffusion

[e.g., Ashkenazy and Tziperman, 2021, Lobo+ 2021, Wong+ 2022, Kang 2023]

ice topography forcing

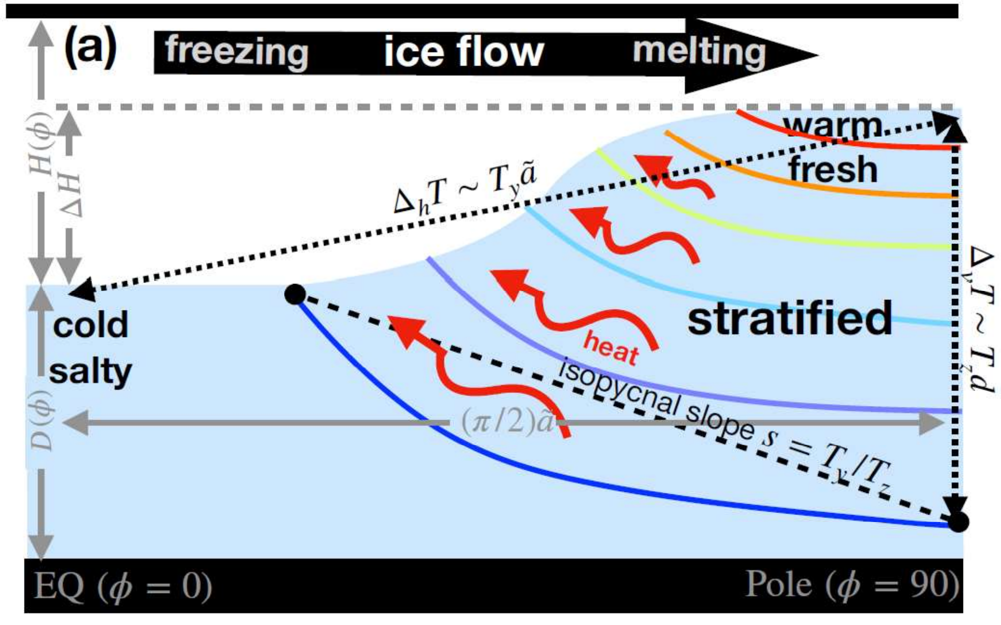

[Kang, MNRAS 2023]

Implication for the ice crust

Underlying hypothesis: **ice shell thickness anti-correlated with the heat flux at the top of the ocean**

CAVEATS

Melting point depression with pressure

- 20-km latitudinal ice thickness variation on Enceladus → **0.2 K difference** at the base of the ice crust
- Thermal gradient could drive **large-scale baroclinic flows** and hamper the convective transport in the polar regions [Kang, MNRAS 2023]

Variations in salinity due to melting/freezing

Double-diffusion

[e.g., Ashkenazy and Tziperman, 2021, Lobo+ 2021, Wong+ 2022, Kang 2023]

Endogenic processes in the ice

- Viscous ice flow (/!\ Uncertainty in basal ice viscosity)
- Solid-state convection

Implication for the ice crust

Underlying hypothesis: **ice shell thickness anti-correlated with the heat flux at the top of the ocean**

CAVEATS

Melting point depression with pressure

- 20-km latitudinal ice thickness variation on Enceladus → **0.2 K difference** at the base of the ice crust
- Thermal gradient could drive **large-scale baroclinic flows** and hamper the convective transport in the polar regions [Kang, MNRAS 2023]

Variations in salinity due to melting/freezing

Double-diffusion

[e.g., Ashkenazy and Tziperman, 2021, Lobo+ 2021, Wong+ 2022, Kang 2023]

Endogenic processes in the ice

- Viscous ice flow (/!\ Uncertainty in basal ice viscosity)
- Solid-state convection

Dynamical feedback of the topography on the ocean flow

Feedback of the ice: coupled models

Gastine and Favier, Icarus 2024: rotating convection with a melting boundary (phase field method)

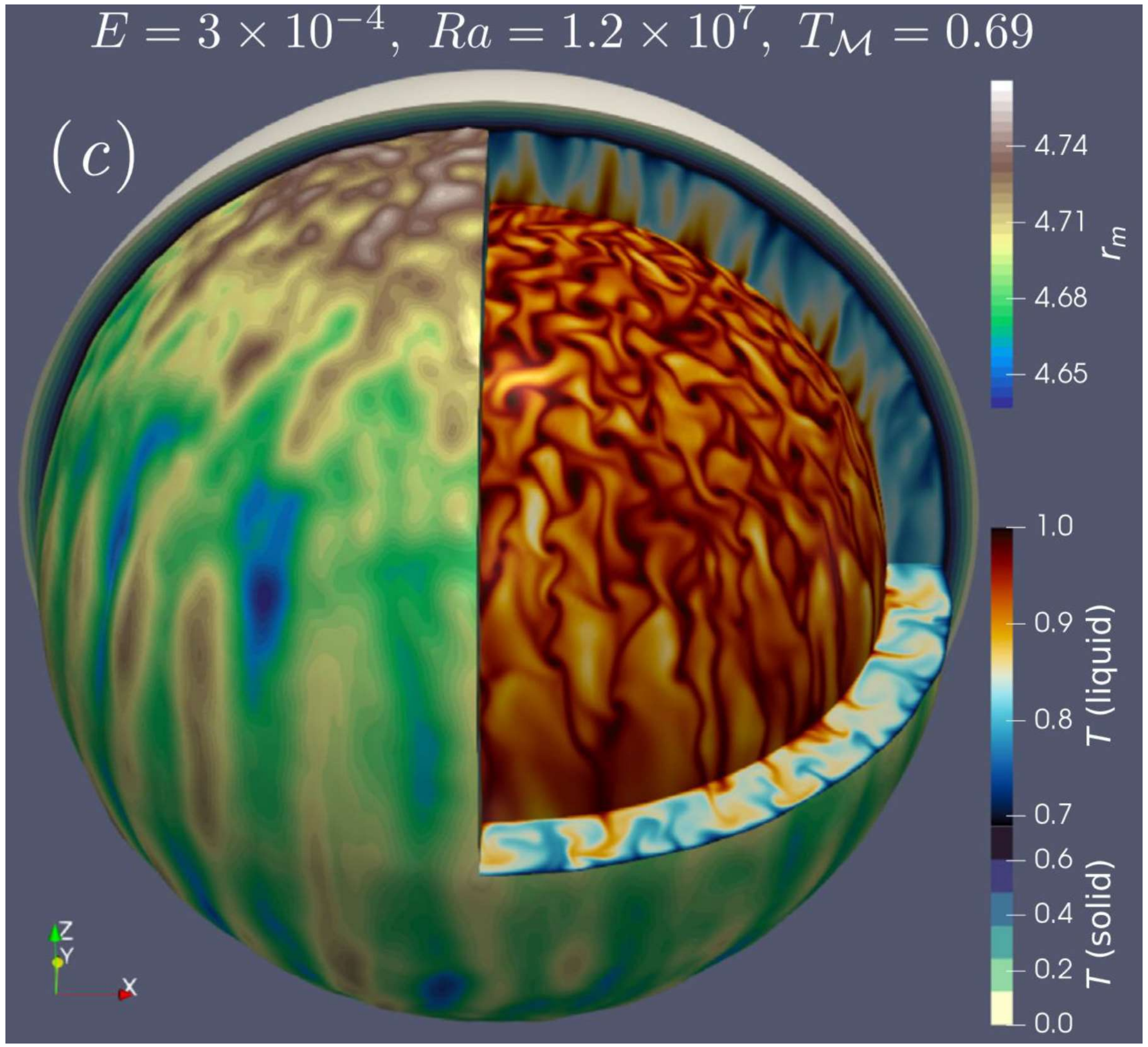

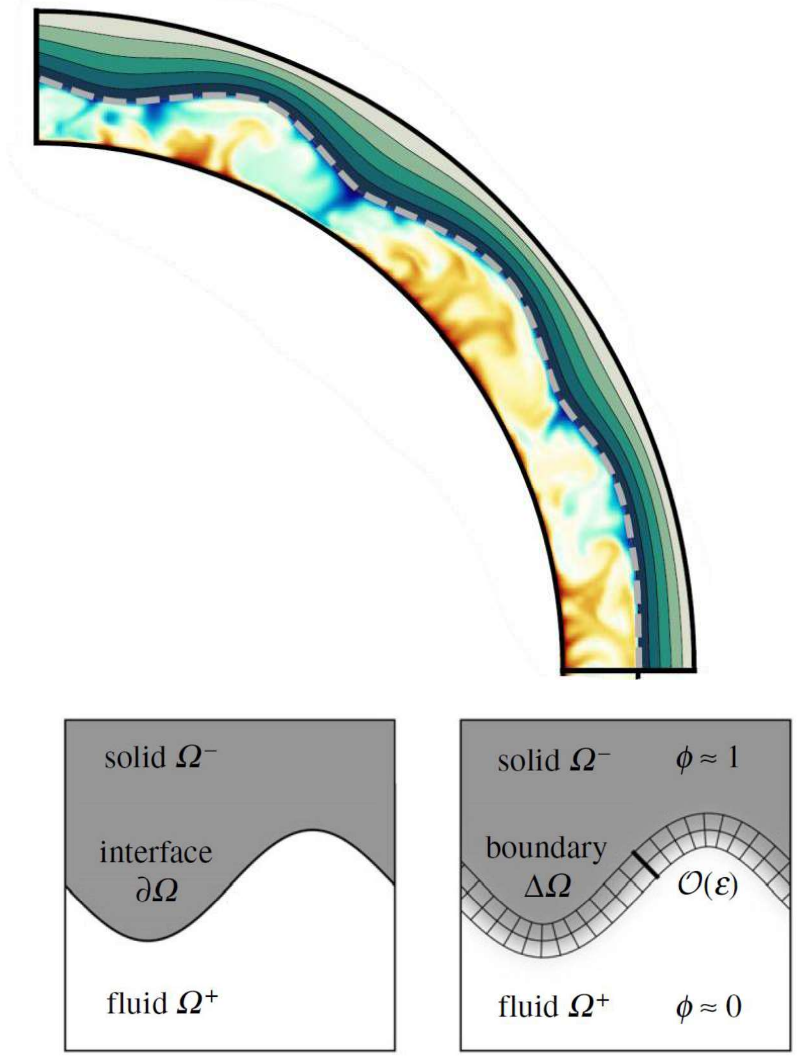

[Hester+, 2020]

Feedback of the ice: coupled models

Gastine and Favier, Icarus 2024: rotating convection with a melting boundary (phase field method)

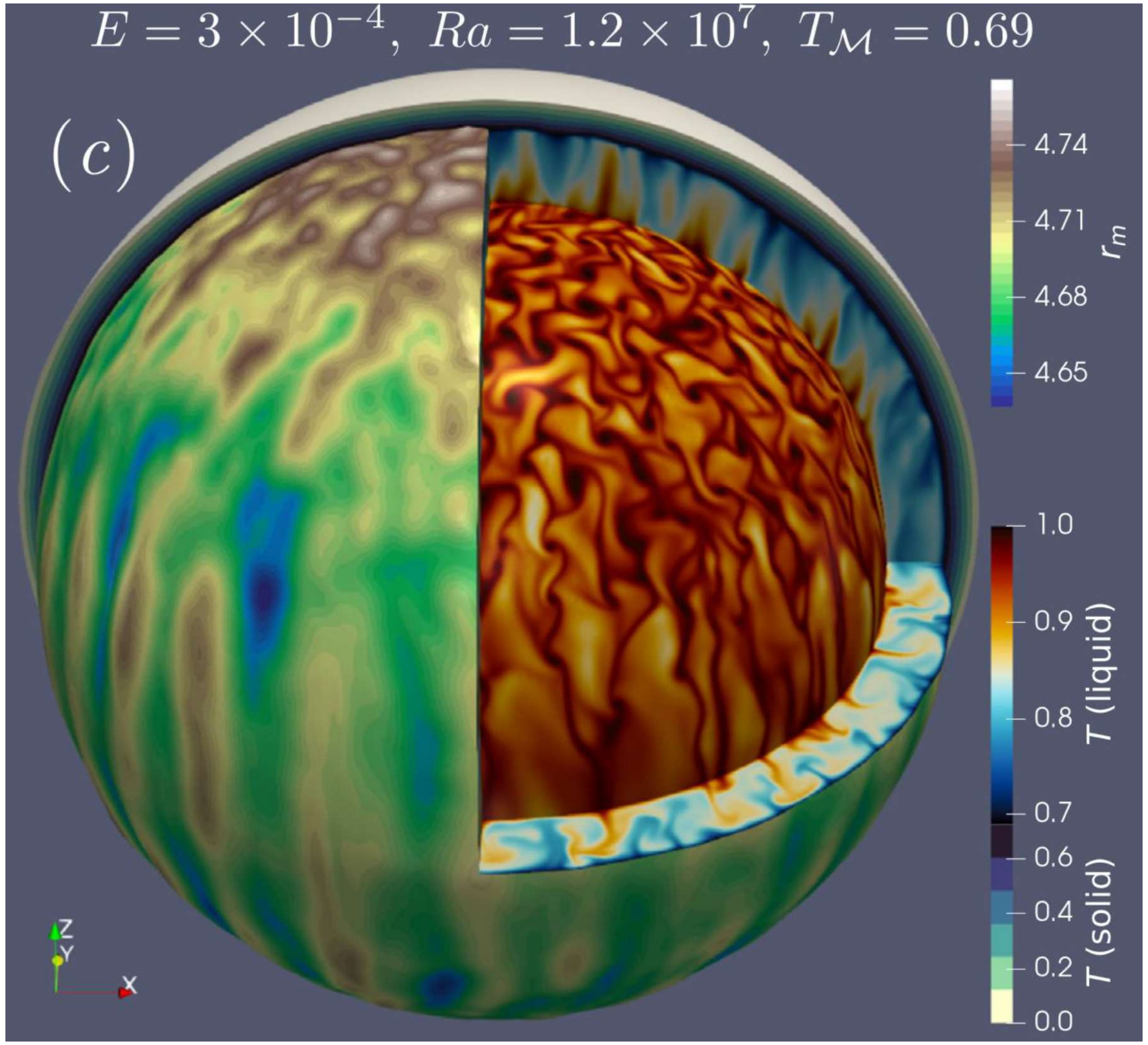

Governing equations [Hester+, 2020]:

Penalization term (velocity->0 in ice)

$$\nabla \cdot \boldsymbol{u} = 0,$$

$$\frac{\partial \boldsymbol{u}}{\partial t} + \boldsymbol{u} \cdot \nabla \boldsymbol{u} + \frac{2}{E} \boldsymbol{e}_z \times \boldsymbol{u} = -\nabla p + \frac{Ra}{Pr} g \boldsymbol{e}_r + \nabla^2 \boldsymbol{u} \boxed{- \frac{1}{\tau_p \epsilon^2} \phi \boldsymbol{u}},$$

$$\frac{\partial T}{\partial t} + \boldsymbol{u} \cdot \nabla T = \frac{1}{Pr} \nabla^2 T + \boxed{St \frac{\partial \phi}{\partial t}},$$

Latent heat

$$\frac{5}{6} St Pr \frac{\partial \phi}{\partial t} = a \nabla^2 \phi - \frac{1}{\boxed{\epsilon^2}} \phi(1-\phi) \left[a(1-2\phi) + T - T_{\mathcal{M}} \right].$$

Phase change interface width

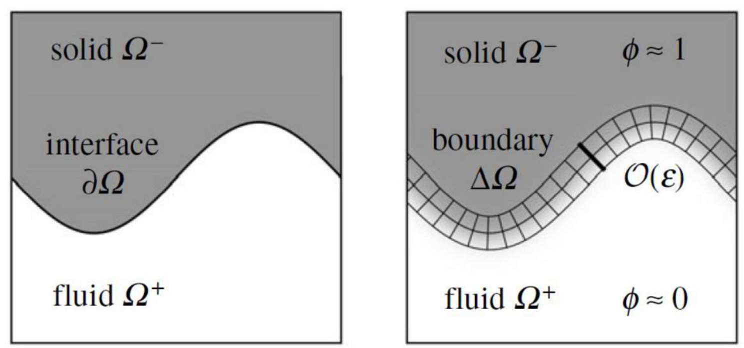

[Hester+, 2020]

Feedback of the ice: coupled models

Gastine and Favier, Icarus 2024: rotating convection with a melting boundary (phase field method)

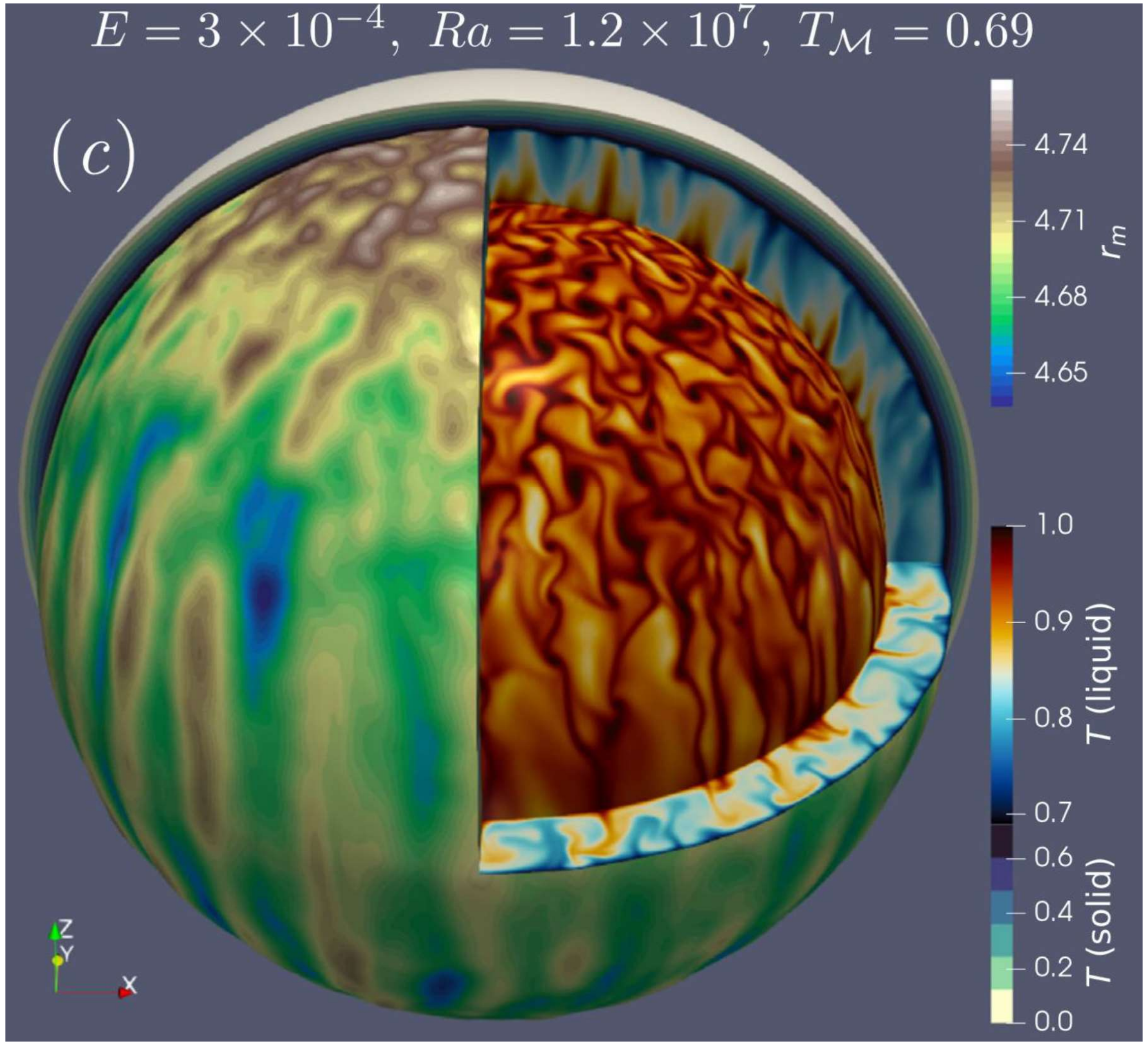

Governing equations [Hester+, 2020]:

$$\nabla \cdot \boldsymbol{u} = 0,$$

$$\frac{\partial \boldsymbol{u}}{\partial t} + \boldsymbol{u} \cdot \nabla \boldsymbol{u} + \frac{2}{E} \boldsymbol{e}_z \times \boldsymbol{u} = -\nabla p + \frac{Ra}{Pr} g \boldsymbol{e}_r + \nabla^2 \boldsymbol{u} \boxed{- \frac{1}{\tau_p \epsilon^2} \phi \boldsymbol{u}},$$

Penalization term (velocity->0 in ice)

$$\frac{\partial T}{\partial t} + \boldsymbol{u} \cdot \nabla T = \frac{1}{Pr} \nabla^2 T + \boxed{St \frac{\partial \phi}{\partial t}},$$

Latent heat

$$\frac{5}{6} St Pr \frac{\partial \phi}{\partial t} = a \nabla^2 \phi - \frac{1}{\boxed{\epsilon^2}} \phi (1 - \phi) \left[a(1 - 2\phi) + T - T_{\mathcal{M}} \right].$$

Phase change interface width

Stefan condition at the interface (limit $\epsilon \to 0$):

$$\boldsymbol{n} \cdot \left[\nabla T^{(S)} - \nabla T^{(L)} \right] = St Pr\, \boldsymbol{v} \cdot \boldsymbol{n},$$

$$T = T_{\mathcal{M}},$$

Feedback of the ice: coupled models

Gastine and Favier, Icarus 2024: rotating convection with a melting boundary (phase field method)

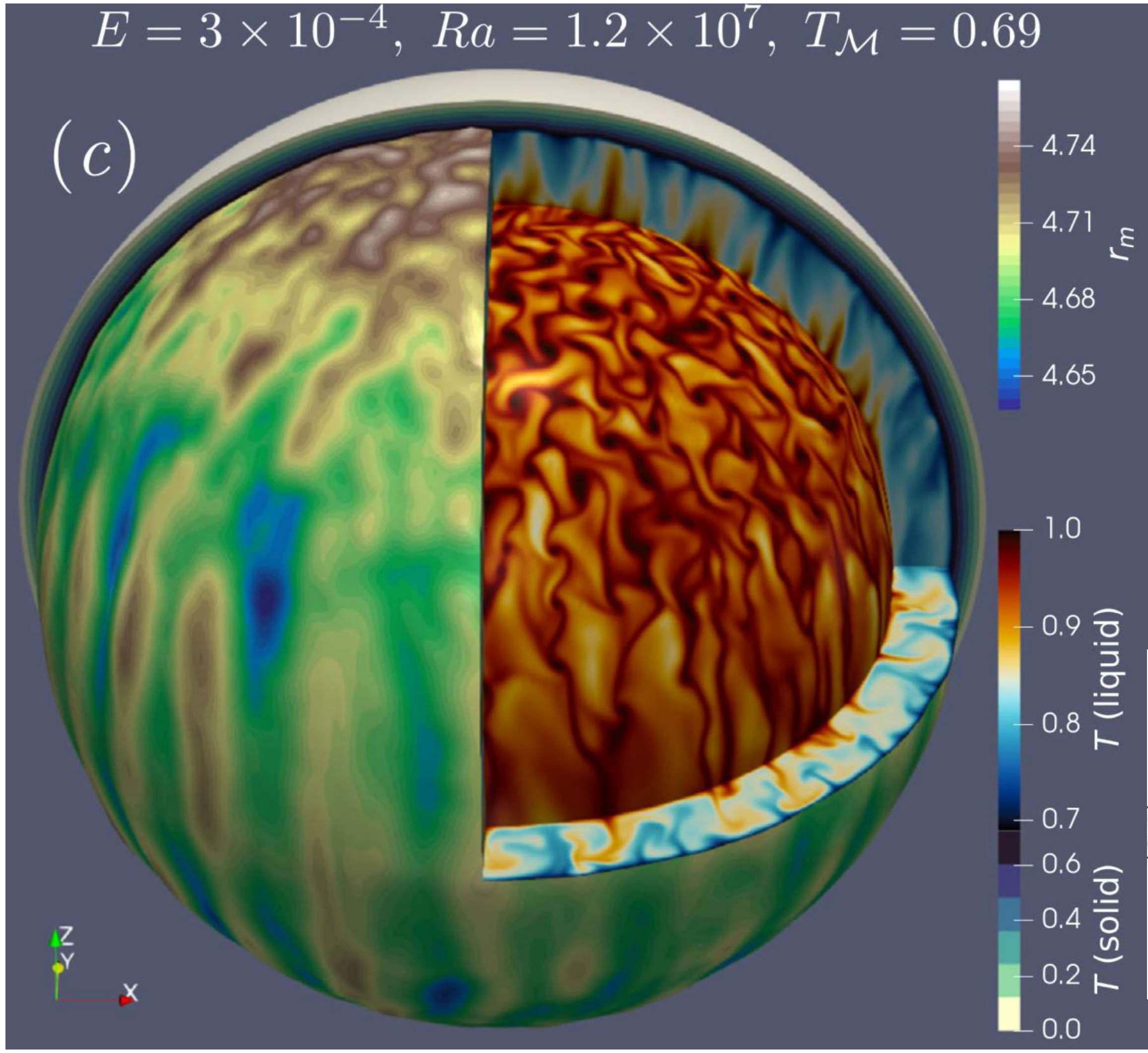

- First study to account for the ***dynamical* generation of topographic features** associated with the turbulent flows
- Transition between polar and equatorial cooling retrieved
- **Small/No feedback of latitudinal thickness variations**: Relative heat flux variations from monophasic simulations provide a good guess of the actual axisymmetric flux as long as the mean axisymmetric topographic changes are small

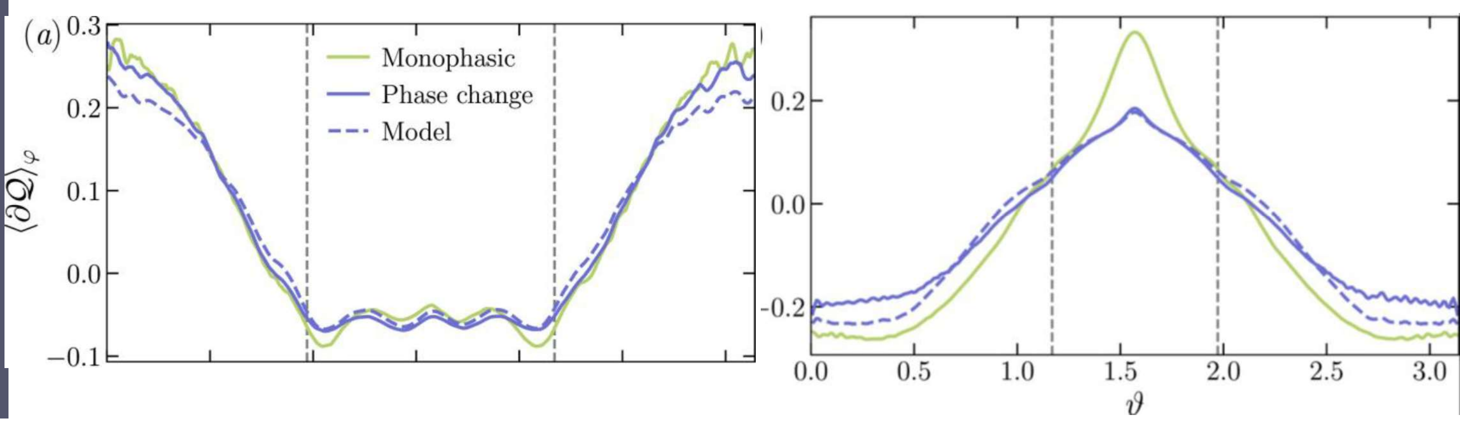

Feedback of the ice: coupled models

Gastine and Favier, Icarus 2024: rotating convection with a melting boundary (phase field method)

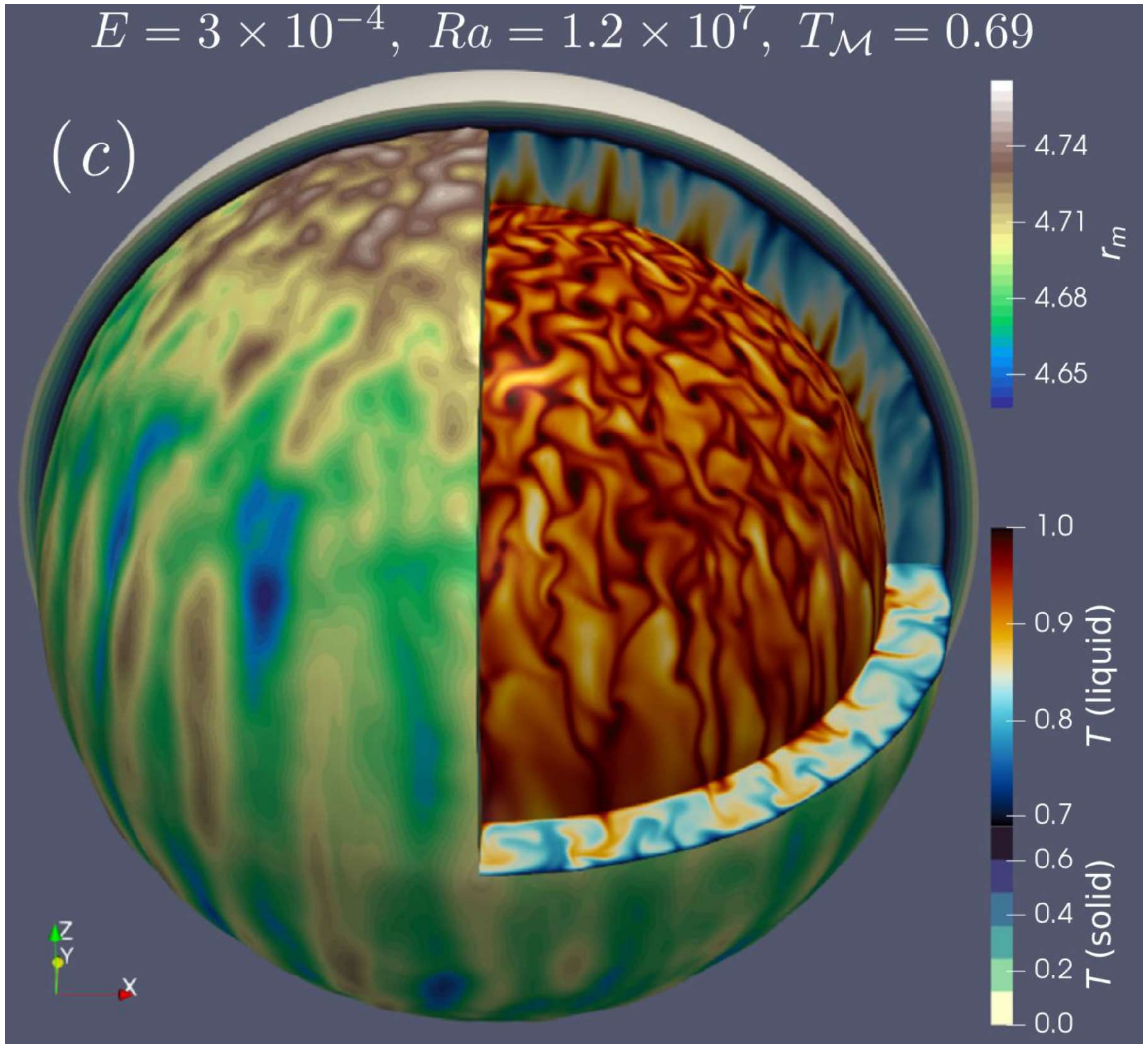

- ❖ First study to account for the ***dynamical* generation of topographic features** associated with the turbulent flows
- ❖ Transition between polar and equatorial cooling retrieved
- ❖ **Small/No feedback of latitudinal thickness variations**: Relative heat flux variations from monophasic simulations provide a good guess of the actual axisymmetric flux as long as the mean axisymmetric topographic changes are small
- ❖ **Stronger feedback of non-axisymmetric** troughs and crests able to lock-in convective upwelling

Missing effect relevant to subsurface oceans:

- Salinity
- Pressure dependence of melting temperature
- Flow in the ice
- Tidal heating in the ice
- Thermal heterogeneities at the seafloor

Conclusions

- Tidal heating could drive large-scale **thermal winds** in Europa's ocean, but it strongly depends on the mechanical BC considered

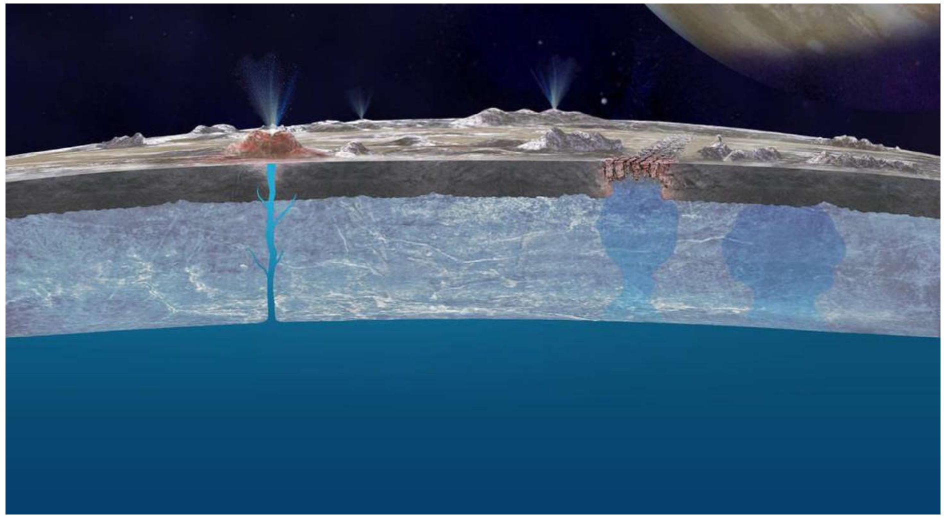

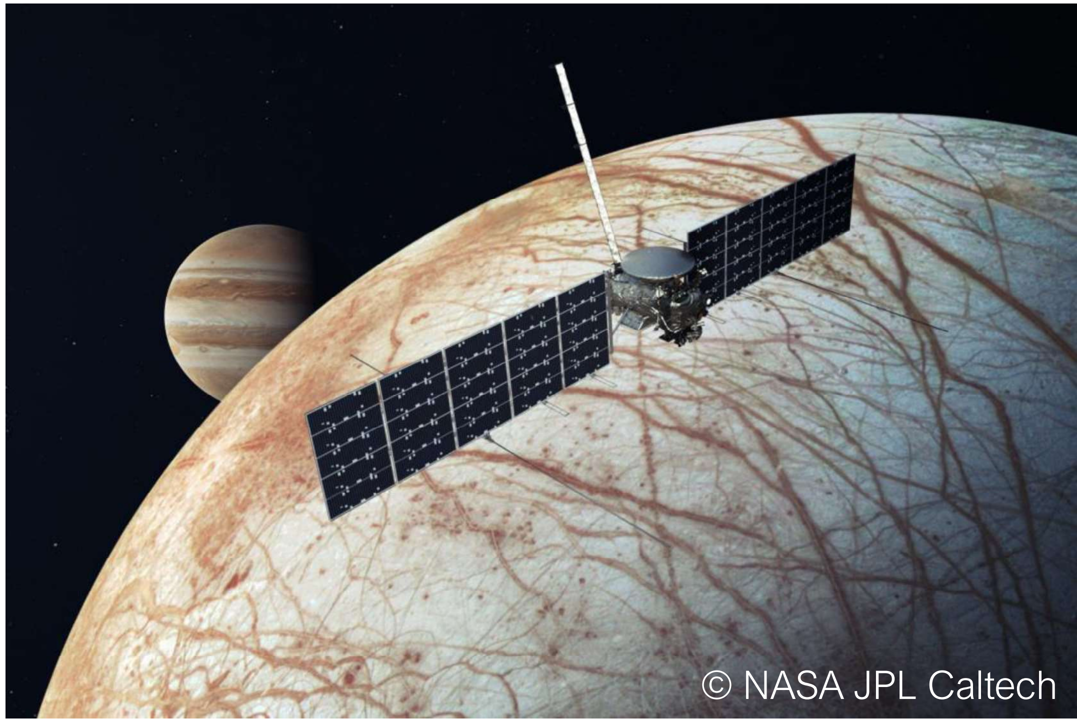

Conclusions

- Tidal heating could drive large-scale **thermal winds** in Europa's ocean, but it strongly depends on the mechanical BC considered

- Despite this uncertainty, in all cases, the tidal heating anomaly in latitude is entirely translated upwards (leading to a **polar cooling** configuration)

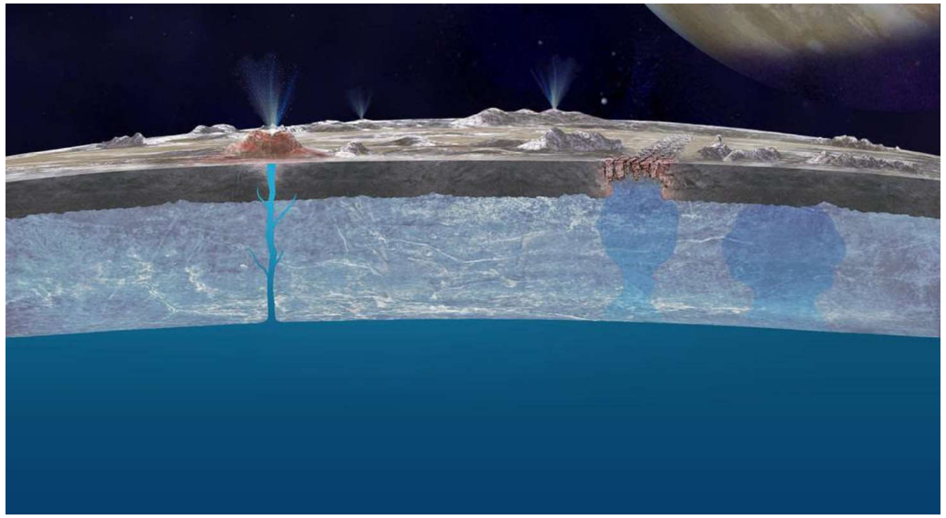

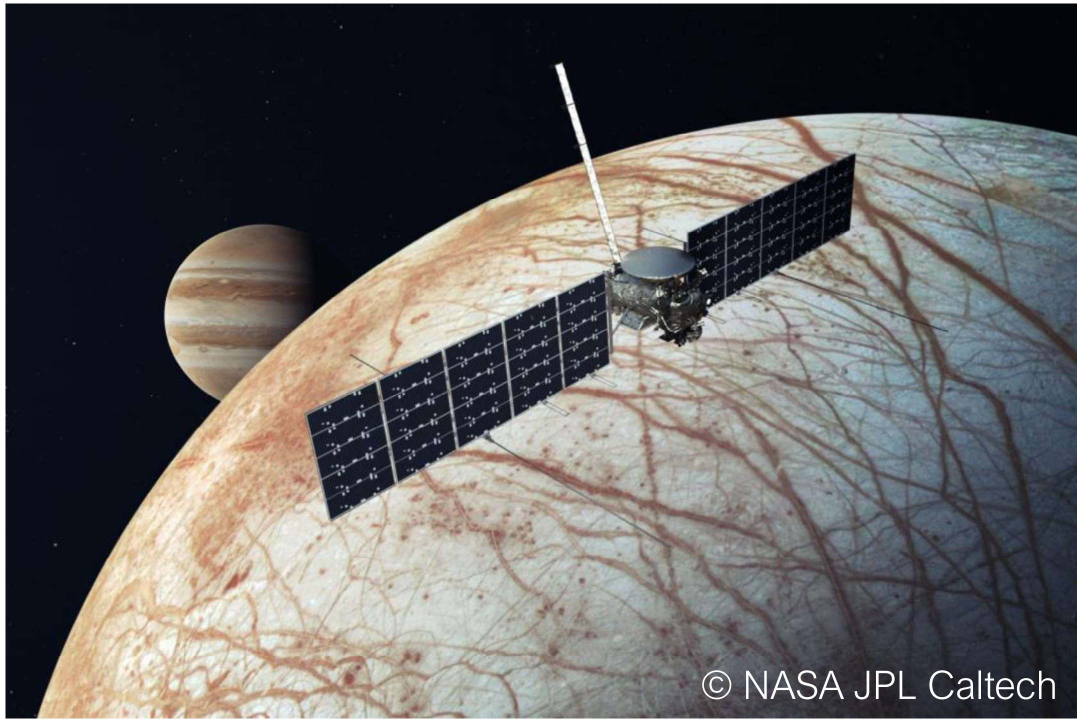

© NASA JPL Caltech

Conclusions

- Tidal heating could drive large-scale **thermal winds** in Europa's ocean, but it strongly depends on the mechanical BC considered

- Despite this uncertainty, in all cases, the tidal heating anomaly in latitude is entirely translated upwards (leading to a **polar cooling** configuration)

- Tidal heating in the silicate mantle could account for **longitudinal variations** of ice crust's features, but robustness at smaller Ekman number needs to be investigated

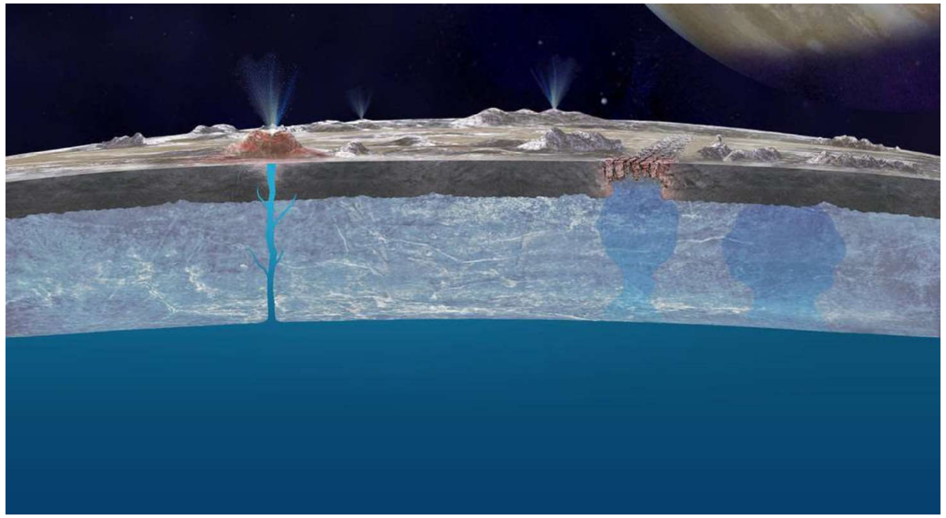

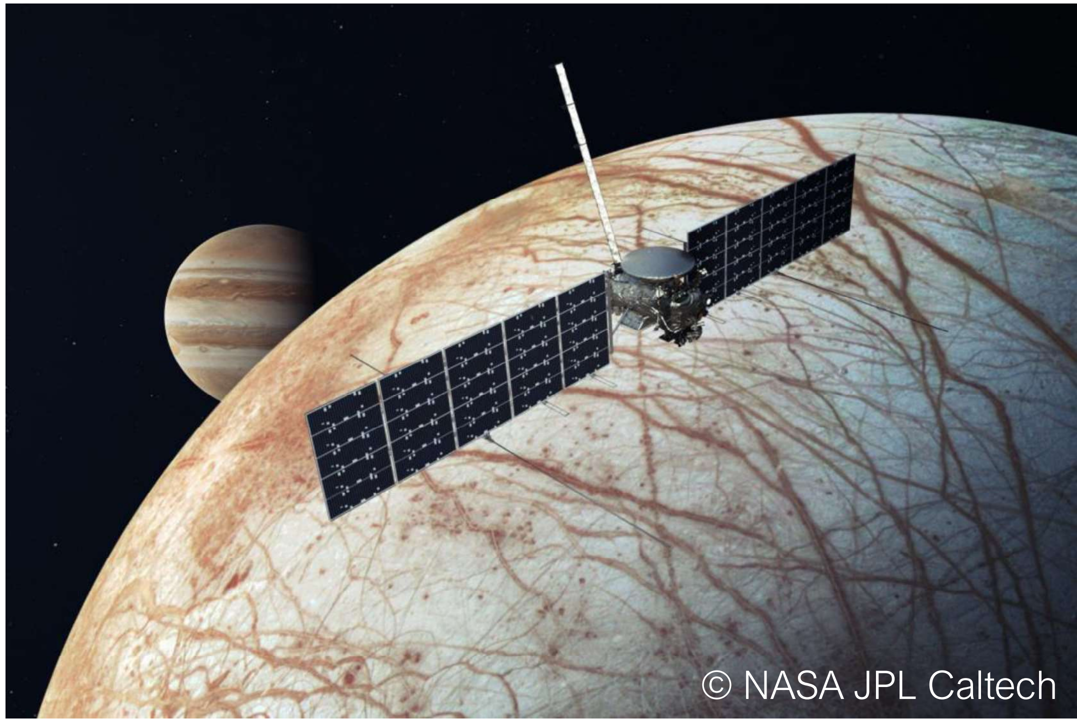

Conclusions

- Tidal heating could drive large-scale **thermal winds** in Europa's ocean, but it strongly depends on the mechanical BC considered

- Despite this uncertainty, in all cases, the tidal heating anomaly in latitude is entirely translated upwards (leading to a **polar cooling** configuration)

- Tidal heating in the silicate mantle could account for **longitudinal variations** of ice crust's features, but robustness at smaller Ekman number needs to be investigated

- Limitations:
    - ✓ Reaching more extreme (Ra,E) regimes
    - ✓ What is the relevant regime of rotational constraint?
    - ✓ The **salinity-driven** circulation and **phase-change** at the ice-ocean boundary need to be incorporated in DNS
    - ✓ Ice thickness variations could induce topographic and thermal feedbacks (promising coupled models, but increased numerical cost)
    - ✓ Role of active processes in the ice?
    - ✓ Interaction with other driving forces (mechanical tides, libration)

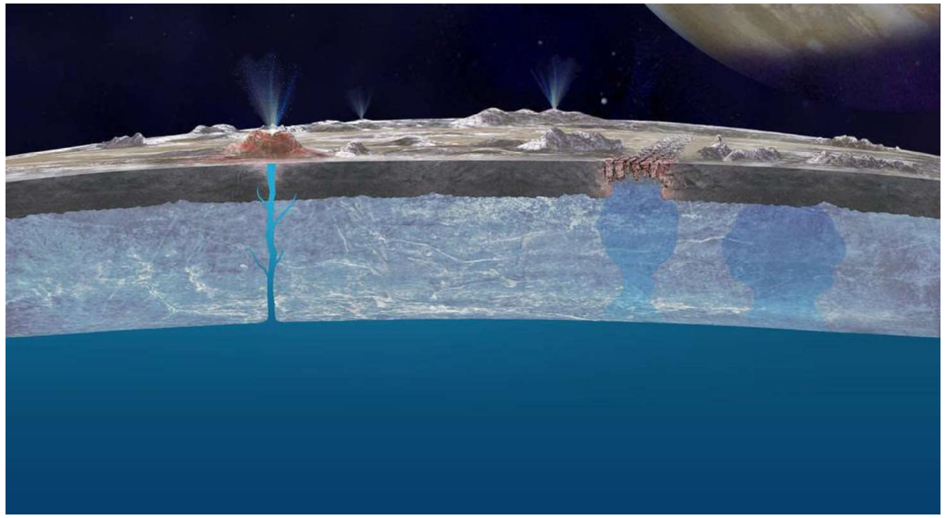

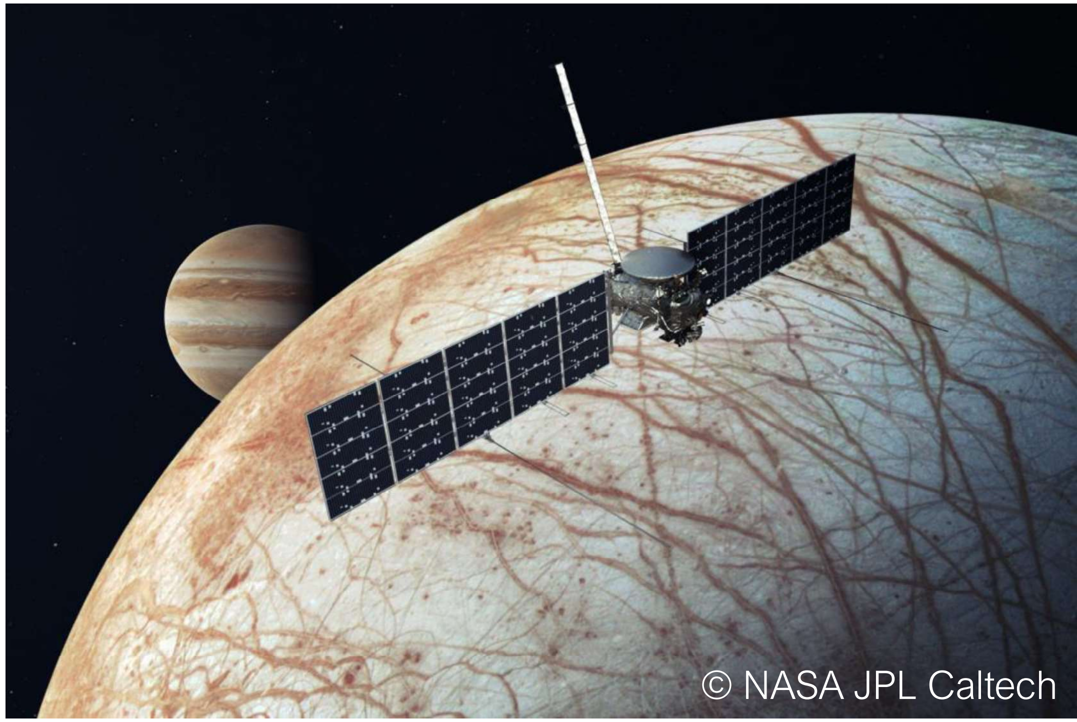

© NASA JPL Caltech